Use of digital image analysis to identify *Rhizoctonia solani* and *Rhizoctonia zeae* resistance in *Festuca arundinacea* plant introductions

Virginia R. Sykes

Thesis submitted to the faculty of the Virginia Polytechnic Institute and State University in partial fulfillment of the requirements for the degree of

Master of Science
In
Plant Pathology, Physiology, and Weed Science

B.J. Horvath, Chair
S.D. Askew
A.B. Baudoin
J.M. Goatley

April 22, 2009
Blacksburg, VA

Keywords: brown patch, tall fescue, turfgrass, disease evaluation, *Schedonorus phoenix*

Use of digital image analysis to identify *Rhizoctonia solani* and *Rhizoctonia zeae* resistance in *Festuca arundinacea* plant introductions

Virginia R. Sykes

ABSTRACT

Brown patch, caused by *Rhizoctonia solani* Kuhn, is an important disease on tall fescue (TF, *Festuca arundinacea* Schreb, synonym *Schedonorus phoenix* (Scop.) Holub). *Rhizoctonia zeae* Voorhees, a related pathogen, causes similar symptoms. Confusion over which *Rhizoctonia* species is causing symptoms and subjective visual evaluations of disease severity may contribute to variability in observed BP resistance of TF cultivars at multiple locations. The objectives of this study were to develop an objective digital image analysis (DIA) method for evaluating disease and to use DIA to screen tall fescue plant introductions (PIs) for resistance to *R. solani* and *R. zeae*. There was a strong correlation ($r^2 = 0.97$) between actual disease severity, measured by applying lesioned tissue of a known area to healthy leaves, and DIA calculated disease severity using scanned images of individual leaves (DIA-IL). The accuracy and precision of visual evaluations and DIA evaluations of entire plants (DIA-WP) were evaluated using DIA-IL as a standard of accuracy. Accuracy of DIA-WP was not significantly different from visual evaluation accuracy. Precision was significantly higher for DIA-WP. Evaluation of PIs and putatively BP resistant TF cultivars for resistance to *R. solani* and *R. zeae* using DIA-WP identified clones within each PI that ranked high for resistance to *R. solani* or *R. zeae*. No clones were identified with high resistance to both *R. solani* and *R. zeae.* Improved precision of DIA evaluation methods and inclusion of *R. zeae* in BP resistance breeding may decrease variability of TF cultivar performance across locations.

Table of Contents

List of Tables

List of Figures

Chapter 1
Literature Review

Introduction

Brown patch, caused by the fungus *Rhizoctonia solani* Kuhn (Piper and Coe, 1919), is frequently the cause of severe damage to tall fescue (*Festuca arundinacea* Schreb, synonym *Schedonorus phoenix* (Scop.) Holub) lawns in the state of Virginia. Resistant cultivars have become an effective and relatively inexpensive option for combating common lawn diseases such as brown patch. While many improvements have been made in grasses with disease resistance, brown patch resistance in tall fescue cultivars remains inconsistent and inadequate. *Rhizoctonia zeae* Voorhees (Voorhees, 1934), a pathogen that presents similar symptoms to those of *R. solani*, typically is not included in the screening process when developing brown patch resistant cultivars. This, along with the subjectivity of visual evaluation methods used in determining disease severity, may contribute to the high variability in brown patch disease resistance observed among currently available cultivars. The primary focus of this thesis will be on the development of a digital image analysis (DIA) method to objectively evaluate disease resistance and the incorporation of *R. zeae* into the brown patch resistance breeding process in an effort to develop tall fescue cultivars with improved brown patch disease resistance.

Turf Industry

The National Agricultural Statistics Service recorded over 1.7 million acres of maintained turf in the state of Virginia in 2004 (NASS, 2004). This was an increase of over 300,000 acres from the 1998 report in which turf already had the highest acreage of any single agronomic crop grown in the state. This acreage can be further divided into a number of areas, with the largest portion consisting of home lawns, which compose nearly 62% of the total turf acreage in Virginia. Maintenance expenses exceed 1.7 billion dollars annually. Approximately 9% of these expenditures, over 1.3 million dollars, are spent on crop protectants such as fungicides and insecticides (NASS, 2004). Virginia homeowners with intensively managed lawns in the

Hampton Roads area spray a fungicide for brown patch control three times on average over the course of a summer (B. Horvath, prs. comm).

The majority of home lawns in the state of Virginia, and throughout much of the transition zone, are tall fescue as this cool-season grass is relatively inexpensive, readily available, and appropriate for Virginia's temperate climate. Tall fescue is susceptible to a number of diseases of which brown patch (*Rhizoctonia solani*), *Pythium* blight (*Pythium* spp.), gray leaf spot (*Pyricularia grisea* (Cooke) Sacc.), and rust (*Puccinia* , *Uromyces*, and *Physopella* species) are the most important. Of these diseases, brown patch, caused by the fungus *R. solani*, is the most common and destructive on tall fescue lawns in Virginia.

Rhizoctonia species

Rhizoctonia species are categorized as imperfect fungi with Basidiomycota teleomorphs. Species within the genus *Rhizoctonia* do not have conidia, clamp connections, or rhizomorphs and sclerotia are undifferentiated into rind and medulla. Taxa within the genus may be differentiated by number of nuclei with binucleate species having only two nuclei per cell and multinucleate species having more than two nuclei per cell. Differences in the architecture and general appearance of vegetative hyphae and sclerotia may also be used as a means of differentiation. Hyphal anastomosis, along with morphological, pathogenic, physiological, and ecological differences, are used to further subdivide groups at the subspecies level (Burpee and Martin, 1992).

Mycelial compatibility, or anastomosis grouping, is based on hyphal fusion, and has been reported to be the principle most helpful to plant pathologists in studying *R. solani* from 1965-1982 (Anderson, 1982). Isolates are placed in anastomosis groups (AGs) based on the interaction of their hyphal cells with those of other isolates. Possible reactions include perfect fusion, which involves dissolution of the membrane and cytoplasmic mixing, imperfect fusion, which involves no cell dissolution or cytoplasmic mixing, and contact fusion, which involves contact but no fusion. Hyphal fusion of compatible isolates results in perfect fusion while fusion of hyphae from dissimilar isolates results in imperfect fusion. Hyphae are often stained to provide greater visual distinction of the anastomosis reaction (Carling, 1996).

Rhizoctonia is a diverse genus causing seed decay, damping off, stem cankers, root rots, fruit decay, and foliar diseases in a wide variety of plant hosts including cereals, cotton,

sugarbeet, potato, vegetables, field crops, turfgrasses, ornamentals, fruit trees, and forest trees (Banniza and Rutherford, 2001; Sneh et al., 1996). All *Rhizoctonia* incited turfgrass diseases were attributed to *R. solani* prior to 1980 (Burpee and Martin, 1992; Donk, 1956). In 1980, a binucleate *Rhizoctonia* species fitting the species concept of *Rhizoctonia cerealis* van der Hoeven was isolated from ring shaped chlorotic and necrotic turfgrass (Burpee, 1980). As the species concept was more fully defined, further species pathogenic to turfgrass were identified within the genus. The most common of these diseases are those caused by the fungal pathogen *R. solani,* the causal agent of brown patch on cool season grasses and large patch on warm season grasses. Other turfgrass diseases that have been identified within the genus include leaf and sheath spot diseases caused by *R. zeae* and *Rhizoctonia oryzae* Ryker & Gooch (Ryker and Gooch, 1938), and yellow patch caused by *R. cerealis* (Burpee, 1980). Recently, a new disease, brown ring patch caused by a fungus with the teleomorph *Waitea circinata* var. *circinata* (Leiner and Carling, 1994) has been added to the genus (Toda et al., 2005). These species are genetically diverse and often require identification based on both morphological and physiological characteristics. Some key identification characteristics are summarized in Table 1.1 (Burpee and Martin, 1992; Leiner and Carling, 1994; Toda et al., 2005). Differences in fungicide sensitivity also exist between species (Elliot, 1999; Martin et al., 1984; Royals et al., 2005).

R. solani

Rhizoctonia solani, the causal agent of brown patch on turfgrass, is the most commonly known turfgrass pathogen within the *Rhizoctonia* genus as it was originally thought to be the sole species to incite turfgrass diseases within the genus. Though the genus *Rhizoctonia* has been expanded to include a greater number of species, *R. solani* is still the most commonly found turf pathogen within the genus, causing damage to at least twelve turfgrass species. Both warm and cool season turfgrass species are susceptible, with tall fescue, St. Augustinegrass (*Stenotaphrum secundatum* (Walter) Kuntze), zoysiagrass (*Zoysia* spp.) and bentgrass (*Agrostis* spp.) suffering the most damage in the U.S. *Rhizoctonia solani* is multinucleate with buff to brown hyphae greater than 5 µm in diameter (Burpee and Martin, 1992). Sclerotia are irregularly shaped and brown (Stalpers and Andersen, 1996). *Rhizoctonia solani* sub-species are numerous and are defined through hyphal anastomosis.

Table 1.1. Key morphological and physiological differences in *Rhizoctonia* species causing disease on turfgrass (adapted from (Burpee and Martin, 1992; Leiner and Carling, 1994; Toda et al., 2005).

Anamorph	***R. solani***	***R. zeae***	***R. oryzae***	***R. cerealis***	**Unknown**
Teleomorph	*Thanatephorus cucumeris*	*Waitea circinata* var. *zeae*	*W. circinata* var. *oryzae*	*Ceratobasidium cereale*	*W. circinata var. circinata*
Disease Incited	Rhizoctonia blight (brown patch)	Rhizoctonia leaf and sheath spot	Rhizoctonia leaf and sheath spot	Yellow patch	Brown ring patch[b]
Anastomosis groups	AG 1-1 A, AG 2-2 IIIB, AG 4, AG 5	WAG-Z	WAG-O	AG-D (CAG-1)	WAG
Nuclear count	multinucleate	multinucleate	multinucleate	binucleate	multinucleate
Colony color	buff to brown	white to salmon	white to salmon	white to buff	white to salmon
Temperature Optimum	18-28 °C	~32 °C	~32 °C	~23 °C	~30 °C
Phenol reaction	light brown	dark brown	dark brown		

R. zeae and R. oryzae

Rhizoctonia oryzae and *R. zeae* produce similar symptoms, have the same optimal growing temperature, and are often grouped together as Rhizoctonia leaf and sheath spot (Martin and Lucas, 1983; Haygood and Martin, 1990). Symptoms are difficult to distinguish from those induced by *R. solani*, and often cannot be distinguished without observation in culture. Like *R. solani*, *R. zeae* and *R. oryzae* create a rapidly increasing brown to tan patch of blighted grass. A darkened brown to purple periphery, referred to as a smoke ring, is more likely to occur in *R. solani* infections, though the ring may occasionally be present during infections by *R. zeae* or *R. oryzae* (Smiley et al., 2005).

Rhizoctonia oryzae and *R. zeae* have an optimum growth temperature of 33°C (Ryker and Gooch, 1938). In culture, hyphae are 4 to 10 µm wide and white to salmon in color. *Rhizoctonia oryzae* produces salmon colored sclerotia that vary in size between less than 1mm to greater than 3 mm in diameter. Sclerotia form imbedded on the media surface and are irregularly shaped. *Rhizoctonia zeae* produces sclerotia that are more uniform in size and shape between 0.5 and 1 mm in diameter and spherical. These are frequently formed beneath the surface of the media and are typically more numerous than sclerotia formed by *R. solani* (Burpee and Martin, 1992).

R. cerealis

Rhizoctonia cerealis infection symptoms are distinct from those of *R. solani*, showing extended chlorosis without the necrosis seen in *R. solani* infections. *Rhizoctonia cerealis* also prefers a cooler temperature for disease development compared to *R. solani*, thus the reference to *R. cerealis* as cool-weather brown patch prior to its distinction from *R. solani* (Sanders et al., 1978). In culture, hyphae of *R. cerealis* are very similar to those of *R. solani* with the exception of *R. cerealis*' binucleate nature. The two may be differentiated through anastomosis grouping as well as nuclear staining. *Rhizoctonia cerealis* forms sclerotia that are 0.3 to 1.2 mm in diameter and white to yellow to dark brown in color (Burpee, 1980).

Waitea circinata var. circinata

A fungus with the teleomorph *Waitea circinata var. circinata* was discovered in Alaska in 1994 (Leiner and Carling, 1994). In 2005, this fungus was isolated from brown rings on bentgrass putting greens in Japan and the name brown ring patch was proposed (Toda et al.,

2005). Symptoms of infections occurring in the western United States include yellow rings surrounding healthy turf that are similar in appearance to yellow patch. These alternate expressions of symptoms have brought the name brown ring patch, also called *Waitea* patch by some, under dispute. Further naming disputes continue concerning the anamorphic and teleomorphic name and its distinction from the other turf pathogenic *Rhizoctonia* species (de la Cerda et al., 2007).

Waitea circinata var. circinata is multinucleate and forms orange to dark brown globose sclerotia up to 2 mm in diameter. Hyphae are white to orange in color with a diameter ranging from 3.9 to 10.0 μm. *Waitea circinata* var. *circinata* can anastomose with both *R. oryzae* and *R. zeae*. All three species, *R. zeae, R. oryzae*, and *Waitea circinata var. circinata*, are categorized as having *Waitea circinata* teleomorphs (Leiner and Carling, 1994). The inconsistency in anamorph name for these three has been contested and possible alternative categorization of anamorph and teleomorph names are summarized in Table 1.2 (de la Cerda et al., 2007; Leiner and Carling, 1994).

Breeding Efforts for Disease Resistance

Growing concern over environmental problems associated with excessive pesticide use, along with pesticide resistance concerns and the cost of purchasing and applying these products, has led to an increased public interest in cultivars bred for disease resistance (Bonos et al., 2006). Even with continued efforts and improvements in resistance breeding, tall fescue cultivars with a consistent, acceptable amount of brown patch resistance are rare. Disease ratings taken by evaluators participating in the National Turfgrass Evaluation Program (NTEP) are made visually using an ordinal 1-9 scale with 1 representing complete disease and 9 representing no disease (Morris, 2004). Of the tall fescue cultivars observed for brown patch resistance through NTEP in 2002, the top ten cultivars received a disease rating of 8.7 or above in at least one of the states in which a trial was established. However, the resistance response of these cultivars was highly variable across locations, with disease ratings as low as 4 and as high as 9 being recorded for the same cultivar rated at different locations (Table 1.3). A number of influences may be contributing to the high variability in brown patch disease resistance observed among currently available cultivars. Two factors that have been identified as possible contributors are: *R. zeae*

Table 1.2. Proposed anamorph and teleomorph names for turf pathogenic fungi with the teleomorph *Waitea circinata* in response to the characterization of a turf pathogenic fungus with the teleomorph *Waitea circinata* var. *circinata* and an uncharacterized anamorph.

Teleomorph	***Waitea circinata* var. *zeae***	***W. circinata* var. *oryzae***	***W. circinata var. circinata***
Anamorph (current)	*R. zeae*	*R. oryzae*	unknown
Anamorph (alternative 1)	*R. circinata var. zeae*	*R. circinata var. oryzae*	*R. circinata var. circinata*
Anamorph (alternative 2)	*R. zeae*	*R. oryzae*	*R. circinata*

Table 1.3. Variability in brown patch disease ratings across locations for ten of the top ranked tall fescue cultivars in the 2002- 2005 NTEP trials. Disease ratings performed using a scale of 1-9 with 1 representing complete disease and 9 representing healthy turfgrass.

	AR1	GA1	IL2	IN1	MA1	MD1	MO1	NJ1	NJ2	OK1	PA1	VA1	WI1	MEAN
REBEL IV (R-4)	7.2	6.3	5.2	8	8.7	9	4	5.6	6.2	7	8.1	8.7	8	6.8
TAR HEEL II (PST-5TR1)	7.5	6	4.8	7	8	9	5.3	5.9	6	7.7	8.3	8.3	8.3	6.8
MAGELLAN (OD-4)	7.5	6.3	5.3	8.7	8.3	8.7	6.3	5	6.2	7.3	7.8	8	8	6.8
TITANIUM (SBM)	7	6.3	6.5	8	8.3	8.7	4.3	5.6	5.8	8	8	7.7	8.3	6.8
KY-31 E+	8.3	7	6.3	8.7	8.7	9	6	5.8	4.6	7	7.8	8.7	8	6.8
TAR HEEL	7.5	6.7	5.2	8	9	8.7	5.3	6.1	5.3	6.7	8.1	8	8.3	6.8
FINELAWN ELITE (DLSD)	7	6.3	5.7	6.7	6	8.7	6.3	6.1	6	7.3	7.9	8.3	8.7	6.8
MUSTANG 3	7.3	6.7	6	8.3	8.3	9	5	4.9	6	7.7	7.8	7.7	8	6.7
PADRE (NJ4)	7.3	6.3	5.7	8.3	8.7	8	5.7	5.4	6.1	6.3	7.8	6.3	8.3	6.7
INNOVATOR (PST-5KI)	7.2	6.3	5.7	8.3	8.7	9	4.7	5.2	5.2	7.7	8.1	8.3	8.3	6.7
For All Cultivars by location														
LSD VALUE[a]	2.6	1.3	2.6	1.5	2.1	0.9	1.8	1.9	1.5	1.6	1.6	2.4	0.9	0.8
C.V. (%)[b]	24	12.7	33.5	12.1	16.4	6.4	22.6	25	21.5	15.1	14.3	21.4	6.7	18.8

[a]To determine statistical differences among entries, subtract one entry's mean from another entry's mean. Statistical differences occur when this value is larger than the corresponding LSD value (LSD 0.05)
[b]C.V. (Coefficient of Variation) indicates the percent variation of the mean in each column.

artificially inflating disease ratings by producing symptoms similar to brown patch and disease ratings taken using subjective visual evaluation methods.

Screening for resistance in grasses that are seed propagated and cross pollinated, such as tall fescue, is accomplished through phenotypic or genotypic recurrent selection (Bonos et al., 2006). Using phenotypic plant selection, a germplasm collection is subjected to environmental stresses in accordance with the breeding objective and plants exhibiting superior performance are selected visually. This initial selection is usually followed by a progeny test in which the superior plants are crossed with a common tester genotype or a combination of testers. The practice of single plant selection is common in the initial screening process. Superior genotypes, once identified, are then crossed to produce progeny with improved expression of the desired characteristic. This process of screening and crossing, known as recurrent selection, continues as long as improved genotypes are being produced. Genotypic recurrent selection, which is based on progeny performance, may also be used. This is typically used when more complex characteristics are being improved. Phenotypic recurrent selection is more appropriate for characteristics such as disease resistance where phenotype can accurately identify superior genotypes (Bonos et al., 2006; Sleper and Poehlman, 2006).

Phenotypic plant selection for brown patch resistance in tall fescue uses the pathogen *R. solani* as an environmental stressor in identifying superior genotypes. Once these genotypes have been established as cultivars they are evaluated under field conditions in relation to other cultivars in programs such as the NTEP trials. During these field trials, other pathogens such as *R. zeae*, which causes nearly identical symptoms to those caused by *R. solani*, may cause symptoms that are included as brown patch when evaluating disease severity. Since the optimal growing temperature for *R. zeae* is higher than *R. solani,* geographical distribution of these two pathogens may differ. This may explain some of the variability in cultivar resistance between states.

In southern regions, *R. zeae* is thought to be the dominant *Rhizoctonia* pathogen, while *R. solani* is thought to be dominant in northern regions (Elliot, 1999). However, higher than expected frequencies of *R. zeae* isolations have been reported within transition zone states, including New Jersey, South Carolina, and Virginia (Martin et al., 2001; McCall, 2006; Plumley, 1988). Martin et al. (2001) reported significant differences in isolation frequency of *R. zeae* and *R. solani* between two locations in South Carolina. Comparing *R. solani* to *R. zeae* frequency, *R.*

zeae was more frequently isolated at the Clemson location, while *R. solani* was more frequently isolated at the Florence location. A 2006 study in Virginia also showed variation in the frequency of *R. zeae* isolations by location. In this study isolates were collected across the state of Virginia from tall fescue, Kentucky bluegrass (*Poa pratensis* L.), creeping bentgrass (*Agrostis stolonifera* L.), and bermudagrass (*Cynodon dactylon* (L.) Pers.) showing symptoms of *Rhizoctonia* disease (McCall, 2006). These were then identified as either *R. zeae* or not *R. zeae*. Geographical distribution of these isolates showed *R. zeae* to be more prevalent in the Eastern part of the state. Isolates that were not identified as *R. zeae* were not further identified as *R. solani* or any other *Rhizoctonia*. Differences in the geographical distribution between *R. solani* and *R. zeae*, combined with the similarity of symptoms they exhibit on tall fescue, may cause variability in the disease ratings taken from multiple locations for cultivars bred only for resistance to *R. solani*.

Disease Evaluation

Subjective Disease Evaluation Methods

The currently accepted method for turfgrass disease evaluation may also be a factor affecting the consistency in the resistance response of available brown patch resistant tall fescue cultivars. There are many methods for measuring or estimating disease. In an effort to provide consistency when presenting results, evaluators have tried to standardize their rating methods with systems such as the Horsfall-Barratt, or logarithmic, scale, various ordinal scales, and percentage scales.

The Horsfall-Barratt method was developed in 1945 and is based on the idea that grades should be based on "equal ability to distinguish, not on equal disease" (Horsfall and Barratt, 1945). In this method, grades are broken into 12 unequal scales with greater accuracy required for very small and very large disease severity and less accuracy required for disease severity between 25% and 75% (Horsfall and Barratt, 1945). The accuracy of this method compared to direct percent disease assessment has been questioned by several authors (Forbes and Korva, 1994; Nita et al., 2003). Although the Horsfall-Barratt scale is logarithmic, Forbes and Korva found that raters tended to linearize the scale, treating scale units as if they had approximately equal intervals. Disease evaluated in-field using estimated percent disease and later converted

to a Horsfall-Barratt scale was significantly more accurate and precise compared to disease evaluated in-field using a Horsfall-Barratt scale (Forbes and Korva, 1994).

Various ordinal scales are also used for evaluating disease. These can vary by the disease, host plant, or plant part being researched. Different scales may also be used on studies of the same disease and host making it difficult to compare results across studies. The National Turfgrass Evaluation Program (NTEP), the largest turfgrass evaluation program in the United States, evaluates various turfgrass characteristics using a standardized 1-9 ordinal scale. In this scale, 1 represents the least desirable characteristic and 9 represents the most desirable characteristic possible (Morris, 2004). Even a standardized scale such as this can be problematic when people interpret the categories within it differently. A ranking of 9 may represent an idealized best and 1 and idealized worst, or 9 may represent the best within that trial that day and 1 the worst within that trial that day. While ranking using these two different interpretations may be the same, the information they portray is no longer standardized and the comparison of trial results across multiple locations becomes limited.

In turfgrass research, a percentage scale is also common. A percentage scale is less open to interpretation allowing more accurate comparisons of results by providing a uniform rating system across studies. However, none of these scales can eliminate the variability inherent in visual ratings due to their subjective nature.

A study on the assessment of visual evaluation techniques done by Horst et al. (1984) showed visual assessment to be inadequate at evaluating turf quality and density. Ten evaluators took quality and density ratings of ten cultivars of Kentucky bluegrass and tall fescue grown in Oregon in 1980 and Texas in 1981. There were significant differences among evaluator ratings and rankings. These inconsistencies suggest that the criteria used for evaluation was inconsistent among evaluators and that the criteria each evaluator did use did not remain consistent throughout the study. Studies performed by Nutter Jr. et al. (1993) on visual assessment of dollar spot severity in creeping bentgrass showed similar results with significant variation in both intra-rater repeatability (variability within ratings performed by a single evaluator over multiple assessments) and inter-rater reliability (variability within ratings performed by multiple evaluators on a single assessment). These inconsistencies bring into question the reliability of regional and national testing program data in which visual ratings are used as the primary method of disease resistance evaluation.

Though the study by Horst et al. was done more than 20 years ago, turfgrass is still evaluated using the same visual evaluation method assessed as lacking accuracy and precision by this and other, more recent, studies (Nutter Jr. et al., 1993; Richardson et al., 2001). Further complications brought about by using a visual scale lie in the statistical test used to distinguish significant differences in treatments. Many evaluators distinguish significant differences between treatments using a one-way analysis of variance, a statistical test that assumes a continuous variable, not an ordinal variable.

Visual evaluation is a preferred disease evaluation method because it is quick, easy, and inexpensive. More objective evaluation methods, such as line intersect analysis (LIA), multispectral radiometry, and digital image analysis (DIA), could reduce the intra-rater and inter-rater variability of subjective visual evaluations. Until now, high equipment costs and excessive time inputs have limited the economic feasibility of these alternatives. Reductions in equipment prices and improved methods have increased interest in developing more objective alternatives to visual evaluation.

Objective Disease Evaluation Methods

Line intersect analysis is performed using a grid system set over a plot where the characteristic to be measured is evaluated at each intersection of the grid. The accuracy of this system is dependent on the extent of the grid used. Although this type of evaluation is less variable than visual evaluation, studies done by Richardson et al. (2001) found LIA to be 20 times more variable than DIA when used to determine turfgrass cover. This method is effective, however it is time and labor intensive compared to DIA and visual evaluation.

Variation in evaluator rankings and results may be due to a number of factors, including different wavelength perception among individuals, eye strain, or fatigue. Multispectral radiometry is a method that removes this bias by using a device that can consistently measure reflectance values. Disease assessments measure reflectance in the visible and near infrared (NIR) spectrum. As plants become stressed and chlorophyll content decreases, light reflectance in the visible spectrum increases. NIR reflectance values decrease as the cells deep within the leaf degenerate. Since reduction in NIR reflectance is an early sign of plant stress, this method can detect possible disease onset. However, this method is unable to differentiate between biotic and abiotic stressors and a trained evaluator is necessary to confirm infection is by a pathogen.

This method also cannot differentiate between pathogens when the cause is biotic. Equipment costs are high using this method compared to visual evaluation (Richardson et al., 2001). In turfgrass disease evaluation, multispectral radiometry's effectiveness has been assessed at evaluating *Rhizoctonia* blight on creeping bentgrass. Although percent reflectance did decrease as visual disease ratings increased, linear regression of visual disease severity ratings and percent reflectance explained less than fifty-five percent of the variability in each of three experiments (Raikes and Burpee, 1998).

Digital image analysis (DIA), like multispectral radiometry, removes the bias of visual evaluation. This option is less expensive than multispectral radiometry and can evaluate more characteristics. However, it is also limited by its inability to distinguish between different diseases and between biotic and abiotic stress. Using this method, disease is evaluated using a digital image of the subject that is then analyzed using computer software. A number of software programs have been used for DIA of various plant characteristics including SigmaScan (Systat Software Inc., Richmond, CA)(Karcher and Richardson, 2003; Karcher and Richardson, 2005; Niemira et al., 1999; Olmstead and Lang, 2001; Richardson et al., 2001), Scion Image software (Scion Corporation, Frederick, MD)(Wijekoon et al., 2008), Matrox Inspector (Matrox Electronic Systems, Dorval, Quebec, Canada) (Kwack et al., 2005), and Assess (APS Press, St. Paul, MN) (Bock et al., 2008). These programs use the number, hue, saturation, intensity, and location of pixels within an image to calculate image characteristics. For disease, a spectral range is chosen to represent healthy leaf tissue while another spectral range is selected to represent diseased tissue. Percent disease is determined from the ratio of pixels classified as diseased to pixels classified as healthy.

DIA is becoming more common in automating quality control in both agronomic and trade industries. It has provided an accurate and rapid method for determining wood failure percentages in plywood using the contrast of wood to glue (Zink and Kartunova, 1998). Continued work is also being done using DIA to evaluate in vitro stored plants in a non-destructive manner, a task that until now has been both tedious and subjective (Aynalem et al., 2006). Human and plant pathological endeavors are also benefiting from DIA. It has been used in screening for late blight susceptibility in potato tubers as well as monitoring liver fibrosis in patients with chronic hepatitis C (Lazzarini et al., 2005; Niemira et al., 1999). In these studies,

digital analysis alone or combined with visual evaluation was found to be an accurate and preferable evaluation method compared to subjective visual evaluations alone.

Applications for DIA techniques are becoming more numerous; however, research into possible uses in turfgrass evaluation has been limited. DIA has been quantified as accurately assessing disease severity on numerous agricultural and horticultural crops (Lindow and Webb, 1983). In turfgrass research, the accuracy of DIA has been quantified in evaluating turfgrass color and percent cover (Karcher and Richardson, 2003; Richardson et al., 2001). Digital image analysis has also been successful at detecting dollar spot disease severity and was able to produce a disease progress curve not significantly different from a disease progress curve produced using counts of dollar spot foci (Horvath and Vargas, 2005). A quantification of DIA's accuracy at evaluating turfgrass disease has not been performed.

Some DIA studies have relied on comparison of visual evaluations to DIA evaluations to calibrate and determine the effectiveness of these techniques. This method of calibration is inherently flawed as visual ratings are subjective and may be inaccurate (Zink and Kartunova, 1998). Calibrating DIA to visual evaluations creates a method that is fast and consistent, however it limits the accuracy for which DIA has the potential since it is calibrated to a subjective evaluation. Calibration studies have also assessed the accuracy of DIA by physically determining percent disease and comparing these values to values obtained using DIA. In this manner, the accuracy of DIA at evaluating plant disease has been quantified on a number of plants with varying leaf and lesion shapes (Lindow and Webb, 1983).

Lindow and Webb (1983) assessed DIA's accuracy at evaluating disease on leaves of varying shapes and sizes. A digital video camera was used to capture and digitize images that were then converted to grayscale. Actual disease values were determined physically by tracing necrotic areas on enlarged photographs using a planimeter. DIA showed high correlations to actual disease values in leaves of pinto beans ($\rho = 0.99$.), California buckeye ($\rho = 0.97$), sycamore ($\rho = 0.99$), tomato ($\rho = 0.97$), and bracken fern ($\rho = 0.98$).

In turfgrass research, DIA's accuracy at evaluating turfgrass cover and color has been quantified. Studies in turfgrass evaluation by Richardson et al. in 2001 calibrated DIA values to known areas of cover. 'Tifway' bermudagrass plugs of a known diameter were set against a soil background and images were taken using a digital camera and saved as JPEGs. Sixteen plots containing a range of 1-16 plugs were evaluated creating a percent cover range of 0.75 – 12%.

The images were processed using SigmaScan with a hue range set at 57 – 107 and a saturation range from 0 – 100 to select green tissue and from the ratio of green pixels to total pixels, percent cover was calculated. This calibration study showed DIA percent cover predictions to be closely correlated to actual percent cover values ($r^2 = 0.99$) with a slope of 1.01 and an intercept near 0. Once the accuracy of DIA was quantified in the calibration study, DIA, LIA, and subjective analysis (SA) were compared. Of these three evaluation techniques, variability in SA was 152 times greater than DIA and LIA was 20 times more variable than DIA (Richardson et al., 2001).

Turfgrass color is another area in which DIA is being introduced as an alternative to subjective visual evaluations. A study performed by Karcher and Richardson in 2003 assessed the ability of digital image analysis to quantify visual color differences among turf plots due to nitrogen treatments. Colors were calibrated by taking digital images of color chips from Munsell Color Charts for Plant Tissues (GretagMacbeth LLC, New Windsor, NY). RGB values were converted to hue, saturation, and brightness values. Calibration results showed hue and saturation values to be statistically equal to actual values. Brightness was slightly less accurate but could be corrected with a formula. To evaluate the efficacy of DIA at evaluating turfgrass color, nitrogen treatments were applied to both zoysiagrass and creeping bentgrass plots. Images were evaluated based on hue, saturation, and brightness. Results showed no significant differences among saturation and brightness values, though hue values were significantly affected by the nitrogen treatments applied to the zoysiagrass plots. All values were affected by the nitrogen treatment applied to creeping bentgrass plots (Karcher and Richardson, 2003).

While both of these studies effectively used DIA to evaluate various turfgrass characteristics, turfgrass pathologists have been reluctant to use DIA in disease evaluation. Research reported by Horvath and Vargas (2005) evaluated DIA as a method for measuring dollar spot disease parameters and compared dollar spot foci counts to DIA estimates of disease severity as a means to measure disease progress. Throughout the 2001 season, images were taken of two 0.3 m^2 areas, one of creeping bentgrass and the other of annual bluegrass. Assess image analysis software (APS Press, St. Paul, MN) was used to evaluate percent disease severity. The number of dollar spot foci were counted three times per week from June through September and the disease progress curve generated from these values was compared to that generated by the values obtained using Assess. Dollar spot foci counts and DIA disease severity values were weakly related using regression analysis. Since individual dollar spots vary in size, especially as

disease severity increases and spots coalesce, dollar spot foci counts and total disease area were weakly related. Disease progress curves obtained using DIA and visual evaluations were similar and not statistically different from one another ($p < 0.13$). Results from this study suggest DIA can effectively distinguish disease on turfgrass and may provide a less time consuming method for evaluating disease progress curves of dollar spot infections comparing to dollar spot foci counts (Horvath and Vargas, 2005).

DIA has been quantified as accurately assessing disease on plants with varied leaf size and shape. DIA has also been quantified as accurately assessing turfgrass cover and turfgrass color and has been effective at distinguishing the disease dollar spot on turfgrass and tracking the disease progress curve of a dollar spot infection. These studies suggest DIA may be an effective evaluation method for estimating brown patch disease severity on tall fescue.

Objectives

The objective of this study is to reduce the variability observed in the brown patch resistance response of currently available cultivars through the following objectives and sub-objectives:

1) Develop a digital image analysis method to objectively determine disease severity of brown patch on greenhouse grown tall fescue.
    a. Quantify and compare DIA methods
    b. Compare DIA and visual evaluation methods
2) Use digital image analysis to evaluate the resistance response of tall fescue germplasm to both *R. solani* and *R. zeae.*
    a. Use DIA to perform an initial screening of plant accessions
    b. Use DIA to perform a screen of 20 seeds, each maintained as a genetic clone, from plant accessions showing good resistance in the initial screen.

Literature Cited

Anderson, N.A. 1982. The genetics and pathology of *Rhizoctonia solani*. Annual Review of Phytopathology 20:329-347.

Aynalem, H.M., T.L. Righetti, and B.M. Reed. 2006. Non-destructive evaluation of *in vitro*-stored plants: a comparison of visual and image analysis. In Vitro Cellular and Developmental Biology 42:562-567.

Banniza, S., and M.A. Rutherford. 2001. Diversity of isolates of *Rhizoctonia solani* AG-1 1A and their relationship to other anastomosis groups based on pectic zymograms and molecular analysis. Mycological Research 105:33-40.

Bock, C.H., P.E. Parker, A.Z. Cook, and T.R. Gottwald. 2008. Visual rating and the use of image analysis for assessing different symptoms of citrus canker on grapefruit leaves. Plant Disease 92:530-541.

Bonos, S.A., B.B. Clarke, and W.A. Meyer. 2006. Breeding for disease resistance in the major cool-season turfgrasses. Annual Review of Phytopathology 44:213-234.

Burpee, L., and B. Martin. 1992. Biology of Rhizoctonia species associated with turfgrasses. Plant Disease 76:112-117.

Burpee, L.L. 1980. *Rhizoctonia cerealis* causes yellow patch of turfgrasses. Plant Disease 64:1114-1116.

Carling, D.E. 1996. Grouping in *Rhizoctonia solani* by hyphal anastomosis reaction, p. 37-47, *In* B. Sneh, et al., eds. *Rhizoctonia* Species: Taxonomy, Molecular Biology, Ecology, Pathology and Disease Control. Kluwer Academic Publishers, Dordrecht.

de la Cerda, K.A., G.W. Douhan, and F.P. Wong. 2007. Discovery and characterization of *Waitea circinata* var. *circinata* affecting annual bluegrass from the western United States. Plant Disease 91:791-797.

Donk. 1956. Notes on resupinate Hymenomycetes-II. The tulasnelloid fungi. Reinwardtia 3:363-379.

Elliot, M.L. 1999. Comparison of *Rhizoctonia zeae* isolates from Florida and Ohio turfgrass. HortScience 34:298-300.

Forbes, G.A., and J.T. Korva. 1994. The effect of using a Horsfall-Barratt scale on precision and accuracy of visual estimation of potato late blight severity in the field. Plant Pathology 43:675-682.

Horsfall, J.G., and R.W. Barratt. 1945. An improved grading system for measuring plant diseases. Phytopathology 35:655.

Horvath, B.J., and J.M. Vargas. 2005. Analysis of dollar spot disease severity using digital image analysis. International Turfgrass Society Research Journal 10:196-201.

Karcher, D.E., and M.D. Richardson. 2003. Quantifying turfgrass color using digital image analysis. Crop Science 43:943-951.

Karcher, D.E., and M.D. Richardson. 2005. Batch analysis of digital images to evaluate turfgrass characteristics. Crop Science 45:1536-1539.

Kwack, M.S., E.N. Kim, H. Lee, K.D. Kim, J.-W. Kim, and S.-C. Chun. 2005. Digital image analysis to measure lesion area of cucumber anthracnose by *Colletotrichum orbiculare*. Journal of General Plant Pathology 71:418-421.

Lazzarini, A.L., R.A. Levine, R.J. Ploutz-Snyder, and S.O. Sanderson. 2005. Advances in digital quantification technique enhance discrimination between mild and advanced liver fibrosis in chronic hepatitis C. Liver International 25:1142-1149.

Leiner, R.H., and D.E. Carling. 1994. Characterization of *Waitea circinata* (*Rhizoctonia*) isolated from agricultural soils in Alaska. Plant Disease 78:385-388.

Lindow, S.E., and R.R. Webb. 1983. Quantification of foliar plant disease symptoms by microcomputer-digitized video image analysis. Phytopathology 73:520-524.

Martin, S.B., C.L. Campbell, and L.T. Lucas. 1984. Response of *Rhizoctonia* blights of tall fescue to selected fungicides in the greenhouse. Phytopathology 74:782-785.

Martin, S.B., S.N. Jeffers, and A. Rogers. 2001. Isolation frequency and pathogenicity of Rhizoctonia species from tall fescue crown and leaf tissues from two locations in South Carolina. International Turfgrass Society Research Journal 9:689-694.

McCall, D.S. 2006. Influence of isolate, cultivar, and heat stress on virulence of *Rhizoctonia zeae* on tall fescue, Virginia Polytechnic Institute and State University, Blacksburg.

Morris, K.N. 2004. A Guide to NTEP Turfgrass Ratings [Online]. Available by NTEP http://www.ntep.org/reports/ratings.html (posted April 16, 2004; verified March 31, 2009).

NASS. 2004. Virginia's Turfgrass Industry. Virginia Office of the National Agricultural Statistics Service.

Niemira, B.A., W.W. Kirk, and J.M. Stein. 1999. Screening for late blight susceptibility in potato tubers by digital analysis of cut tuber surfaces. Plant Disease 83:469-473.

Nita, M., M.A. Ellis, and L.V. Madden. 2003. Reliability and accuracy of visual estimation of Phomopsis leaf blight of strawberry. Phytopathology 93:995-1005.

Nutter Jr., F.W., M.L. Gleason, J.H. Jenco, and N.C. Christians. 1993. Assessing the accuracy, intra-rater repeatability, and inter-rater reliability of disease assessment systems. Phytopathology 83:806-812.

Olmstead, J.W., and G.A. Lang. 2001. Assessment of severity of powdery mildew infection of sweet cherry leaves by digital image analysis. HortScience 36:107-111.

Piper, C.V., and H.S. Coe. 1919. *Rhizoctonia* in lawns and pastures. Phytopathology 9:7.

Plumley, K.A. 1988. *Rhizoctonia* spp. associated with golf course turfgrass in southern New Jersey. Phytopathology 78:1510.

Raikes, C., and L.L. Burpee. 1998. Use of multispectral radiometry for assessment of *Rhizoctonia* blight in creeping bentgrass. Phytopathology 88:446-449.

Richardson, M.D., D.E. Karcher, and L.C. Purcell. 2001. Quantifying turfgrass cover using digital image analysis. Crop Science 41:1884-1888.

Royals, J.K., S.B. Martin, J.J. Camberato, and S.N. Jeffers. 2005. Development and evaluation of strategic fungicide programs for control of warm weather diseases in creeping bentgrass. International Turfgrass Society Research Journal 10:237-246.

Ryker, T.C., and F.S. Gooch. 1938. Rhizoctonia sheath spot of rice. Phytopathology 28:233-246.

Sanders, P.L., L.L. Burpee, and R.T. Sherwood. 1978. Preliminary studies on binucleate turfgrass pathogens that resemble *Rhizoctonia solani.* Phytopathology 68:145-148.

Sleper, D.A., and J.M. Poehlman. 2006. Breeding of Field Crops. 5th ed. Blackwell Publishing, Ames.

Smiley, R.W., P.H. Dernoeden, and B.B. Clarke. 2005. Compendium of Turfgrass Diseases. 3rd ed. APS Press, St. Paul.

Sneh, B., S. Jabaji-Hare, S. Neate, and G. Dijst. 1996. Rhizoctonia species: Taxonomy, Molecular Biology, Ecology, Pathology and Disease Control Kluwer Academic Publishers, Dordrecht.

Stalpers, J.A., and T.F. Andersen. 1996. A synopsis of the taxonomy of teleomorphs connected with *Rhizoctonia* S.L., p. 49-63, *In* B. Sneh, et al., eds. Rhizoctonia Species: Taxonomy,

Molecular Biology, Ecology, Pathology and Disease Control. Kluwer Academic Publishers, Dordrecht.

Toda, T., T. Mushika, T. Hayakawa, A. Tanaka, T. Tani, and M. Hyakumachi. 2005. Brown ring patch: a new disease on bentgrass caused by *Waitea circinata* var. *circinata*. Plant Disease 89:536-542.

Voorhees, R.K. 1934. Sclerotial rot of corn caused by *Rhizoctonia zeae*, N. SP. Phytopathology 24:1290-1303.

Wijekoon, C.P., P.H. Goodwin, and T. Hsiang. 2008. Quantifying fungal infection of plant leaves by digital image analysis using Scion Image Software. Journal of Microbiological Methods 74:94-101.

Zink, A.G., and E. Kartunova. 1998. Wood failure in plywood shear samples measured with image analysis. Forest Products 48:69-74.

Chapter 2

Quantifying the accuracy of digital image analysis in assessing percent disease severity of *Rhizoctonia solani* on *Festuca arundinacea*

Introduction

Brown patch is caused by the fungus *Rhizoctonia solani* and is both a common and destructive disease on turfgrass. This disease is especially problematic on cool season grasses grown in the transition zone. In Eastern Virginia, this disease is a major problem on tall fescue, reducing aesthetic appeal and increasing chemical, monetary, and labor inputs. Many cultivars bred for brown patch resistance are available, however evaluations of the resistance response of these cultivars vary across multiple locations (NTEP, 2005). A possible cause of this variation is the visual evaluation system used to assess the resistance response of tall fescue cultivars to brown patch.

Visual evaluation, using an ordinal scale or a percentage scale, is a standard method for evaluating turfgrass disease. While this method is quick and easy, its accuracy and precision have been questioned due to the subjective nature of visual evaluations (Horst et al., 1984; Nutter Jr. et al., 2006; Nutter Jr. et al., 1993). Digital image analysis (DIA) is an alternative method to visual evaluation that removes the subjectivity of visual evaluation and may offer a more accurate and precise evaluation method.

Digital image analysis has been shown to accurately assess disease severity on numerous agricultural and horticultural crops (Lindow and Webb, 1983). In turfgrass research, DIA has been successful at detecting the disease dollar spot and disease progress curves formed using DIA evaluations showed no significant difference from disease progress curves formed using physical counts of dollar spot foci (Horvath and Vargas, 2005). The accuracy of DIA has been quantified in evaluating turfgrass color and percent cover (Karcher and Richardson, 2003; Richardson et al., 2001). A quantification of DIA's accuracy at evaluating percent disease severity on turfgrass has not been performed.

To accurately assess the effectiveness of DIA as a disease evaluation method, the true disease value must be known and compared to the DIA estimated value. A number of methods

have been used to determine actual values in order to quantify the accuracy of an evaluation method.

In assessments of actual percent disease, necrotic areas have been visually selected and then physically measured to improve accuracy over a visual estimation of percent disease. Nita et al. (2003) determined actual disease values of Phomopsis leaf blight on strawberry leaflets by photographing infected leaflets, cutting the leaflet from the image and weighing it, and then cutting the necrotic area from the image and weighing it. Percent disease was calculated as a ratio of the necrotic area weight to the total leaf weight.

James et al. (1971) created a set of diagrammatic keys with actual disease values listed for black and white images portraying a wide range of disease severity on numerous host and disease combinations. Disease values were measured by drawing leaf images on Cronaflex media and measuring diseased areas using an IBM drum scanner.

In evaluating turfgrass cover, quantification was done by taking established turfgrass plugs of a known diameter and placing these on a bed of bare soil. Percent cover was determined using a ratio of physical measurements of the area of the turfgrass plugs to the area of bare soil (Richardson et al., 2001).

A number of software programs have been used for DIA of various plant characteristics including SigmaScan (Systat Software Inc., Richmond, CA)(Karcher and Richardson, 2003; Karcher and Richardson, 2005; Niemira et al., 1999; Olmstead and Lang, 2001; Richardson et al., 2001), Scion Image software (Scion Corporation, Frederick, MD)(Wijekoon et al., 2008), Matrox Inspector (Matrox Electronic Systems, Dorval, Quebec, Canada) (Kwack et al., 2005), and Assess (APS Press, St. Paul, MN) (Bock et al., 2008). These programs range in the number of characteristics they can evaluate, ease of use, and cost.

The objective of this chapter is to quantify the accuracy of DIA in evaluating brown patch lesions on individual leaves of tall fescue.

Materials and Methods

Disease Range Preparation

Healthy, fully developed tall fescue leaves and completely necrotic tall fescue leaves infected with *R. solani* were cut to a length of 40 mm. Leaf tips were removed to provide a consistent width along the length of the blade though width varied between blades from 4.5 mm to 6.5 mm. *Rhizoctonia solani* infected tissue from tall fescue leaves and healthy tissue from tall fescue leaves were cut to a length of 5.5 mm and width of 2 mm using a rectangular hole punch. All measurements were taken with a Helix office ruler (model 15015, Helix USA, Ltd., Bensenville, IL). 3M Spray Mount (3M Industrial Adhesives and Tapes Division, St. Paul, MN) was used to attach rectangles of lesioned tissue to healthy leaf blades and rectangles of healthy leaf tissue to completely diseased leaf blades.

In Experiment 1, evaluations were performed on healthy leaves containing 0, 1, 2, 3, and 4 rectangles of necrotic tissue to emulate disease values of 0, 5.5%, 11%, 16.5%, and 22% (Figure 2.1). Actual disease values varied according to blade width. Each disease value was replicated four times.

In Experiment 2, a wider range of disease values was evaluated by placing 0, 4, 9, and 13 rectangles of lesioned tissue on healthy leaves to emulate disease values of 0%, 22%, 49.5%, and 71.5% (Figure 2.2). To emulate disease values of 83.5%, 78%, and 72.5% disease, 3, 4, and 5 rectangles of healthy leaf tissue were placed on completely diseased leaves (Figure 2.3). A completely lesioned leaf was used to create a leaf with 100 percent disease. Actual disease values varied according to blade width. Each disease value was replicated five times.

Disease Evaluation

Disease value measurements were calculated both physically and through the use of Digital Image Analysis (DIA). Physical measurements were taken of the total leaf area and healthy or lesioned rectangle area in mm^2. Actual percent disease was calculated as the ratio of lesion area to total leaf area. DIA was performed on leaves prepared using three different methods: 4 mil thick Hammermill transparency film (International Paper Company, Memphis, TN) with leaves attached using 3M Spray Mount (TF), Boise X-9 white printer paper with a brightness level of 90 (Boise Cascade LLC, Boise, ID) with leaves attached using 3M Spray Mount (PP), and a

Figure 2.1. Scanned images of healthy leaf blades with varying numbers of rectangles of lesioned tissue used to create known disease values of approximately 0-22% disease (approximate percent disease is indicated below each leaf blade). Images are of the three preparation methods used in experiment 1: transparency film (A), printer paper (B), and cover sheet (C).

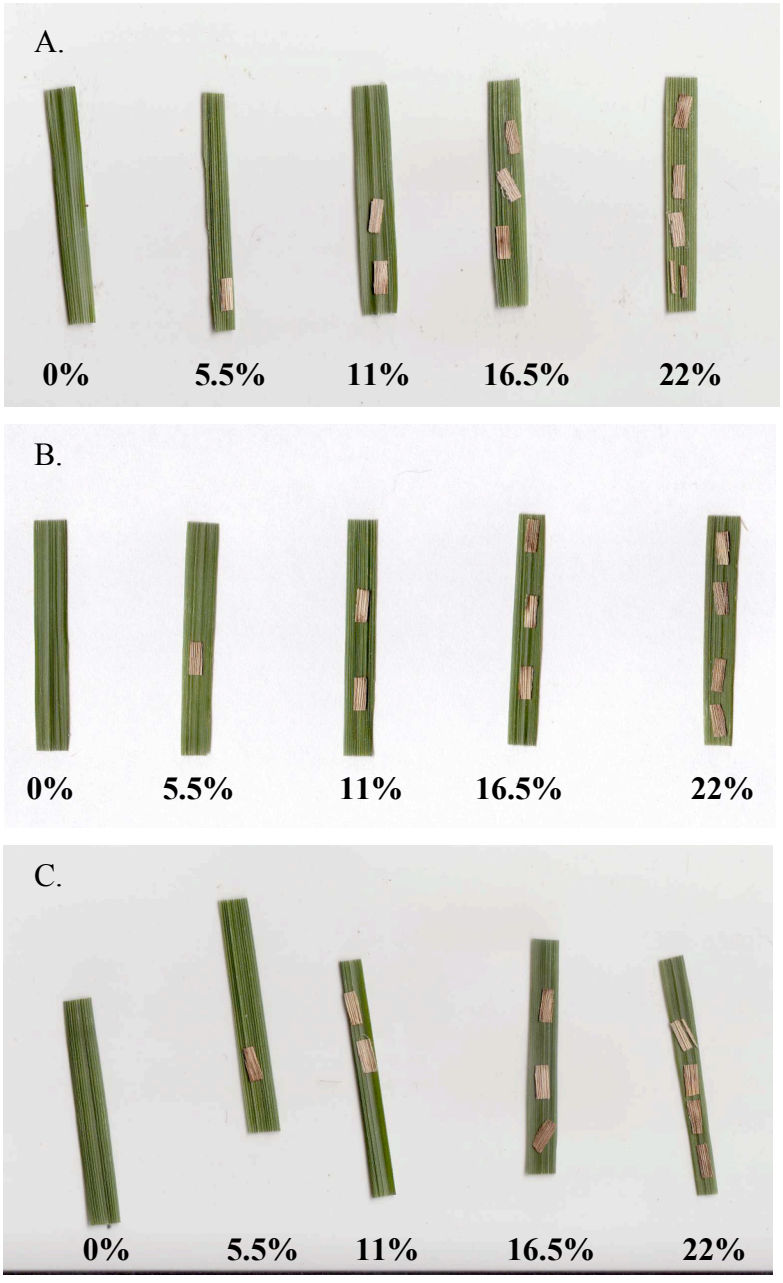

Figure 2.2. Scanned image of healthy leaf blades with varying numbers of rectangles of diseased tissue used to create known disease values of 0 - 100% disease (approximate disease values are shown beneath each leaf blade) using the cover sheet preparation method in experiment 2.

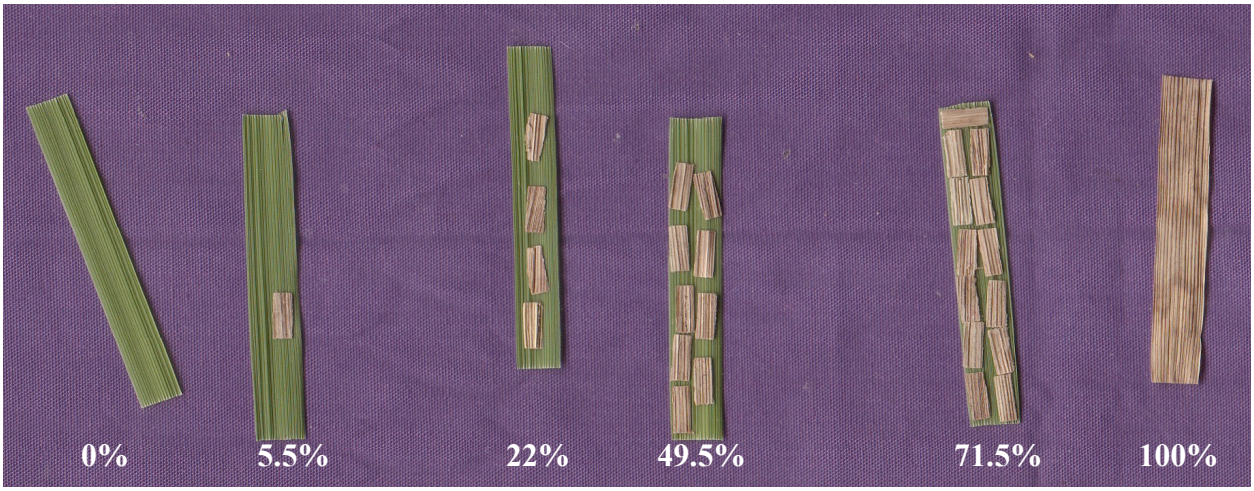

Figure 2.3. Scanned image of a diseased leaf blade with rectangles of healthy tissue attached to create a known disease value (approximately 78% in the image below) using the cover sheet method in experiment 2.

clear Avery sheet protector (Avery Dennison Corporation, Brea, CA) with leaves placed inside and spread out within to prevent overlap (CS) (Figure 2.1).

Leaves were scanned into the computer in JPEG (Joint Photographic Experts Group) format using a CanoScan LiDE 50 scanner (Canon, Inc, Tokyo, Japan) and ArcSoft PhotoStudio 5 (ArcSoft, Fremont, CA) software set to capture an image with 300 dpi (dots per inch). The following steps were taken to evaluate the percent disease of each image using Assess image analysis software (APS Press, St. Paul Minnesota)(Appendix A).

1. Leaves were distinguished from the background by selecting the H (hue) color plane and selecting hue thresholds of 31-low and 191-high in the threshold panel. The background was replaced with a solid blue background by selecting Edit > Substitute background.
2. Leaves were selected from the background using hue thresholds of 31-low and 191-high. The 'Area' button on the threshold panel was selected to calculate the number of pixels within the threshold area.
3. Lesions were selected from the background using hue thresholds of 31-low and 87-high. The 'Area' button on the threshold panel was selected to calculate the number of pixels within the threshold area.
4. Percent disease was calculated by selecting the 'Percent disease' button. This calculated percent disease as a ratio of lesion area (pixels) to total plant area (pixels).

In the second experiment, DIA disease evaluation was performed using only the CS method, with the PP and TF methods omitted. A purple cloth was placed behind the cover sheet when scanning leaves as images. All methods were otherwise performed as noted above.

Statistical Analysis

JMP statistical software (version 7, SAS Institute Inc., Cary, NC) was used for all analyses. Linear regressions were performed using actual disease values, as determined by physical measurements of the leaf and lesion area, as the independent variable and estimated disease values, as calculated by DIA, as the dependent variable. Correlations of these values were determined at an alpha level of 0.05. In experiment 1, regression analyses were performed

for the three DIA preparation methods and a cumulative regression was performed containing data from all three methods. The DIA estimated disease severity of the three preparation methods were compared using $ANOVA_{\alpha = 0.05}$. To further assess the accuracy of each method, the absolute error was calculated for each of the three preparation methods separately and for the combined methods. In experiment 2, a regression analysis was performed and absolute error was calculated.

Results

Experiment 1

In all three methods, disease values obtained using the DIA method were well correlated with actual disease values (TF: $r^2 = 0.97$ (Figure 2.4), PP: $r^2 = 0.97$ (Figure 2.5), CS: $r^2 = 0.98$ (Figure 2.6)). All three methods had slopes close to 1 and intercepts near zero, however, only the CS and the PP method had intercepts not significantly different from 0. The slope for each method was significantly different from 1. All three DIA preparation methods had a low mean absolute error (TF: MAE = 1.81, PP: MAE = 1.86, CS: MAE = 1.78). The DIA estimated mean disease severities for the three preparation methods were not significantly different ($p < 0.0001$) so data were combined and a cumulative regression was performed. Disease values ranged from 0% to 30% with combined DIA methods showing a tendency to overestimate disease slightly as disease severity increased, with a slope of 1.01 and an intercept of 0.75 (Figure 2.7). The slope and intercept were significantly different from 1 and 0 respectively. DIA disease values on average were ±1.82 percentage points from the calculated actual disease value.

Experiment 2

Disease ranged from 0 to 100 percent with a high correlation between actual disease values and disease values determined using DIA ($r^2 = 0.99$). The DIA method tended to overestimate disease slightly within the 40 to 70 percent disease range resulting in a slope of 0.98 and an intercept of 2.33 (Figure 2.8). The slope and intercept were significantly different from 1 and 0 respectively. The DIA method had a low absolute error, on average being ±2.51 percentage points from the actual disease value.

Figure 2.4. Linear regression of actual disease severity by digital image analysis (DIA) estimated disease severity for the Transparency Film method in Experiment 1. Actual disease severity was calculated using physical measurements of diseased and healthy leaf tissue. The dashed line represents a 1:1 relationship.

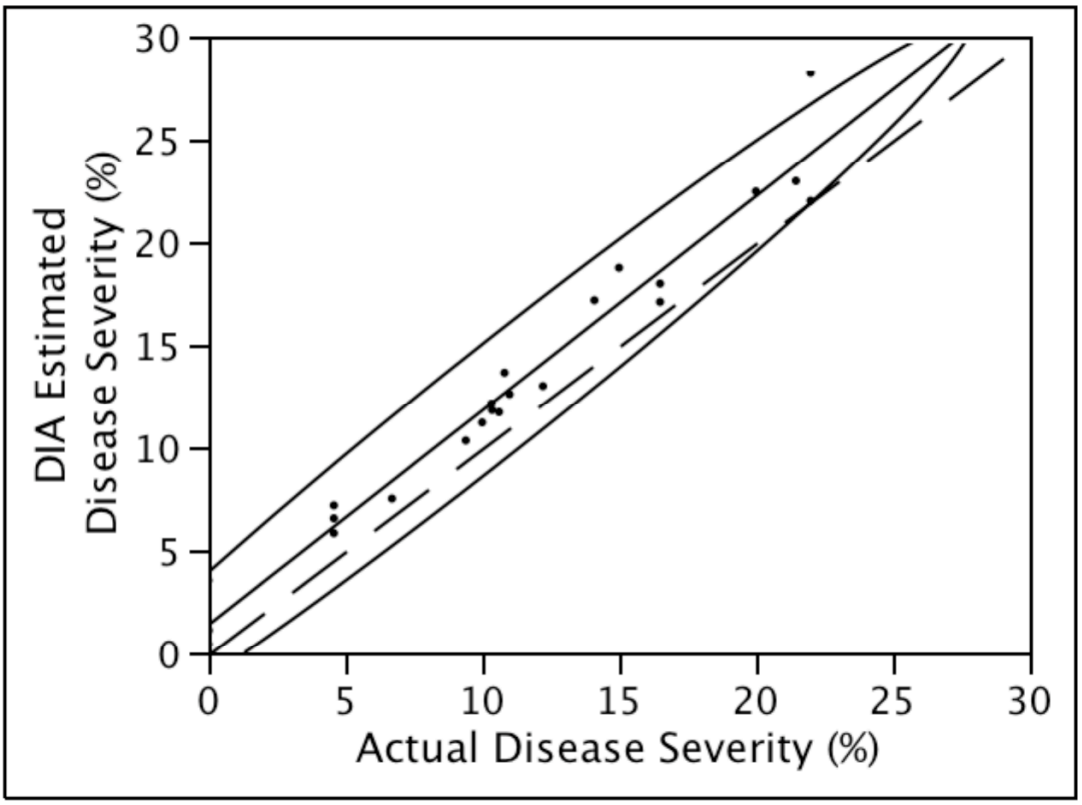

r^2 = 0.97	
Linear Fit[z]:	y = 1.04x + 1.35

[z] An asterisk indicates an intercept or slope not significantly different from 0 or 1 respectively

Figure 2.5. Linear regression of actual disease severity by digital image analysis (DIA) estimated disease severity for the Printer Paper method in Experiment 1. Actual disease severity was calculated using physical measurements of diseased and healthy leaf tissue. The dashed line represents a 1:1 relationship.

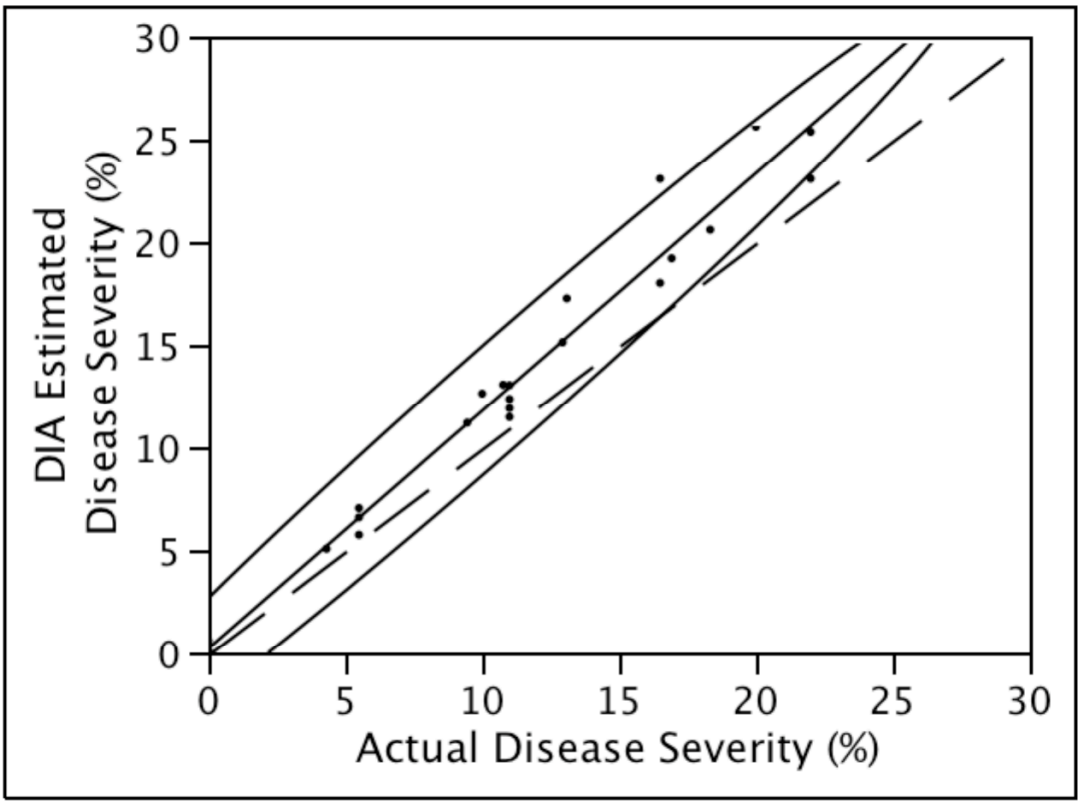

$r^2 = 0.97$
Linear Fit[z]: y = 1.16x + 0.21*

[z] An asterisk indicates an intercept or slope not significantly different from 0 or 1 respectively

Figure 2.6. Linear regression of actual disease severity by digital image analysis (DIA) estimated disease severity for the Cover Sheet method in Experiment 1. Actual disease severity was calculated using physical measurements of diseased and healthy leaf tissue. The dashed line represents a 1:1 relationship.

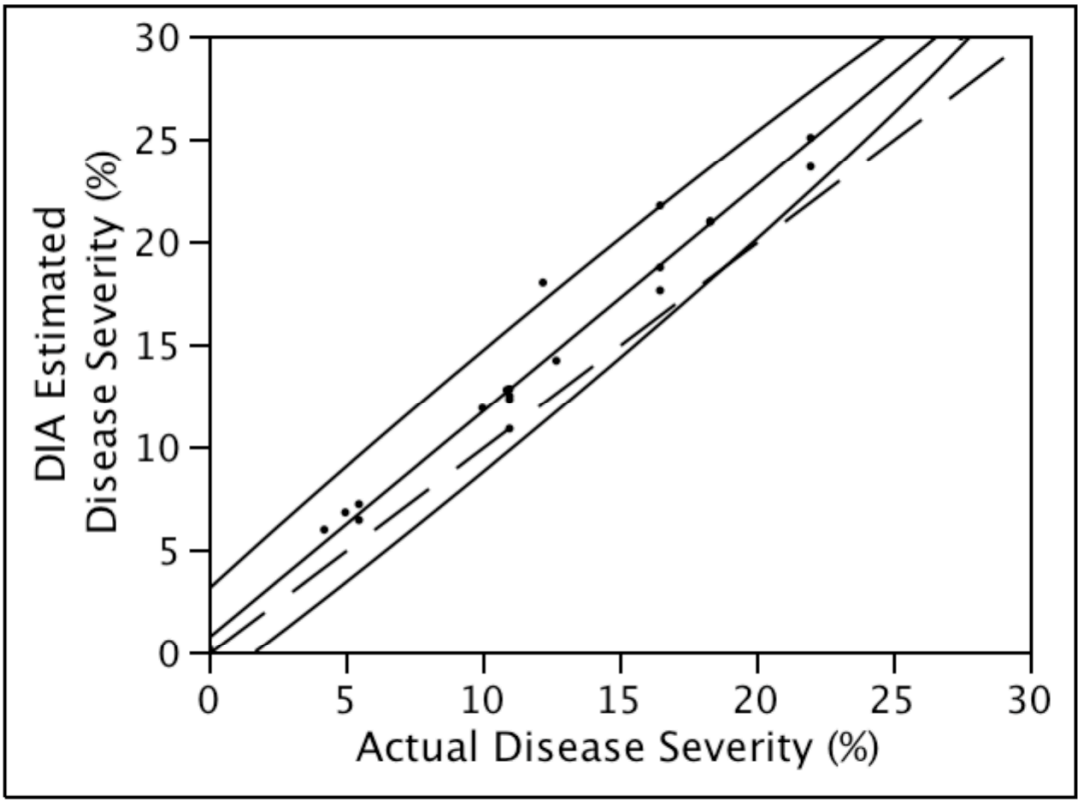

$r^2 = 0.98$

Linear Fit[z]: % disease (DIA) = 1.10x + 0.66*

[z] An asterisk indicates an intercept or slope not significantly different from 0 or 1 respectively

Figure 2.7. Linear regression of actual disease values by digital image analysis (DIA) disease severity for all methods combined in Experiment 1. Actual disease severity was calculated using physical measurements of diseased and healthy leaf tissue. The dashed line represents a 1:1 relationship.

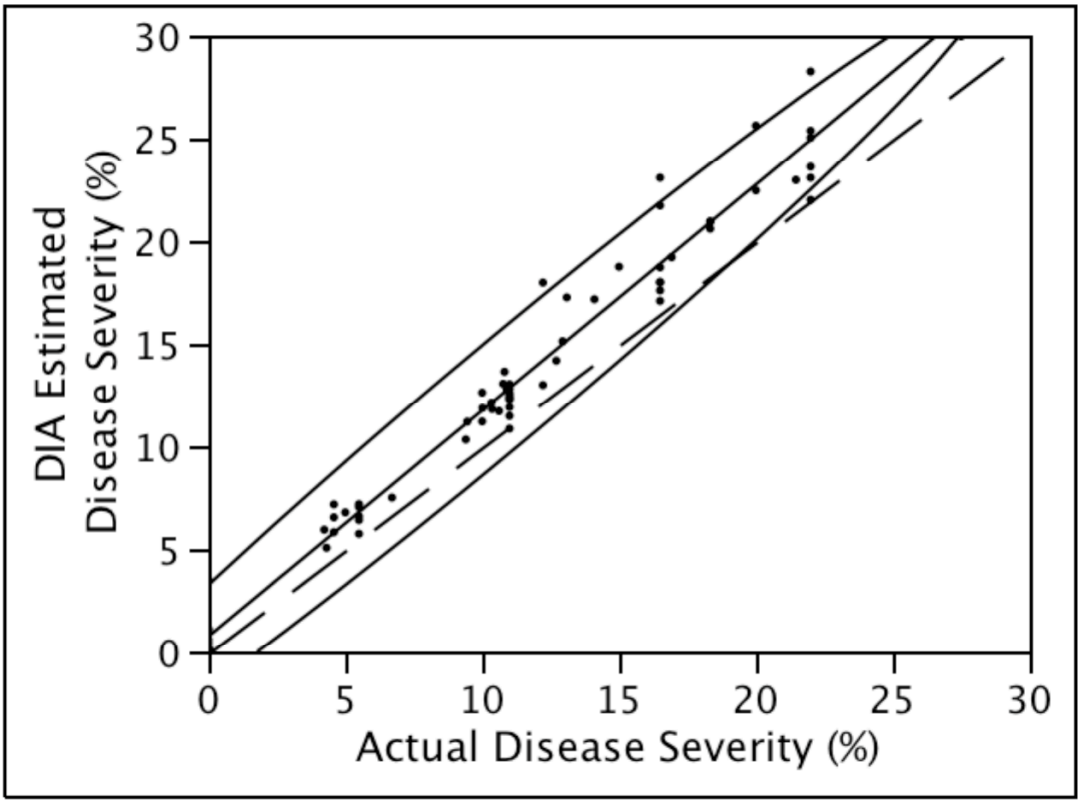

$r^2 = 0.97$
Linear Fit[z]: y = 1.10x + 0.75

[z] An asterisk indicates an intercept or slope not significantly different from 0 or 1 respectively

Figure 2.8. Linear regression of actual disease severity by DIA estimated disease severity using the Cover Sheet method in Experiment 2. Actual disease values were calculated using physical measurements of diseased and healthy leaf tissue.

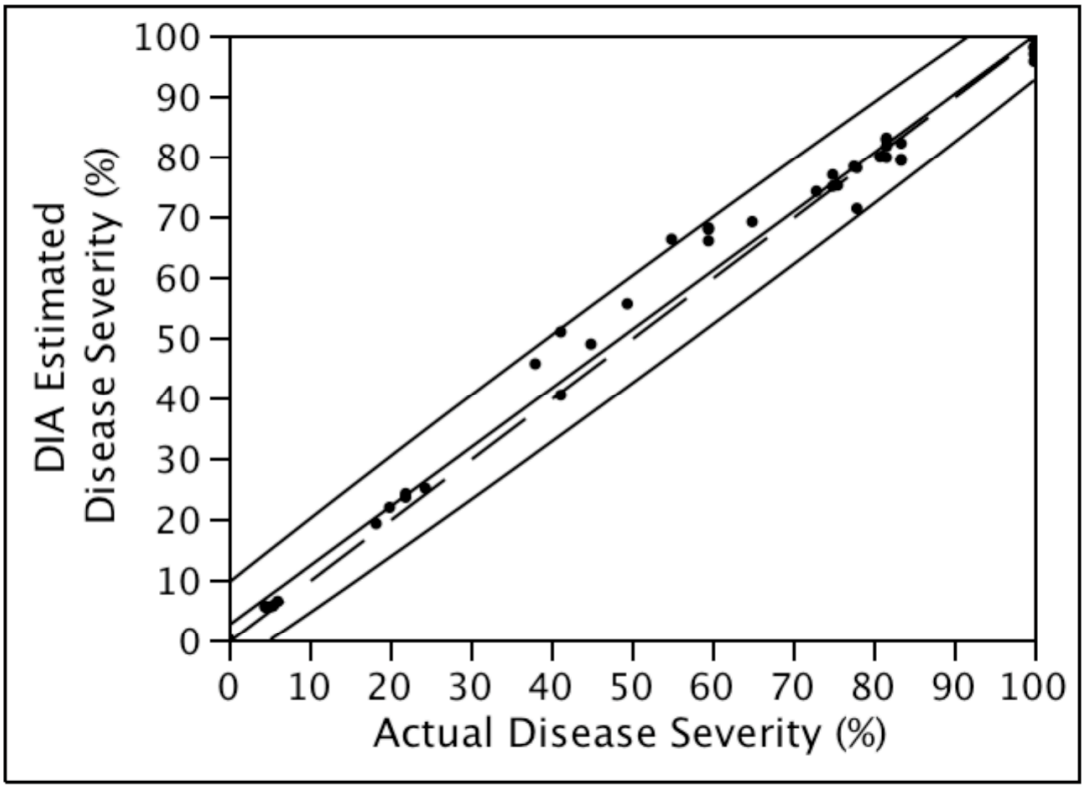

$r^2 = 0.99$
Linear Fit[z]: $y = 0.98x + 2.33$

[z] An asterisk indicates an intercept or slope not significantly different from 0 or 1 respectively

Discussion

In the first experiment, there were no significant differences among the three methods. For this reason, in the second experiment, the cover sheet method was the only method used as it produced the clearest image and was the easiest to use since it did not require the use of any type of adhesive.

Results from both studies showed a strong correlation between actual disease values and those calculated using DIA for disease severity values from 0-100%. Between 40% and 70% disease, DIA estimations varied the most from actual disease values, with a tendency to overestimate disease slightly. When placing the leaf blades, with the lesioned or healthy rectangle side down, on the flatbed scanner, the glued on rectangles prevented the leaf blade from lying completely flat. This caused a slight amount of shadowing around the edges of the leaf blade. When calculating percent disease, portions of this shadowed region were included as disease by the DIA software. Leaf blades showing the greatest amount of shadowing around the edges, were those with the high numbers of lesioned or healthy tissue rectangles required to create disease values between 40% and 70% disease. This may explain why these disease values were less accurate and precise compared to higher and lower disease values. Wijekoon et al. (2008) reported similar problems with the ability of DIA to detect disease on scanned images where shadows were present due to puckering or blistering caused by infections on leaves that were expanding.

The resulting variability in actual percent disease severity accounted for by DIA estimated disease severity in this study was similar to results seen in other DIA quantification studies in which linear regressions between actual and DIA estimated disease severity for all diseases evaluated had r^2 values of 0.97 or greater (Lindow and Webb, 1983).

Only the CS and PP method in experiment 1 had intercepts not significantly different from zero. The slopes for all methods in both experiments were close to, but significantly different from, one. However, DIA estimated disease severity using all methods in both experiments was highly correlated with actual disease values (Ex.1: $r^2 = 0.97$ (Figure 2.7), Ex.2: $r^2 = 0.99$ (Figure 2.8)). The mean absolute error (MAE) was also low in both experiments (Ex. 1: MAE = 1.85, Ex.2: MAE = 2.51). DIA using scanned leaves was very time-consuming and would not be efficient for large-scale disease evaluation. Photographing plants would be an alternative method of DIA preparation that would be faster and, since it would leave the plant

intact, would allow for in-field evaluation and tracking of disease progress curves. Although DIA of scanned leaves does not provide an exact disease severity value, it can provide a close estimate of actual disease severity and could be used as a standard to judge the accuracy and precision of alternative DIA evaluation methods such as photographing plants.

Literature Cited

Bock, C.H., P.E. Parker, A.Z. Cook, and T.R. Gottwald. 2008. Visual rating and the use of image analysis for assessing different symptoms of citrus canker on grapefruit leaves. Plant Disease 92:530-541.

Horst, G.L., M.C. Engelkle, and W. Meyers. 1984. Assessment of visual evaluation techniques. Agronomy Journal 76:619-622.

Horvath, B.J., and J.M. Vargas. 2005. Analysis of dollar spot disease severity using digital image analysis. International Turfgrass Society Research Journal 10:196-201.

James, W.C. 1971. An illustrated series of assessment keys for plant diseases, their preparation and usage. Canadian Plant Disease Survey 51:39-65.

Karcher, D.E., and M.D. Richardson. 2003. Quantifying turfgrass color using digital image analysis. Crop Science 43:943-951.

Karcher, D.E., and M.D. Richardson. 2005. Batch analysis of digital images to evaluate turfgrass characteristics. Crop Science 45:1536-1539.

Kwack, M.S., E.N. Kim, H. Lee, K.D. Kim, J.-W. Kim, and S.-C. Chun. 2005. Digital image analysis to measure lesion area of cucumber anthracnose by *Colletotrichum orbiculare*. Journal of General Plant Pathology 71:418-421.

Lindow, S.E., and R.R. Webb. 1983. Quantification of foliar plant disease symptoms by microcomputer-digitized video image analysis. Phytopathology 73:520-524.

Niemira, B.A., W.W. Kirk, and J.M. Stein. 1999. Screening for late blight susceptibility in potato tubers by digital analysis of cut tuber surfaces. Plant Disease 83:469-473.

Nita, M., M.A. Ellis, and L.V. Madden. 2003. Reliability and accuracy of visual estimation of Phomopsis leaf blight of strawberry. Phytopathology 93:995-1005.

NTEP. 2005. 2002-05 National Tall Fescue Test (NTEP No. 06-12). National Turfgrass Evaluation Program.

Nutter Jr., F.W., P.D. Esker, and R.A.C. Netto. 2006. Disease assessment concepts and the advancements made in improving the accuracy and precision of plant disease data. Phytopathometry 115:95-103.

Nutter Jr., F.W., M.L. Gleason, J.H. Jenco, and N.C. Christians. 1993. Assessing the accuracy, intra-rater repeatability, and inter-rater reliability of disease assessment systems. Phytopathology 83:806-812.

Olmstead, J.W., and G.A. Lang. 2001. Assessment of severity of powdery mildew infection of sweet cherry leaves by digital image analysis. HortScience 36:107-111.

Richardson, M.D., D.E. Karcher, and L.C. Purcell. 2001. Quantifying turfgrass cover using digital image analysis. Crop Science 41:1884-1888.

Wijekoon, C.P., P.H. Goodwin, and T. Hsiang. 2008. Quantifying fungal infection of plant leaves by digital image analysis using Scion Image Software. Journal of Microbiological Methods 74:94-101.

Chapter 3

Quantifying and comparing the accuracy and precision of digital image analysis disease evaluations to visual disease evaluations of *Rhizoctonia solani* on *Festuca arundinacea*

Introduction

Turfgrass cultivars are routinely evaluated for various characteristics across multiple locations with evaluations performed by multiple researchers. This can lead to an inaccurate overall assessment of a cultivar due to inter-rater variability (variability within ratings performed by multiple researchers) and intra-rater variability (variability within ratings performed by a single researcher) (Nutter Jr. et al., 1993). Accuracy and precision in turfgrass evaluation are essential for accurate statistical analysis and research results. Statistically, accuracy is defined as "the nearness of a measurement to the actual value of the variable being measured" and precision is defined as "the closeness to each other of repeated measurements of the same quantity" (Zar, 1999). These two components may be compromised using a visual evaluation method (Horst et al., 1984; Nutter Jr. et al., 1993).

Digital image analysis (DIA) has become increasingly popular for evaluating plant disease because of its objectivity. Digital image analysis has been quantified as accurately assessing disease severity of numerous diseases on agricultural and horticultural crops with varying leaf shapes and sizes based on comparisons of DIA estimated disease severity to actual disease severity (Lindow and Webb, 1983; Martin and Rybicki, 1998). Studies have also assessed the ability of DIA to accurately detect numerous diseases on various host plants based on visual confirmation of accurate selection of the necrotic area by the DIA software (Kwack et al., 2005; Wijekoon et al., 2008). In studies comparing accuracy and precision between DIA disease evaluations and visual disease evaluations, DIA has shown improved accuracy and precision over visual evaluations in symptom evaluations of citrus canker (*Xanthomonas axonopodis* pv. *citri*) on leaves of grapefruit (Citrus x paradisi "Ruby Red") and maize streak virus on corn (*Zea mays*) (Bock et al., 2008; Martin and Rybicki, 1998). However, DIA evaluations of powdery mildew (*Erysiphe cichoracearum* D.C. Ex Merat) on squash (*Cucurbita maxima* Dutch) and powdery mildew (*Podosphaera clandestine* Waller.:Fr.) on sweet cherry

(*Prunus avium* L.) showed no improvement in accuracy over visual evaluations (Moya et al., 2005; Olmstead and Lang, 2001). In turfgrass research, the accuracy of DIA has been quantified in evaluating turfgrass color and percent cover (Karcher and Richardson, 2003; Richardson et al., 2001). Digital image analysis has also been successful at detecting the disease dollar spot on turfgrass and showed no significant difference in disease progress curves produced using DIA evaluations compared to those produced using visual evaluations (Horvath and Vargas, 2005).

In the previous chapter, the accuracy of DIA was quantified and DIA produced a close estimate to actual disease values in estimations of percent brown patch damage on scanned leaves of tall fescue (Chapter 2). Disease values from leaves with a physically calculated percent disease were compared to disease values obtained using DIA of scanned leaf images. This method of DIA was highly correlated with actual disease values but was also tedious and time consuming. The objectives of this study are to develop a more efficient DIA method for evaluating brown patch on tall fescue and to compare the accuracy and precision of this method to that of visual evaluations using the quantified DIA method as a standard of accuracy.

Materials and Methods

Plant Maintenance

Experiment 1

Approximately six seeds of "Kentucky 31" tall fescue were planted in 3.8 cm diameter conetainers™ (Steuwe & Son, Corvallis, OR) filled with Pro-Mix potting media containing biofungicide (*Bacillus subtilis* MBI 600) (Code 0532, Premier Horticulture, Quebec, Canada). Plants were grown to maturity, approximately 6 weeks, until they began to form tillers. Plants were grown in a glass greenhouse with a fan and pad cooling system. Temperature was not consistent and varied according to outside temperature. Plants were watered daily for 2-3 minutes using an overhead irrigation system with between 310 and 414 kPa of pressure. Plants were heavily fertilized with three applications per month of a 20-20-20 mix at 48.8 kg N ha^{-1}. Plants were maintained at a height of approximately 7.6 cm and cut to this height prior to inoculation.

Experiment 2

Twenty seeds from thirteen plant introductions (PIs) obtained from the USDA germplasm database were grown to maturity with each seedling maintained as a genetic clone (Table 3.1). Tillers from each PI were planted in 3.8 cm diameter conetainers and allowed to grow until they formed at least five or six tillers. These were maintained in the same manner as plants used in Experiment 1.

Inoculation

Fourteen isolates of *R. solani* were collected from *Poa annua* putting greens at the Virginia Tech Turfgrass Research Center in Blacksburg, Virginia. A study was performed to assess the virulence of these isolates on tall fescue. Three of the most virulent isolates (data not shown) were used to create inoculum.

Inoculum was created using healthy leaves of K31, rinsed in a 10% bleach solution for 60 seconds then rinsed in sterilized de-ionized water for 60 seconds. These leaves were placed radially around a 4 mm diameter plug of *R. solani* on potato dextrose agar (PDA) resulting in colonization of the leaves. Plants were inoculated by placing three infected leaves, one per isolate, within the plant canopy of each conetainer (Figure 3.1).

Disease Treatment

Cones were placed in a sealed chamber to increase air temperature and provide high humidity for disease development (Figure 3.2). Plants were cut to a height of 7.6 cm prior to inoculation and again prior to disease evaluation.

In experiment 1, cones were arranged in a randomized complete block design with 6 treatments (0, 2, 4, 6, and 8 days exposure to disease pressure) to provide a range of disease severity. Each treatment was replicated five times and the experiment was repeated two times (Ex1.1 and Ex1.2).

In experiment 2, cones were arranged in a randomized complete block design and subject to disease pressure for twelve days. Using the WP macro 1 method described below, four plants were chosen from each of the following percent disease ranges: 0-20, 21-40, 41-60, 61-80, 81-100. This experiment was repeated two times (Ex.2.1 and Ex 2.2)

Table 3.1. Code name, accession name and identifier if applicable, collection location, and identification as cultivar or PI for the tall fescue plants used in Experiment 2 of the comparing methods study (chapter 3) and for the initial and final screens to *R. solani* and *R. zeae* (chapter 4).

PI #	Code #	Accession Name and Identifier	Collection location	Type
578712	1	Alta	Oregon	Cultivar
600801	2	Rebel	New Jersey	Cultivar
634237	3		Oregon	
561431	4	Kentucky 31[a]	Kentucky	
561430	5	Kentucky 31[b]	Kentucky	Cultivar
598927	6		Sardinia, Italy	
598828	7		Morocco	
578715	8	Fawm	Oregon	Cultivar
598918	9		Tunisia	
578719	10	Beltsville 16-1	Maryland	
598574	11		Kazakhstan	
598891	12		Morocco	
469244	13	Asheville	North Carolina	
434045	14	Kentucky 31	Kentucky	Cultivar
598945	15		Sardinia, Italy	
570660	16	SR 8300	US	Cultivar
w6 20487	17		Washington	

Cultivar	Code #
Millenium	18
Falcon IV	19
Stetson	20
K31	21

[a]with endophytes
[b]without endophytes

Figure 3.1. Inoculum used to infect tall fescue plants. Inoculum was composed of 2 cm by 0.5 cm pieces of sterilized filter paper or tall fescue placed radially around a 4 mm diameter plug of either *R. solani* or *R. zeae* grown on potato dextrose agar.

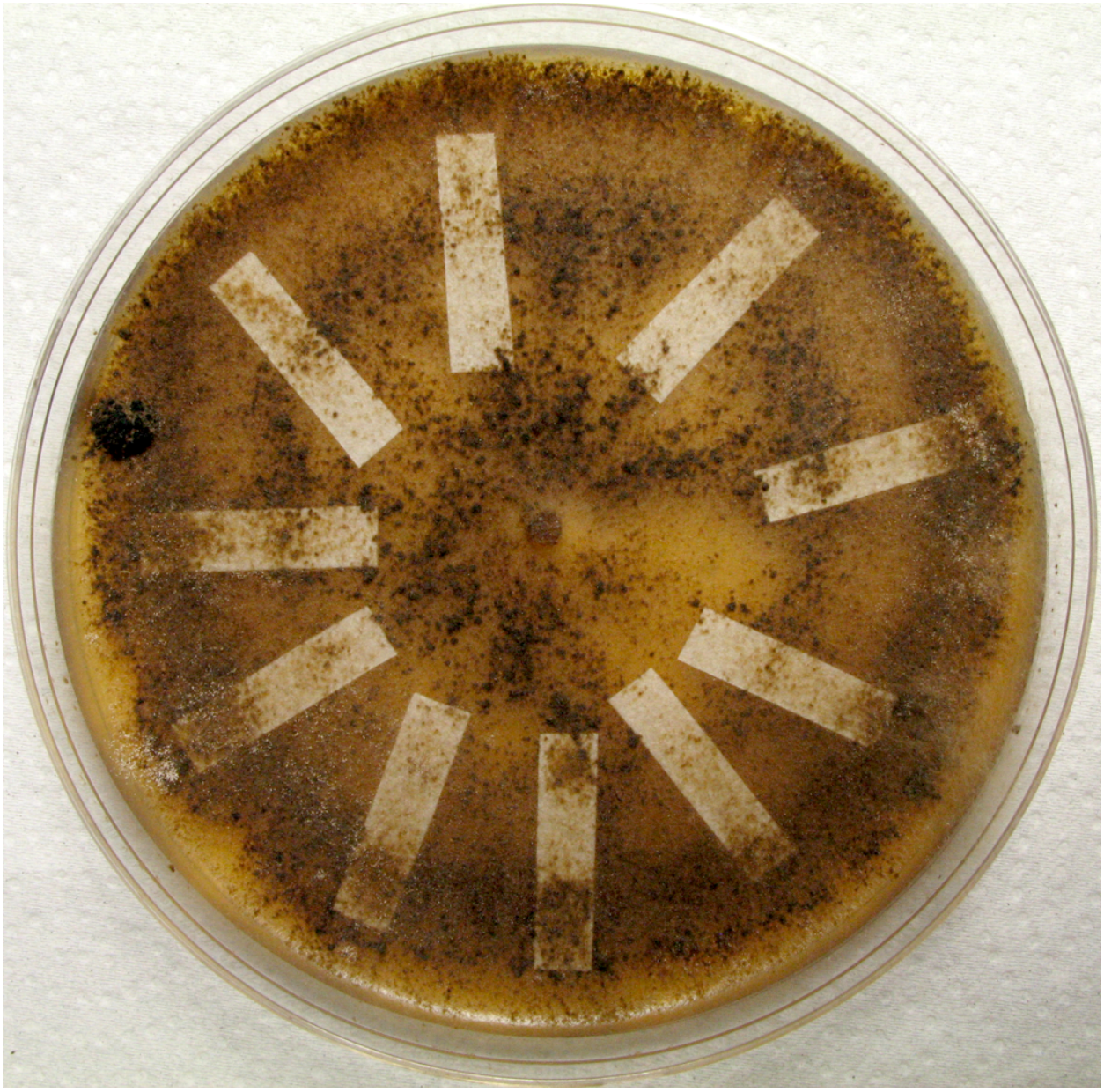

Figure 3.2 Chamber used for increasing temperature and humidity to encourage disease development. Chamber was composed of PVC pipe and plastic sheeting.

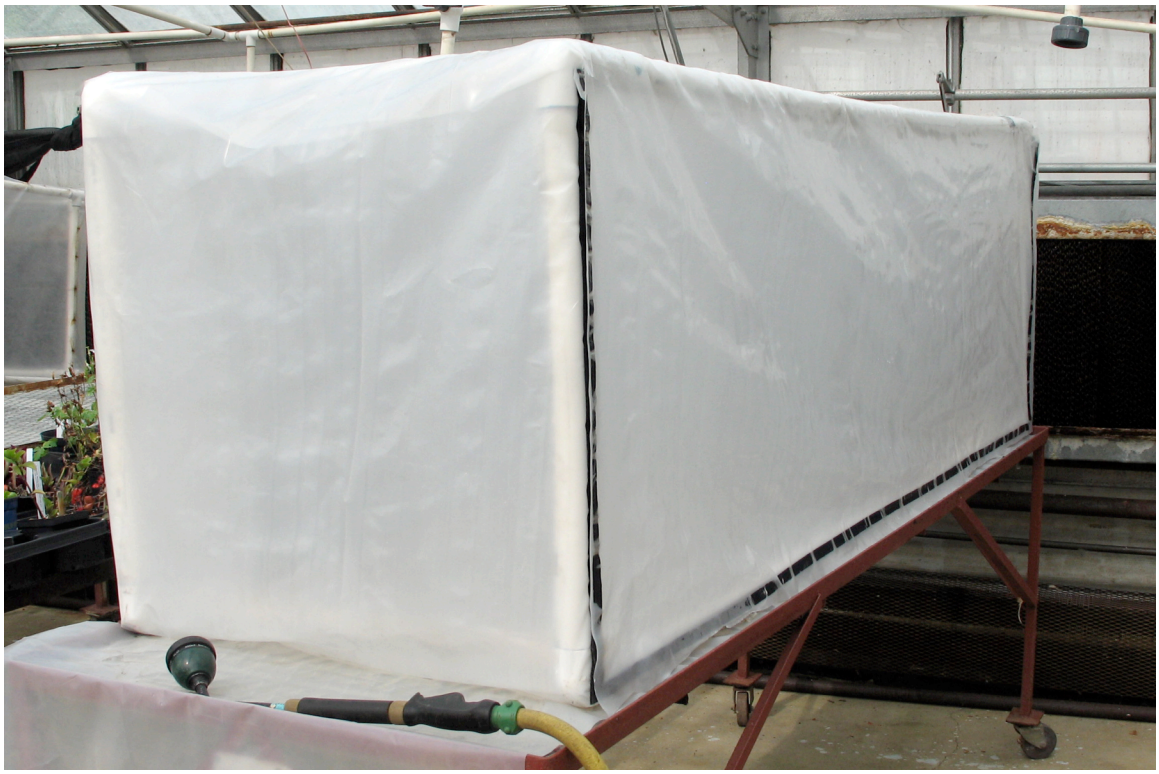

Disease Evaluation

Upon removal from the chamber, plants were sub-irrigated on greenhouse benches for a 24-hr period to allow the leaf canopy to dry prior to disease evaluation. Percent disease severity was evaluated for each cone using the following methods: visual analysis (V), whole pot DIA using two different macros (WP1, WP2), and individual leaf DIA (IL). These methods are described below.

1.) Visual analysis (V): Three evaluators performed visual ratings of disease severity using a percentage scale. All three evaluators were trained in the evaluation of brown patch on tall fescue, though years of experience varied. Evaluators had approximately 1, 3, and 14+ years of experience respectively.

2.) Whole Pot DIA (WP1, WP2): Pictures were taken of each conetainer prior to inoculation and again after the 24-hr drying period. Initial pictures were taken to adjust for any naturally senescing plant tissue that might be present prior to inoculation as this would be included as disease by the DIA software. Most senescent tissue was removed prior to initiation of the study as an added precaution. When capturing images, conetainers were lined up with an index mark placed on the stand and cone prior to inoculation to provide consistent leaf orientation between the Initial and Final pictures. The stand was set at an angle of approximately 45°, and a Canon PowerShot G6 digital camera (Canon, Inc, Tokyo, Japan) was placed on a tripod with the orientation adjusted to take a top down image (Figure 3.3). The aperture on the camera was set to f/8 and the shutter speed was manually adjusted for each image to a setting at which the light meter on the camera read zero. Two Calumet (Calumet Photographic, Inc., Bensenville, IL) light stands, each containing four 40 watt compact semi-spiral, daylight balanced (5500 K) fluorescent bulbs (model 0L2000, Calumet Photographic, Inc. Benesenville, IL), were placed on either side of the stand to provide even illumination. Each cone was placed in the stand, photographed, and removed from the stand three times to assess the variability of this evaluation method.

Pictures were analyzed using Assess image analysis software (Appendix A). Two different macros were used to evaluate disease severity, WP1 and WP2. In both macros,

Figure 3.3. Setup for capturing images using the whole pot (WP) method. The plant stand was set at an angle of approximately 45°, two Calumet light stands, each containing four 40 watt compact semi-spiral, daylight balanced (5500 K) fluorescent bulbs, were placed on either side of the stand, and a Canon PowerShot G6 digital camera was placed in a tripod with the orientation adjusted to take a top down image.

hue thresholds of 31-low and 191-high were used to distinguish the plant from the background. The background was then substituted for a solid blue background. An intensity threshold of 66-low and 255-high was used to select the soil, which was then replaced with a blue background. Hue thresholds of 31-low and 191 high were used to determine the total plant area. Lesion area was determined with hue thresholds of 31-low and 101-high using WP1 and 31-low and 114-high using WP2. A ratio of lesion area to total plant area was used to determine percent disease. Total percent disease was calculated as the difference in disease severity between the pre-inoculation picture and post-inoculation picture.

3.) Individual leaf DIA (IL): All leaves from each plant were removed, placed within a clear plastic cover sheet, and scanned to produce JPEG images using a CanoScan LiDE 50 scanner. Each set of leaves was scanned three times to assess the variability of this evaluation method. The cover sheet was removed and the leaves within it were rearranged between each scan. Assess image analysis software was used to evaluate percent disease in each image. Hue thresholds of 31-low and 191-high were used to distinguish the plant from the background, which was then replaced by a solid blue background. Hue thresholds of 31-low and 191-high were used to determine the total plant area and hue thresholds of 31-low and 87-high were used to determine the lesion area. A ratio of lesion area to total plant area was used to determine percent disease.

In experiment 2, only one picture or scan was taken for each cone and only the accuracy of each method was assessed.

Statistical Analysis

Accuracy

The IL method, which had a high correlation to actual disease values in the previous study ($r^2_{Actual,IL}$=0.98), was used as a standard of accuracy by which to judge the accuracy of the remaining methods: WP1, WP2, and V. In experiments 1.1 and 1.2, each assessment method (IL, WP1, WP2, and V) was used to evaluate disease three times. An $ANOVA_{\alpha = 0.05}$ of mean disease severity showed no significant differences among the three IL scans (p = 0.9984), so only

the value from the first IL scan of each plant was considered the actual disease value for that plant. Disease values from the three images or visual evaluations using the WP1, WP2, and V evaluation methods were treated as independent data points for a total of 108 disease evaluations per method for each experiment.

In experiments 2.1 and 2.2, only one evaluation was performed per method (WP1, WP2, V). Twenty disease evaluations were performed per method for each experiment.

In all experiments, the accuracy of each method was determined by calculating the absolute error. Absolute error was calculated as the absolute difference between predicted percent disease values as determined by WP1, WP2, and V, and actual percent disease values as determined by the first scan using the IL method. To compare the accuracy between methods, mean absolute errors for each method were analyzed in JMP (Version 7.0, SAS Institute, Inc, Cary, NC) using $ANOVA_{\alpha = 0.05}$ and means were differentiated using Tukey's $HSD_{\alpha = 0.05}$.

Precision

Precision calculations were only determined for experiment 1.1 and 1.2. The precision of each method was evaluated by determining the average standard deviation within the three images, scans, or visual evaluations performed on each cone. To compare precision between methods, the standard deviations were analyzed in JMP using $ANOVA_{\alpha = 0.05}$ with means separated using Tukey's $HSD_{\alpha = 0.05}$.

Results

Mean disease severity and the distribution of disease severity varied by experiment. Experiment 1.1 and 1.2 were most evenly distributed, while experiments 1.2 and 2.1 had the greatest range of disease severity. Experiment 2.2 had the highest mean disease severity. Mean disease severity, standard deviation, and coefficient of variation for each experiment are displayed in figure 3.4.

Figure 3.4. Scatterplot matrix showing the distribution of disease severity in experiments 1.1, 1.2, 2.1, and 2.2. Each dot represents a single disease evaluation using a scan of the individual leaves within a cone. The table below shows mean disease severity and standard deviation for each experiment.

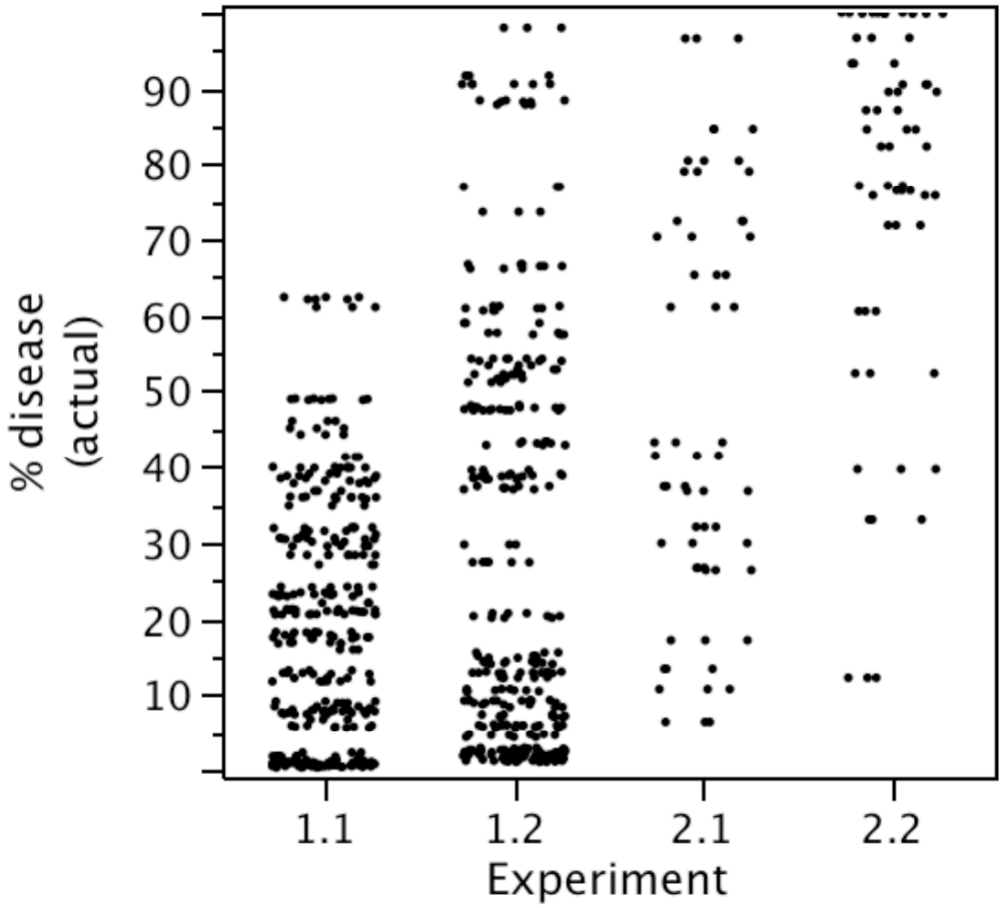

Experiment	Mean % disease	Standard Deviation	Coefficient of Variation
1.1	20.13	15.98	79.38
1.2	28.63	27.24	95.14
2.1	46.56	26.99	57.97
2.2	76.14	24.40	32.05

Comparing DIA WP Macros

The whole pot DIA macros were not consistent in their accuracy across experiments. Comparing the two macros, WP2 had a significantly lower mean absolute error in Ex1.1 (Figure 3.5) and WP1 had a significantly lower mean absolute error in Ex1.2 (Figure 3.6). In Ex2.1 and Ex2.2, the two macros showed no significant difference in accuracy, though macro 1 had a lower mean absolute error in both runs (Figure 3.7, Figure 3.8). Absolute error of the two macros was equally consistent across experiments with no significant differences among absolute errors in three of the four experiments (Figure 3.9).

Comparing the precision of the DIA whole pot macros, WP2 had a lower standard deviation in Ex1.1 (Figure 3.10) while WP1 had a lower standard deviation in Ex1.2 (Figure 3.11). However, the standard deviations of the two WP macros were not significantly different from each other in either run.

Comparing DIA to V

Comparing WP1 to V, WP1 had a significantly higher mean absolute error in Ex1.1 (Figure 3.5), and the two were not significantly different in Ex1.2, Ex2.1, and Ex2.2 (Figure 3.6, Figure 3.7, Figure 3.8). Comparing WP2 to V, WP2 had a significantly lower mean absolute error in Ex1.1 (Figure 2.5), a significantly higher mean absolute error in Ex1.2 (Figure 3.6), and the two were not significantly different in Ex2.1 and Ex2.2 (Figure 3.7, Figure 3.8). Both DIA macros were more consistent in their accuracy across experiments compared to visual evaluations (Figure 3.9). The mean standard deviation was also significantly lower in both WP1 and WP2 compared to V in both runs of the study (Figure 3.11).

Discussion

Image Capture Methods

The method used to obtain images for analysis was effective in obtaining an image in which a set hue threshold could be used to distinguish between plant material and the purple cloth used to mask the background. Preliminary studies, in which a red cloth was used, proved ineffective because of the similarity of the red hue to necrotic areas on the plant. The purple

Figure 3.5. Comparison of mean absolute error by evaluation method for experiment 1.1. Absolute error calculated as the absolute difference between actual disease values, estimated using DIA of scans of individual leaves, and predicted disease values estimated using visual evaluations (V) and DIA macros (WP1, WP2). The diamond indicates points within the 95% confidence interval and the line across each diamond represents the group mean. The short horizontal lines indicate one standard deviation from the mean. The horizontal line crossing the entire graph indicates the grand mean.

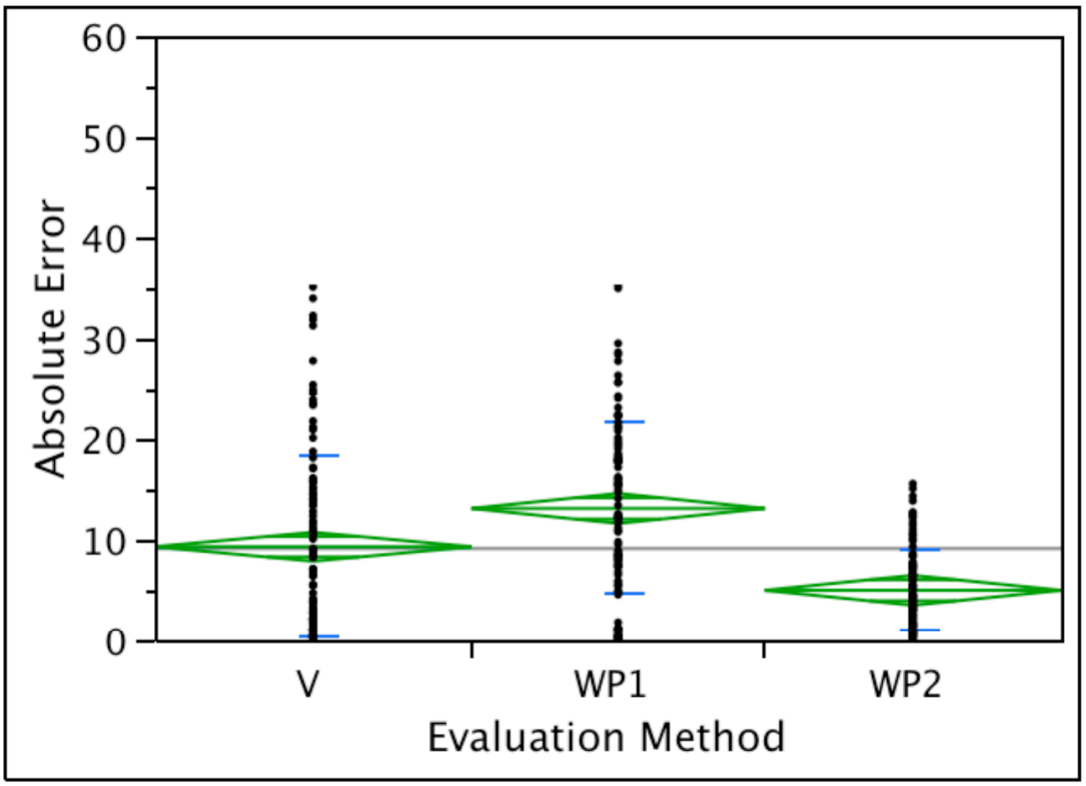

Method	Mean % disease	
V	9.30	B[y]
WP1	13.09	A
WP2	4.98	C
p value	< 0.0001[z]	

[y] means differentiated using Tukey's $HSD_{\alpha = 0.05}$. Means not connected by the same letter are significantly different

[z] means compared using $ANOVA_{\alpha = 0.05}$

Figure 3.6. Comparison of mean absolute error by evaluation method for experiment 1.2. Absolute error calculated as the absolute difference between actual disease values, estimated using DIA of scans of individual leaves, and predicted disease values estimated using visual evaluations (V) and DIA macros (WP1, WP2). The diamond indicates points within the 95% confidence interval and the line across each diamond represents the group mean. The short horizontal lines indicate one standard deviation from the mean. The horizontal line crossing the entire graph indicates the grand mean.

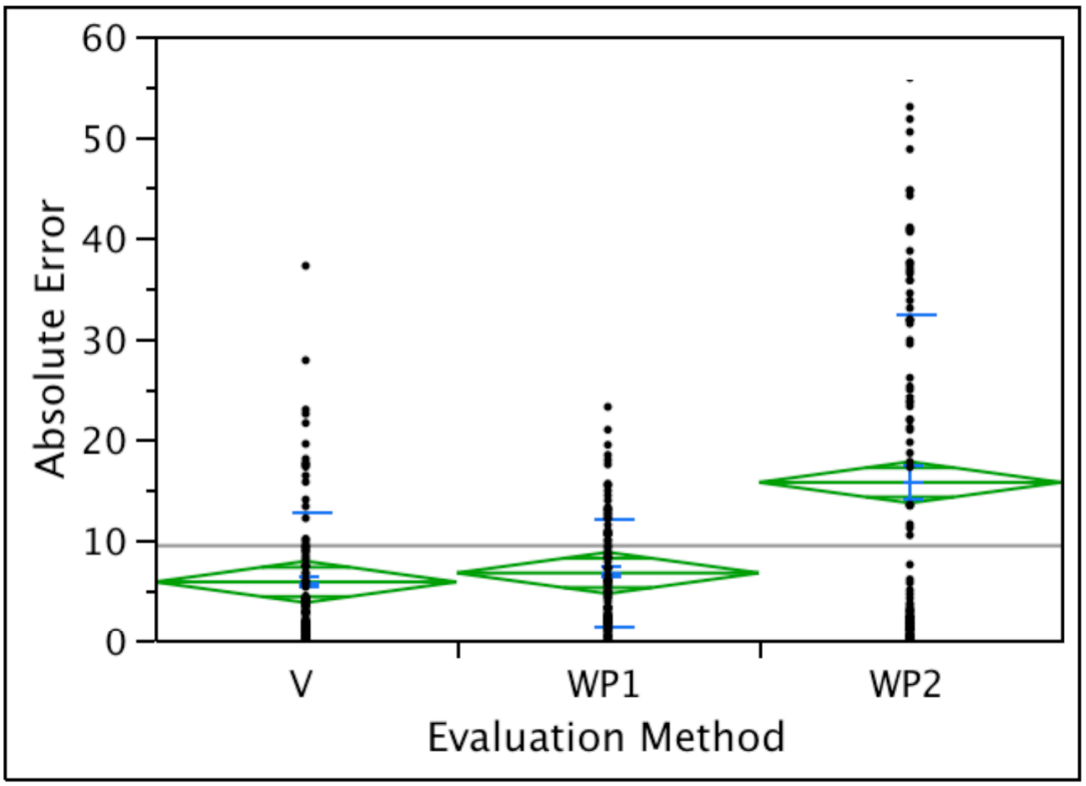

Method	Mean % disease	
V	5.82	B[y]
WP1	6.70	B
WP2	15.68	A
p value	< 0.0001[z]	

[y] means differentiated using Tukey's $HSD_{\alpha = 0.05}$. Means not connected by the same letter are significantly different

[z] means compared using $ANOVA_{\alpha = 0.05}$

Figure 3.7. Comparison of mean absolute error by evaluation method for experiment 2.1. Absolute error calculated as the absolute difference between actual disease values, estimated using DIA of scans of individual leaves, and predicted disease values estimated using visual evaluations (V) and DIA macros (WP1, WP2). The diamond indicates points within the 95% confidence interval and the line across each diamond represents the group mean. The short horizontal lines indicate one standard deviation from the mean. The horizontal line crossing the entire graph indicates the grand mean.

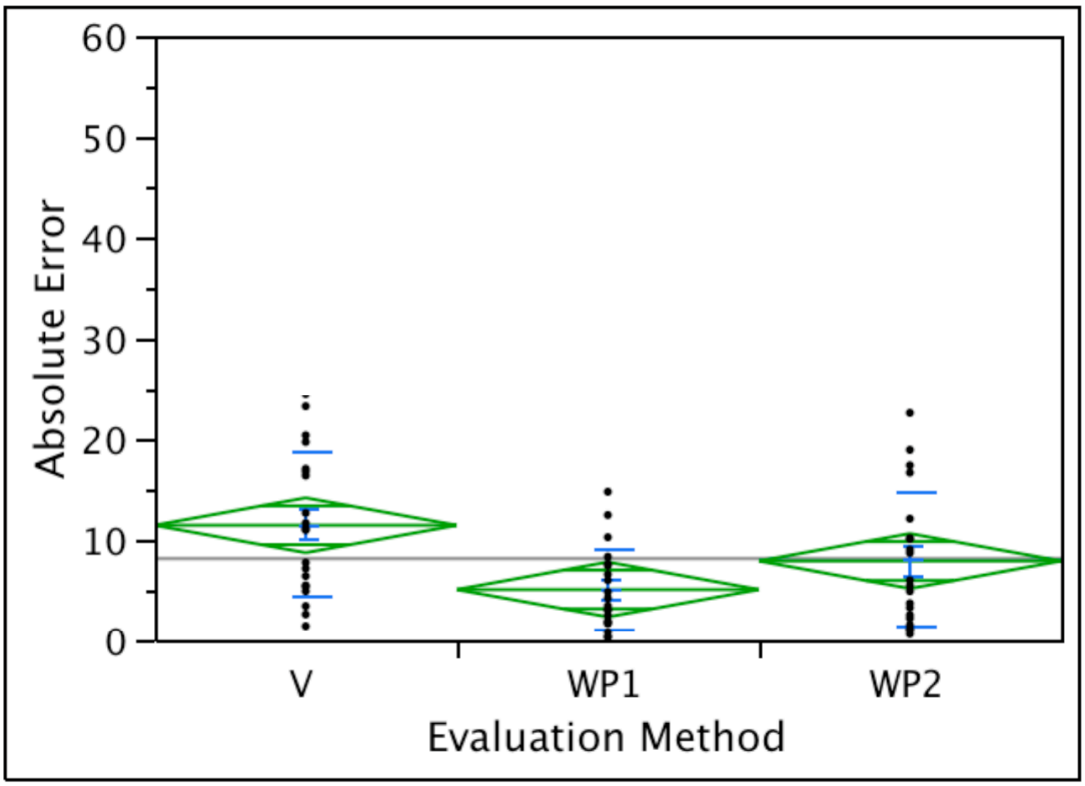

Method	Mean % disease	
V	11.43	A[y]
WP1	5.06	B
WP2	7.88	AB
p value	< 0.0065[z]	

[y] means differentiated using Tukey's $HSD_{\alpha = 0.05}$. Means not connected by the same letter are significantly different

[z] means compared using $ANOVA_{\alpha = 0.05}$

Figure 3.8. Comparison of mean absolute error by evaluation method for experiment 2.2. Absolute error calculated as the absolute difference between actual disease values, estimated using DIA of scans of individual leaves, and predicted disease values estimated using visual evaluations (V) and DIA macros (WP1, WP2). The diamond indicates points within the 95% confidence interval and the line across each diamond represents the group mean. The short horizontal lines indicate one standard deviation from the mean. The horizontal line crossing the entire graph indicates the grand mean.

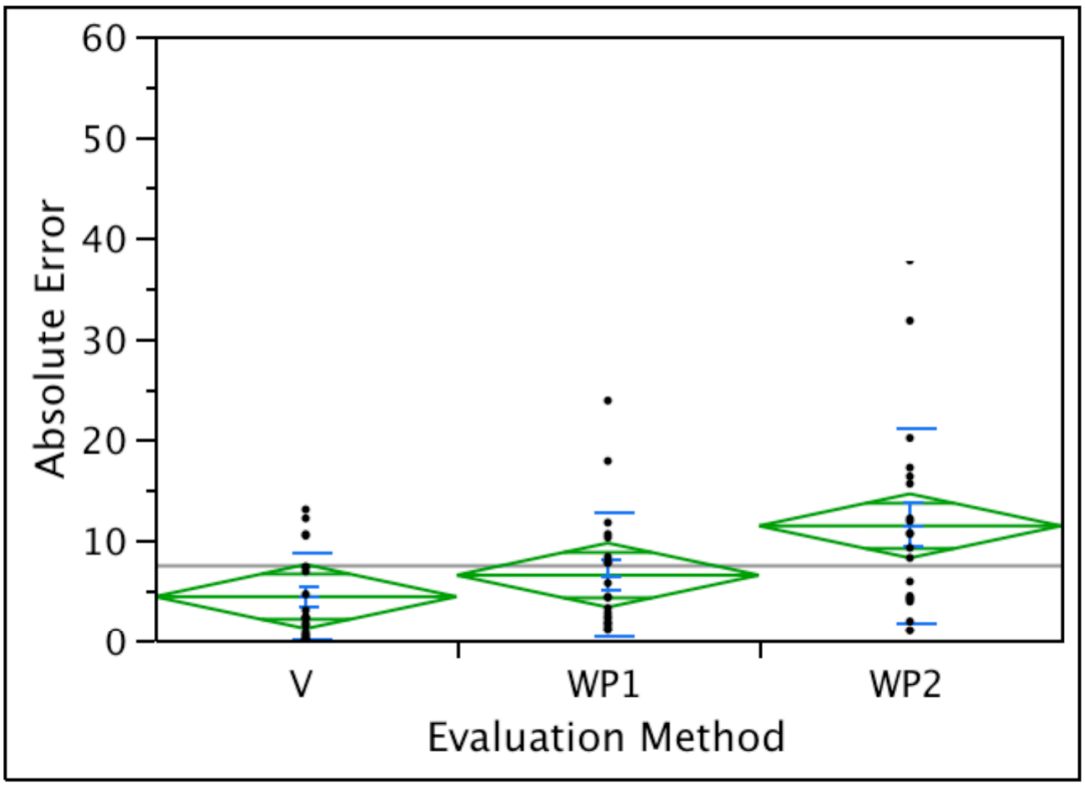

Method	Mean % disease	
V	4.36	B[y]
WP1	6.49	AB
WP2	11.37	A
p value	< 0.0090[z]	

[y] means differentiated using Tukey's $HSD_{\alpha = 0.05}$. Means not connected by the same letter are significantly different

[z] means compared using $ANOVA_{\alpha = 0.05}$

Figure 3.9. Comparison of the mean absolute error among experiments (1.1,1.2,2.1,2.2) by evaluation method. Absolute error calculated as the absolute difference between actual disease values, as calculated using the IL method, and predicted disease values calculated using the WP1, WP2, and V evaluation methods.

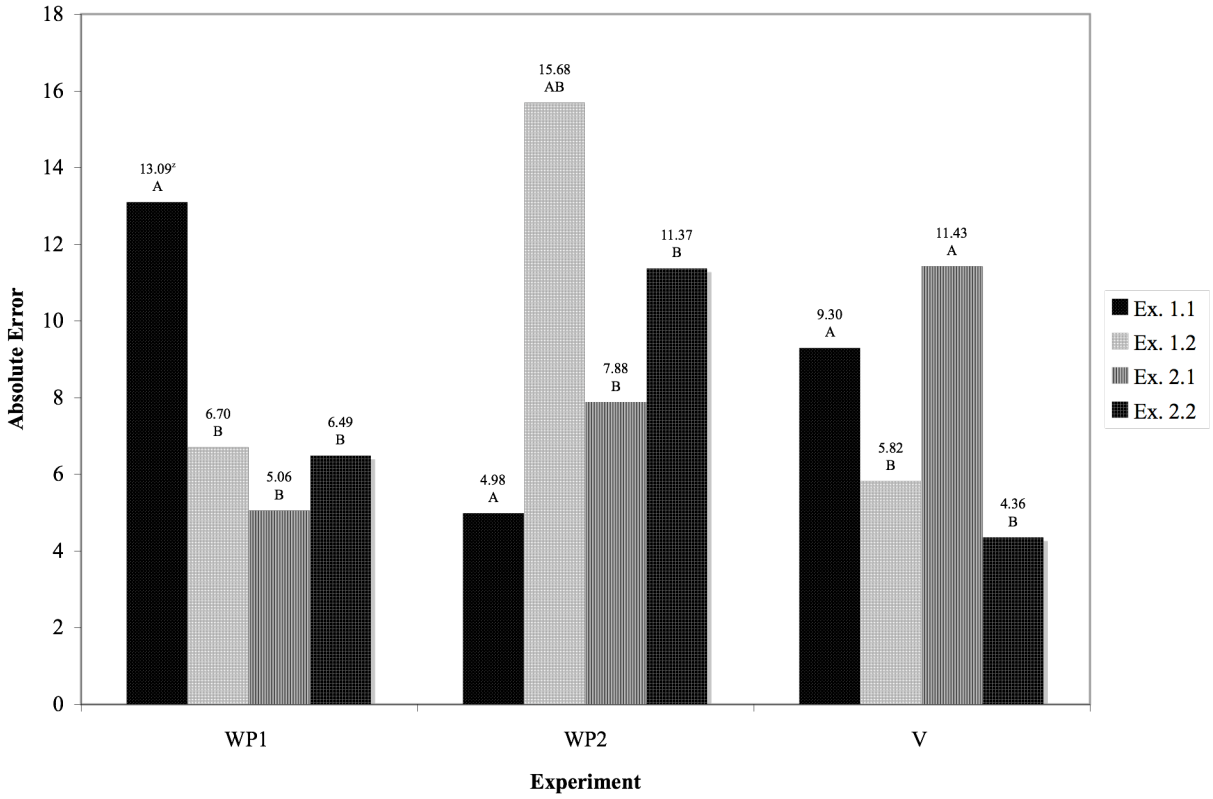

Method	p value
WP1	<0.0001[z]
WP2	<0.0001
V	0.0003

[y] means differentiated using Tukey's $HSD_{\alpha = 0.05.}$ Means not connected by the same letter are significantly different

[z] means compared using $ANOVA_{\alpha = 0.05}$

Figure 3.10. Comparison of precision among evaluation methods for experiment 1.1. Precision calculated as the standard deviation within three disease severity ratings of a single plant evaluated using DIA of three separate images (WP1, WP2), or visual evaluations performed by three separate evaluators (V). The diamond indicates points within the 95% confidence interval and the line across each diamond represents the group mean. The short horizontal lines indicate one standard deviation from the mean. The horizontal line crossing the entire graph indicates the grand mean.

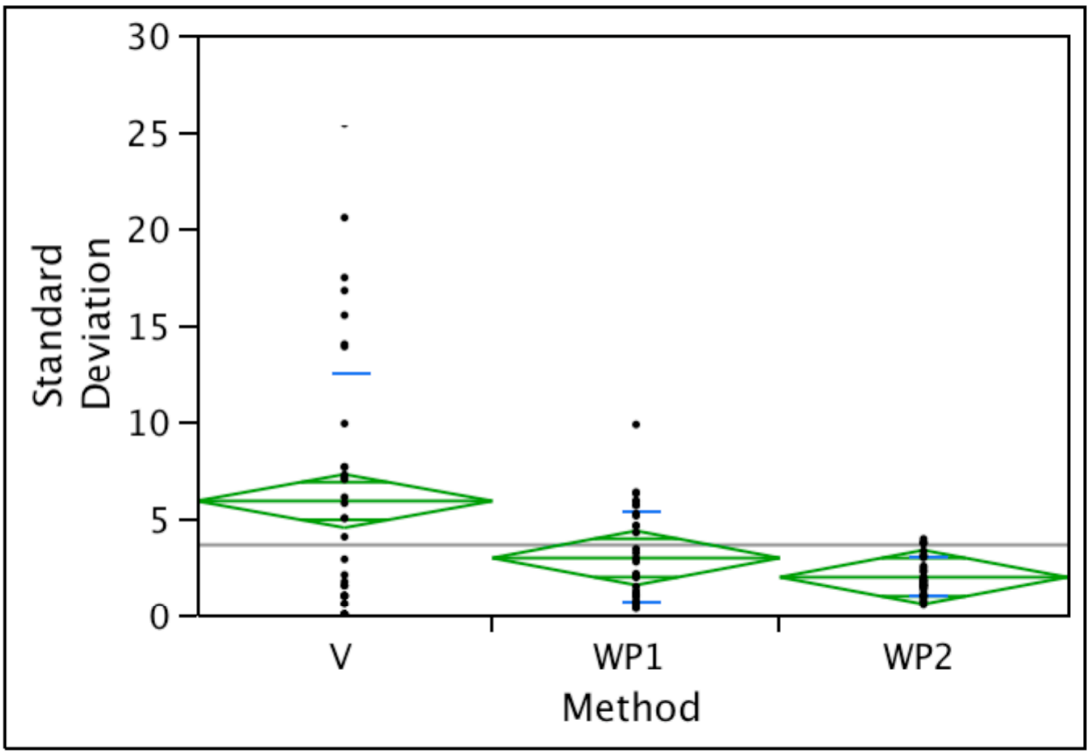

Method	Mean % disease	
V	5.88	A[y]
WP1	2.98	B
WP2	1.83	BC
p value	< 0.0090[z]	

[y] means differentiated using Tukey's HSD$\propto$ = 0.05. Means not connected by the same letter are significantly different

[z] means compared using ANOVA$\propto$ = 0.05

Figure 3.11. Comparison of precision among evaluation methods for experiment 1.2. Precision calculated as the standard deviation within three disease severity ratings of a single plant evaluated using DIA of three separate images (WP1, WP2), or visual evaluations performed by three separate evaluators (V). The diamond indicates points within the 95% confidence interval and the line across each diamond represents the group mean. The short horizontal lines indicate one standard deviation from the mean. The horizontal line crossing the entire graph indicates the grand mean.

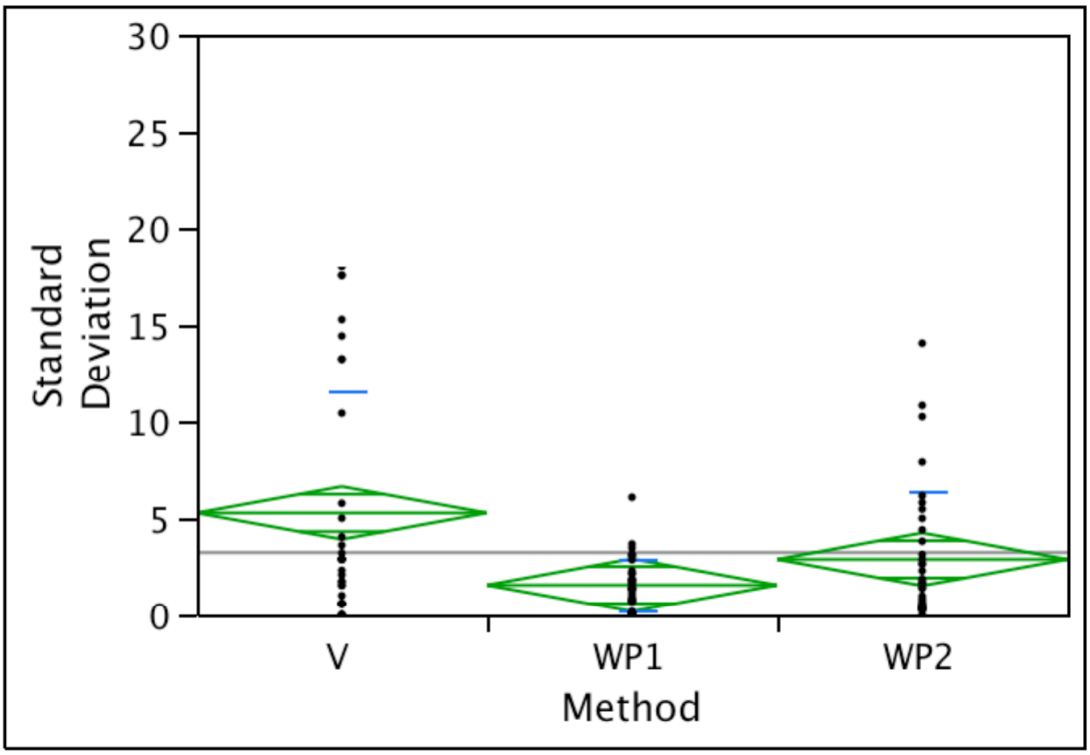

Method	Mean % disease	
V	5.28	A[y]
WP1	1.54	BC
WP2	2.88	B
p value	< 0.0090[z]	

[y] means differentiated using Tukey's $HSD_{\alpha = 0.05}$. Means not connected by the same letter are significantly different

[z] means compared using $ANOVA_{\alpha = 0.05}$

color was far enough removed in hue from both plant and diseased areas on the hue spectrum to provide an effective background.

Placement of the cloth around the base of the plant required extra time and also occasionally created shadows due to folds in the cloth. In future studies, shadows might be avoided by using a cloth to mask the stand only, with a hole left for placement of the cone. Not using a cloth cover would show the soil within the cone, but all macros used for this study replaced the soil in each image with a solid blue background using an intensity threshold. If this were used, it would be necessary to mask the cone top or use cones with a color distinct from both healthy and necrotic tissue.

Although the same cloth was used for each image capture, the color appears different in certain images. Two possible factors influencing this variability are the light source and exposure during image capture. Color temperature of a light source can produce appearance differences both visually and in captured images (Russ, 2007). Differences in light temperature from varying intensity of sources beyond the light stands may have caused some variability. The images were not closed off from outside light sources and pictures were not taken at the same time every day. Hue variance may also have been caused by the method used to balance the aperture when capturing an image. The aperture should have been set to f/8 and the shutter speed adjusted to balance the light meter to zero for one neutral image. This setting should then have been used for all remaining images. Instead, the shutter speed was adjusted for each picture, overexposing images with greater disease severity.

Lindow et al. (1983) found that using a closed light box with a red filter placed over fluorescent lights greatly enhanced the contrast between lesions and healthy tissue. Image analysis in the study showed high correlations to actual disease values in leaves of pinto beans (*Phaseolus vulgaris* L.)($\rho = 0.99$.), California buckeye (*Aesculus californica* (Spach) Nutt.)($\rho = 0.97$), sycamore (*Platanus racemosa* Nutt.)($\rho = 0.99$), tomato (*Lycopersicon esculentum* L.)($\rho = 0.97$), and bracken fern (*Pteridium aquilinum* L.)($\rho = 0.98$). A digital video camera was used to capture images that were then digitized and converted to a grayscale. Although the method used in Lindow et al.'s study differs from the method used in our study, a red filter may still provide greater contrast between healthy and non-healthy tissue in color images. Providing consistent illumination between images, balancing the exposure prior to image capture, and deepening the

contrast between healthy tissue and diseased tissue may all reduce some of the variability seen in the performance of the DIA macros used in this study.

Image Storage

Two types of image compression methods exist for image storage, lossy and lossless. A lossy method, such as JPEG storage, compresses an image by averaging pixels whose pixel values differ only slightly. A lossless method does not compromise pixel values and can exactly reconstruct each pixel value, requiring larger amounts of storage (Russ, 2007). In our study, images were stored in JPEG (Joint Photographic Experts Group) format since this format requires less memory. Storing images in JPEG format may or may not have had an affect on the accuracy of the DIA method. Unlike lossless formats, such as TIFF (Tagged Image File Format), JPEG is a lossy format, which eliminates redundant or near redundant information. Individual pixel information is deleted resulting in an image that is compressed, but also degraded from the original. Such degradation can distort sharp lines, change colors by averaging pixels, and introduce artifacts into the image. Image degradation resulting from image compression may reduce the accuracy of DIA measurements. Lossless formats are generally preferred for any image being analyzed digitally (Russ, 2007).

At image resolutions of higher than 0.8 MP, Steddom et al. (2005) saw little difference in the accuracy of DIA performed on scanned leaves of diseased wheat between original 8.4 MP TIFF images and JPEG images compressed at quality settings of 100, 75, 50, and 25. Results suggest JPEG may be a preferred storage method as it has little effect on DIA accuracy while offering greater storage capacity. The effect of image storage format's on DIA accuracy was not evaluated in images taken by a digital camera. Images taken with a camera are more likely to have brightness and shading differences compared to images obtained using a scanner. Whether JPEG storage impacted the accuracy of images in this study cannot be determined at this time.

Disease Evaluation

The accuracy of DIA evaluations using the most accurate hue threshold was greater than visual evaluations in two of the four experiments and not significantly different from visual evaluations in two of the four experiments with the hue threshold required to most accurately distinguish lesions varying among experiments. The hue threshold used in WP1 tended to have a lower, more consistent absolute error compared to WP2 in experiments 1.2, 2.1, and 2.2, which

had a wider range of disease severity. The hue threshold used in WP2 was more effective than WP1 in Ex 1.1 where mean disease severity was lower and disease severity was less distributed across the entire range of disease. This variability suggests a user defined hue threshold may be more accurate compared to using a set hue threshold when evaluating disease using DIA. The average absolute error was more consistent for WP1 and WP2 compared to V. Because of this, a correction factor might be used to provide more accurate assessment. Providing consistent illumination between images, balancing the exposure prior to image capture, and deepening the contrast between healthy tissue and diseased tissue may also provide greater accuracy in DIA evaluations and eliminate variability in the hue threshold range required to accurately detect lesions.

The variability within ratings performed using either WP DIA macro was significantly lower than the variability within ratings performed by three evaluators using traditional visual evaluation. Overall the most accurate evaluation method varied by experiment while precision was significantly higher in DIA evaluations compared to visual evaluations performed by three evaluators. The improved precision of DIA evaluation methods would allow better comparisons of results across studies performed by multiple evaluators.

Our study was performed in a greenhouse setting with highly controlled disease conditions. Disease evaluations were also performed in a highly controlled setting with uniform plant placement and lighting. The inability of DIA to differentiate between abiotic stress and biotic stress or between diseases caused by pathogens would limit the effectiveness of this method at evaluating disease in the field. Future research would be required to tailor the DIA method used in our study so that it could be used in field evaluations. Precision of this method is improved over visual evaluation. Although accuracy was not significantly improved compared to visual evaluations, the consistency of this method suggests adjustments to the method or a correction factor may improve accuracy. This method provides an objective precise alternative to visual evaluations under controlled conditions.

Literature Cited

Bock, C.H., P.E. Parker, A.Z. Cook, and T.R. Gottwald. 2008. Visual rating and the use of image analysis for assessing different symptoms of citrus canker on grapefruit leaves. Plant Disease 92:530-541.

Horst, G.L., M.C. Engelkle, and W. Meyers. 1984. Assessment of visual evaluation techniques. Agronomy Journal 76:619-622.

Horvath, B.J., and J.M. Vargas. 2005. Analysis of dollar spot disease severity using digital image analysis. International Turfgrass Society Research Journal 10:196-201.

Karcher, D.E., and M.D. Richardson. 2003. Quantifying turfgrass color using digital image analysis. Crop Science 43:943-951.

Kwack, M.S., E.N. Kim, H. Lee, K.D. Kim, J.-W. Kim, and S.-C. Chun. 2005. Digital image analysis to measure lesion area of cucumber anthracnose by *Colletotrichum orbiculare*. Journal of General Plant Pathology 71:418-421.

Lindow, S.E., and R.R. Webb. 1983. Quantification of foliar plant disease symptoms by microcomputer-digitized video image analysis. Phytopathology 73:520-524.

Martin, D.P., and E.P. Rybicki. 1998. Microcomputer-based quantification of maize streak virus symptoms in *Zea mays*. Phytopathology 88:422-427.

Moya, E.A., L.R. Barrales, and G.E. Apablaza. 2005. Assessment of the disease severity of squash powdery mildew through visual analysis, digital image analysis and validation of these methodologies. Crop Protection 24:785-789.

Nutter Jr., F.W., M.L. Gleason, J.H. Jenco, and N.C. Christians. 1993. Assessing the accuracy, intra-rater repeatability, and inter-rater reliability of disease assessment systems. Phytopathology 83:806-812.

Olmstead, J.W., and G.A. Lang. 2001. Assessment of severity of powdery mildew infection of sweet cherry leaves by digital image analysis. HortScience 36:107-111.

Richardson, M.D., D.E. Karcher, and L.C. Purcell. 2001. Quantifying turfgrass cover using digital image analysis. Crop Science 41:1884-1888.

Russ, J.C. 2007. The Image Processing Handbook. 5th Edition ed. Taylor & Francis Group, LLC, Boca Raton.

Steddom, K., M. McMullen, B. Schatz, and C.M. Rush. 2005. Comparing Image Format and Resolution for Assessment of Foliar Diseases of Wheat. Plant Health Progress doi: 10.1094/PHP-2005-0516-01-RS.

Wijekoon, C.P., P.H. Goodwin, and T. Hsiang. 2008. Quantifying fungal infection of plant leaves by digital image analysis using Scion Image Software. Journal of Microbiological Methods 74:94-101.

Zar, J.H. 1999. Biostatistical analysis. 4th ed. Prentice-Hall, Inc, Upper Saddle River.

Chapter 4

Screening *Festuca arundinacea* plant introductions for resistance to *Rhizoctonia solani* and *Rhizoctonia zeae* using digital image analysis

Introduction

In Eastern Virginia, tall fescue is one of the most common turfgrasses grown in home lawns since it is well adapted to Virginia's temperate, transition zone climate. Tall fescue is a cool season turfgrass that is susceptible to a number of diseases. Of these, brown patch, caused by the fungus *Rhizoctonia solani*, is one of the most common and destructive. There are a number of chemical and cultural control options for brown patch on tall fescue. As environmental concern and regulations increase, alternatives to chemical controls, such as planting disease resistant cultivars, are becoming more popular as a means of disease control.

Planting disease resistant cultivars is a simple, inexpensive disease control option and there are many tall fescue cultivars available that have some brown patch resistance. However, this resistance often is not consistent across locations as can be seen in data collected for the National Turfgrass Evaluation Program (NTEP), a widely used and recognized U.S. program for evaluating various turfgrass characteristics in trials performed across multiple locations (NTEP, 2005)(Table 1.3). This variability is influenced by varying disease severity and climatic conditions across locations. Other possible influences include the visual evaluation system used to evaluate the resistance response of cultivars and artificial inflation of disease values by pathogens that cause symptoms similar to those of *R. solani*.

Turfgrass disease is traditionally evaluated using a visual assessment. Visual evaluations are inexpensive and easy to perform, however visual evaluation of turfgrass disease, turfgrass quality, and turfgrass cover have all been shown to have high inter-rater variability, variability among ratings done by multiple researchers, and intra-rater variability, variability within ratings done by a single researcher (Horst et al., 1984; Nutter Jr. et al., 1993; Richardson et al., 2001).

Digital image analysis has been shown to accurately assess disease severity on numerous agricultural and horticultural crops (Lindow and Webb, 1983). In turfgrass research, DIA has been successful at detecting the disease dollar spot and disease progress curves formed using DIA evaluations showed no significant difference from those formed using physical counts of

dollar spot foci (Horvath and Vargas, 2005). The accuracy of DIA also has been quantified in evaluating turfgrass color and percent cover (Karcher and Richardson, 2003; Richardson et al., 2001).

Another possible source of variability in the resistance response of many brown patch resistant cultivars may be the influence of the pathogen *Rhizoctonia zeae.* *Rhizoctonia* leaf and sheath spot is caused by *R. zeae,* a pathogen related to *R. solani* that can produce symptoms very similar, and frequently indistinguishable, from those produced by *R. solani*. Often the two can only be distinguished through examination of cultured isolates. However, *R. zeae* is typically not included in brown patch resistance breeding programs. If cultivars vary in their resistance to *R. solani* versus *R. zeae,* yet both pathogens present brown patch-like symptoms, cultivars bred for *R. solani* resistance may have artificially inflated disease ratings in areas where *R. zeae* is causing disease.

Rhizoctonia solani is thought to be dominant in Northern regions, while *R. zeae* is thought to be dominant in Southern regions (Elliot, 1999). Studies performed in New Jersey, South Carolina, and Virginia have found higher than expected frequencies of *R. zeae* (Martin et al., 2001; McCall, 2006; Plumley, 1988). In 2001, Martin et al. reported significant differences in isolation frequency of *R. zeae* and *R. solani* between two locations in South Carolina. Research by McCall (2006) showed similar results in Virginia. *Rhizoctonia zeae* was isolated from brown patch-like symptoms in Virginia and appeared to be more prevalent in the eastern half of the state. *Rhizoctonia zeae*, which has a higher temperature optimum compared to *R. solani*, may be more prevalent at lower elevations or in areas with higher average temperatures. Cultivars with resistance to *R. solani* but not *R. zeae* may perform better in cultivar evaluations studies performed in areas where *R. solani* is dominant and perform poorly in studies done in areas where *R. zeae* is dominant.

Determining whether cultivar resistance differs between the two pathogens, *R. solani* and *R. zeae*, and then identifying resistance to both pathogens using DIA, may reduce some of the variability seen in current cultivar evaluation programs for brown patch resistance in tall fescue. The objective of this study is to use DIA to evaluate the resistance response of tall fescue germplasm and cultivars in an initial screen and final screen to the pathogens *R. solani* and *R. zeae.*

Materials and Methods

Plant Materials and Maintenance

An initial screen was performed first to eliminate plant introductions with poor resistance to either *R. solani* or *R. zeae*. The initial screen included seventeen tall fescue plant introductions (PI) that were selected from the National Plant Germplasm System (NPGS) based on similarity of collection location climate to the climate of Eastern Virginia (Table 3.1). Four commercial cultivars were chosen based on their average rank across all locations in the 2002 National Turfgrass Evaluation Program (NTEP) trials for brown patch resistance on tall fescue. These included Falcon IV, a high-ranking cultivar, Kentucky 31 and Millennium, both medium-ranking cultivars, and Stetson, a low-ranking cultivar. Plant introductions that performed well in the initial screen were subject to a more thorough final screen in which 20 seeds were selected from each PI with each seed grown and maintained as a vegetative clone.

Each PI or cultivar was assigned a number from 1-21. PIs will be referred to by the prefix PI followed by their number (ex. PI 4) and cultivars will be referred to by a prefix consisting of the first two letters of the cultivar name followed by their number (ex. KE 21). Tall fescue clones will have a dash following this with a number from 1-20 (ex. PI 4-1). This reference system will be used throughout the remainder of this document (Table 3.1).

Initial Screen

Four seeds from each PI were planted in 3.8 cm diameter conetainers™ (Steuwe & Son, Corvallis, OR) filled with Pro-Mix potting media containing biofungicide (*Bacillus subtilis* MBI 600) (Code 0532, Premier Horticulture, Quebec, Canada). These were allowed approximately 6 weeks to mature prior to screening. Plants were grown in a glass greenhouse with a fan and pad cooling system. Temperature was not consistent and varied according to outside temperature. Plants were watered daily for 2-3 minutes using an overhead irrigation system with between 310 and 414 kPa of pressure. Plants were heavily fertilized with 3 applications per month of 20-20-20 at 48.8 kg N ha^{-1}. Plants were maintained at a height of approximately 7.6 cm and cut to this height prior to inoculation. Two PIs (PI-10, PI-14) and the cultivar ME-18 were excluded from initial screens due to poor germination.

Final Screen

PIs were selected based on their performance in the Initial screen. Twenty seeds were selected from each PI and these were grown and maintained each as vegetative clones. As these plants produced tillers, they were divided and planted in 3.8 cm diameter conetainers filled with Pro-Mix containing biofungicide. Sixteen conetainers of each tall fescue clones were planted and maintained for use in the final screen. PIs were planted in order beginning with PI 1-1 and ending with KE 21-20. PIs without enough plant material were screened in only one screen for each pathogen. These included the following PI clones: 1-8, 12-7, 12-15, 13-13, 15-2, 15-5, 15-16, 15-20. The following PI clones were excluded from all screens because of plant death: 4-13, 13-5, 13-12, 13-17.

Plant maintenance mirrored the initial screens with exception to fertility. Fertility was applied in the form of 20-20-20 through the month of July at which point fertilizer was switched to 28-8-18. Heavy fertility (3 applications at 48.8 kg N ha^{-1}) was applied during March and April to increase plant susceptibility to disease. These rates caused disease in the greenhouse prior to inoculation and were reduced to between 24.4 and 73.2 kg N ha^{-1} applied over 1 or 2 applications per month for the months of May through September. One application of Daconil Ultrex Turf Care (Syngenta Group Co., Wilmington, DE) at a rate of 9.9 kg ha^{-1} was made on June 22, 2009 to treat brown patch and leaf spot diseases. This was applied five weeks prior to final screen inoculations.

Inoculation

Three isolates of *R.solani* were chosen for use as inoculum based on their performance in virulence tests done prior to this study (data not shown). These isolates were collected from *Poa annua* putting greens from the Virginia Tech Turfgrass Research Center in Blacksburg, Virginia in 2006. Three isolates of *R. zeae* were chosen based on their performance in virulence studies done by McCall (McCall, 2006). These were collected from tall fescue and Kentucky bluegrass at a variety of locations across the state of Virginia.

Initially, inoculum was grown on healthy leaves of "Kentucky 31" tall fescue (K31). These were surface sterilized in a 10% bleach solution for 60 seconds and then rinsed in sterilized de-ionized water for 30 seconds. Many plates were contaminated with other fungi, possibly due to endophytes contained within the K31. To reduce contamination and provide a

more consistent inoculum size, filter paper was used in place of the K31 leaves. These were cut to 2 cm by 0.5 cm and autoclaved for 1 hr prior to use. Filter paper rectangles were placed radially around a 4 mm diameter plug of *R. solani* or *R. zeae* on potato dextrose agar (PDA) resulting in colonization of the paper (Figure 3.1). Plants were inoculated by placing three infected filter paper pieces, one piece from each isolate, within the plant canopy of each conetainer.

Disease Treatment

Cones were placed in a randomized complete block design with four replications of each PI or cultivar (Initial Screen) or PI clone or cultivar clone (Final Screen). Two initial screens and two final screens were performed for *R. solani* resistance (ISRS1, ISRS2, FSRS1, FSRS2) and two initial screens and two final screens were performed for *R. zeae* resistance (ISRZ1, ISRZ2, FSRZ1, FSRZ2).

The final screen contained 256 treatments and occupied 3 m^2 of space. Because of space limitations, two chambers were required for each run. Blocking was based on location within each chamber with block 2 and 4 placed in the rear of chamber A and B respectively and blocks 1 and 3 placed at the front of chamber A and B respectively (Figure 4.1).

A heating mat set to 100 °C was placed across the bottom of each chamber to provide high temperatures (see results) for disease development. High humidity (approximately 99%) was maintained through a mist irrigation system consisting of three irrigation heads per chamber with tubing threaded through holes cut in the top of the chamber. Irrigation was applied for 3 minutes each morning.

Plants were inoculated and placed within the chambers for a period of 12 days. Upon removal, plants were placed on sub-irrigated greenhouse benches for a 24-hr period to allow the canopy to dry.

Disease Evaluation

Image Capture

Pictures were taken prior to inoculation and again after the 24-hr drying period. Initial pictures were taken to adjust for any naturally senescing plant tissue that might be present prior to inoculation as this would be included as disease by the DIA software. Most senescent tissue

Figure 4.1. Diagram illustrating a top down view of the randomized block design used in screening tall fescue plants for resistance to *R. solani* or *R. zeae*. Two chambers were used (KC A, KC B) with blocking indicated in the left corner. Plants were randomly numbered and placed in stands from front to back then left to right within each block. Un-inoculated tall fescue plants were placed along the side, front, and back of the chamber.

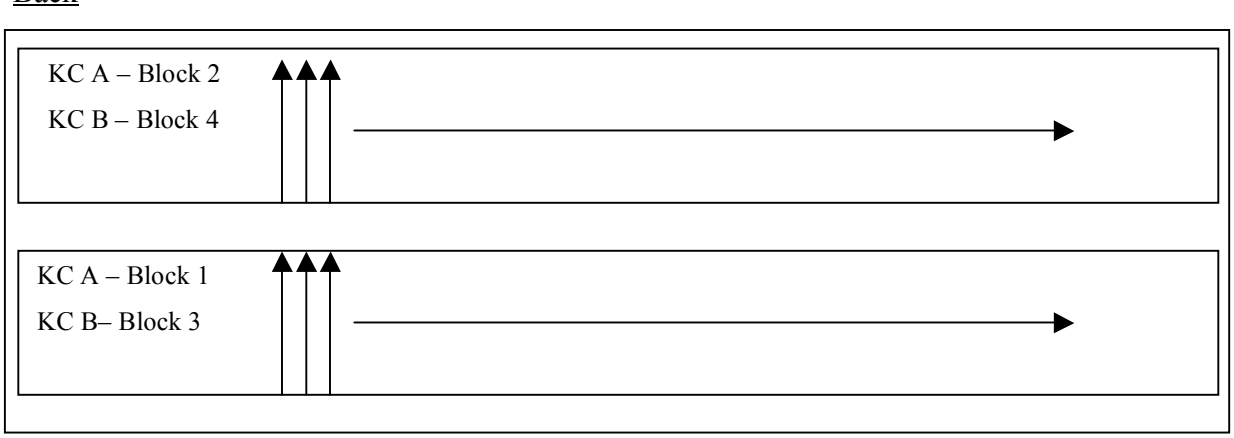

was removed prior to initiation of the study as an added precaution. An index mark was placed on conetainers and the stand prior to inoculation to provide consistent leaf orientation between the pre-inoculation and post-inoculation pictures. A Canon PowerShot G6 digital camera was placed on a tripod with the orientation adjusted to take a top down picture. The camera's aperture was set at f/8 with the shutter speed adjusted to balance the light meter at zero. Two Calumet (Calumet Photographic, Inc., 2007) light stands, each containing four 40-watt compact spiral fluorescent bulbs, were placed on either side of the stand (Figure 3.3).

Digital Image Analysis

Disease evaluation was performed using a macro written for use with APS Assess (APS Press, 2002) that performed the following procedures (Appendix A):

Assess DIA macro 1

1) The plant area was selected from the background using a hue threshold of 31-low and 191-high. The background was replaced with a solid blue background using the command: Edit > Substitute background.
2) The soil was selected using an intensity threshold of 66-low and 255-high. The soil was replaced with a solid blue background using the command: Edit > Substitute background.
3) The total leaf area selected using hue threshold of 31-low and 191-high. The total area in pixels was calculated by selecting the 'Area' button on the threshold panel.
4) The total lesion area was selected using a hue threshold. Results from chapter 3 showed increased accuracy with a user defined hue threshold for picking out lesions. In this study, viewing a random selection of pictures from each screen and visually determining the average hue threshold values that most accurately selected the lesioned areas determined the hue threshold for each replication within each screen. Eight images were evaluated for each of the initial screens (approximately 10% of all images) and forty images were evaluated for each of the final screens (approximately 4% of all images). The hue threshold used to pick out lesions was modified within the macro to correspond with the chosen value for each replication within each screen. The hue values used for each screen to select lesions are listed below:

a) ISRS1, ISRS2, ISRZ1: 31-low, 115-high
b) ISRZ2: 31-low, 120-high
c) FSRS1 rep 1-2, FSRS2 rep 1-2: 31-low, 110-high
d) FSRS1 rep 3-4, FSRS2 rep 3-4: 31-low, 115-high
e) FSRZ1, FSRZ2: 31-low, 101-high

5) Disease was calculated as a ratio of total lesion area to total leaf area
6) Total disease was calculated as the percent disease of the post-inoculation picture minus the percent disease of the pre-inoculation picture.

Statistics

Differences in the mean disease values of PIs and PI clones were evaluated using ANOVA ($\alpha = 0.05$). In screens showing a significant difference in mean disease severity, superior performance was identified using Wards hierarchical cluster analysis in JMP (SAS Institute Inc, Cary, NC). Evaluations of PIs and cultivars as a whole were divided into three clusters classified as highest resistance, medium resistance, and lowest resistance. PI and cultivar clones were broken into nine clusters. The cluster containing PI or cultivar clones with the lowest disease values was considered highest resistance.

Results

Initial Screen

Mean disease severity was significantly different between all screens. *R. solani* screens had significantly higher disease severity than *R. zeae* screens (Figure 4.2).

Of the two screens performed per pathogen, only ISRS1 ($p = 0.0055$) and ISRZ1 ($p = 0.0013$) showed significant differences in mean disease severity among PIs and cultivars (Table 4.1). Two screens, ISRS2 ($p = 0.3748$) and ISRZ2 ($p = 0.3343$), showed no significant difference in mean disease severity among PIs and cultivars (Table 4.1). The established cultivars, FA-20, ST-19, and KE-21, and PIs 5 and 13, were in the highest resistance cluster in both the *R. solani* and *R. zeae* screen. PIs 1, 2, 8, and 15 were in the highest resistance cluster only in the *R. solani* screen and PIs 4, 12, and 17 were in the highest resistance cluster only in the *R. zeae* screen (Figure 4.3, Figure 4.4)

Figure 4.2. Scatterplot matrix showing the distribution of disease severity and table showing mean disease severity in initial screens to *R. solani* and *R. zeae* (ISRS1, ISRS2, ISRZ1, ISRZ2).

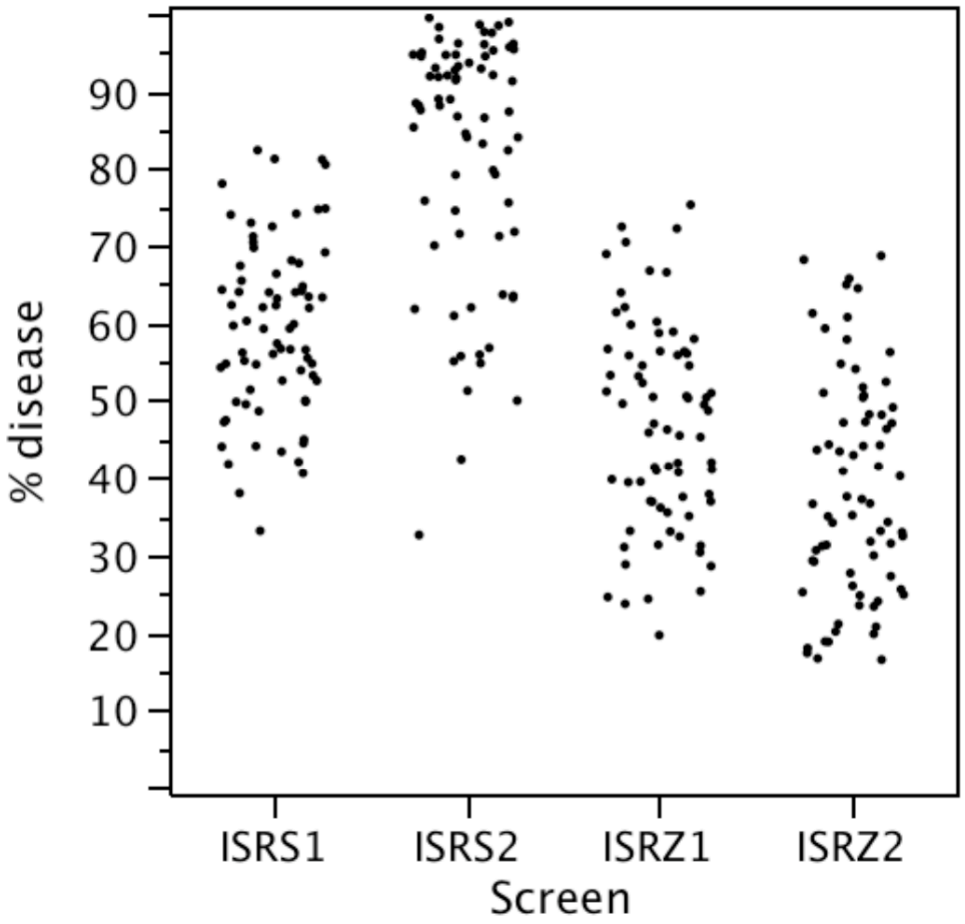

Experiment	Mean % disease	
ISRS1	59.38[y]	B[z]
ISRS2	82.08	A
ISRZ1	46.66	C
ISRZ2	38.62	D

[y] means separated using $ANOVA_{\alpha = 0.05}$

[z] means differentiated using Tukey's $HSD_{\alpha = 0.05}$. Means not connected by the same letter are significantly different.

Table 4.1. ANOVA, means, and standard deviation (SD) table for initial screens to *R. solani* (ISRS1, ISRS2) and *R. zeae* (ISRZ1, ISRZ2).

	ISRS1			ISRS2			ISRZ1			ISRZ2		
ID	Mean	SD	Cluster[y]	Mean	SD	Cluster	Mean	SD	Cluster	Mean	SD	Cluster
PI 1	50.85	5.22	H	86.92	10.83	-	49.13	18.65	M	37.91	18.14	-
PI 2	55.49	5.55	H	79.76	18.59	-	51.71	11.29	M	33.69	18.05	-
PI 3	63.13	4.70	M	80.33	14.23	-	51.46	12.99	M	29.54	17.00	-
PI 4	63.85	9.08	M	84.73	19.60	-	41.59	12.53	H	39.94	15.11	-
PI 5	55.62	6.53	H	81.00	21.48	-	41.52	13.67	H	36.28	21.59	-
PI 6	65.11	4.67	M	71.13	20.60	-	54.59	13.08	M	46.59	17.55	-
PI 7	61.80	14.94	M	82.63	15.81	-	55.79	13.37	M	40.33	13.61	-
PI 8	56.48	9.16	H	71.82	15.80	-	47.17	6.87	M	31.17	5.78	-
PI 9	76.17	4.23	L	94.89	3.08	-	67.73	8.05	L	55.47	21.38	-
PI 11	63.18	8.14	M	92.39	8.42	-	47.24	8.93	M	33.76	6.41	-
PI 12	62.79	19.72	M	81.40	20.30	-	42.78	10.72	H	43.95	12.28	-
PI 13	49.29	5.82	H	94.35	4.09	-	32.63	9.19	H	43.65	19.62	-
PI 15	55.06	13.45	H	82.02	18.45	-	54.08	8.64	M	48.12	11.82	-
PI 16	67.42	12.28	M	80.27	13.25	-	55.03	2.97	M	37.07	10.55	-
PI 17	67.01	6.54	M	75.51	18.04	-	39.29	13.62	H	30.10	3.09	-
ST 19	56.56	7.06	H	69.17	27.63	-	37.80	10.15	H	30.11	13.38	-
FA 20	43.97	9.28	H	82.09	12.08	-	36.88	7.18	H	37.10	6.50	-
KE 21	55.00	9.87	H	87.03	11.95	-	33.35	9.77	H	40.32	6.23	-
Mean	59.38	8.68		82.08	15.24		46.66	10.65		38.61	13.23	
R^2	0.47			0.45			0.54			0.40		
W- p value[z]	0.0055*			0.3748			0.0013*			0.3343		
Rep- p value	0.5349			0.0003*			0.0529			0.0057*		

[y] Means showing significant differences in ANOVA differentiated into three clusters using Wards hierarchical cluster analysis: highest resistance (H), medium resistance (M), lowest resistance (L).

[z] means separated using $ANOVA_{\alpha = 0.05}$ with replication (Rep) and plant introductions and cultivars as a whole (W) as effects. An asterisk indicates a significant p-value

Figure 4.3. Dendrogram of PI clustering determined by Wards hierarchical clustering for the first run of the initial screen to *R. solani* (ISRS1). Clusters designated as high resistance (·), medium resistance (+), and low resistance (x)

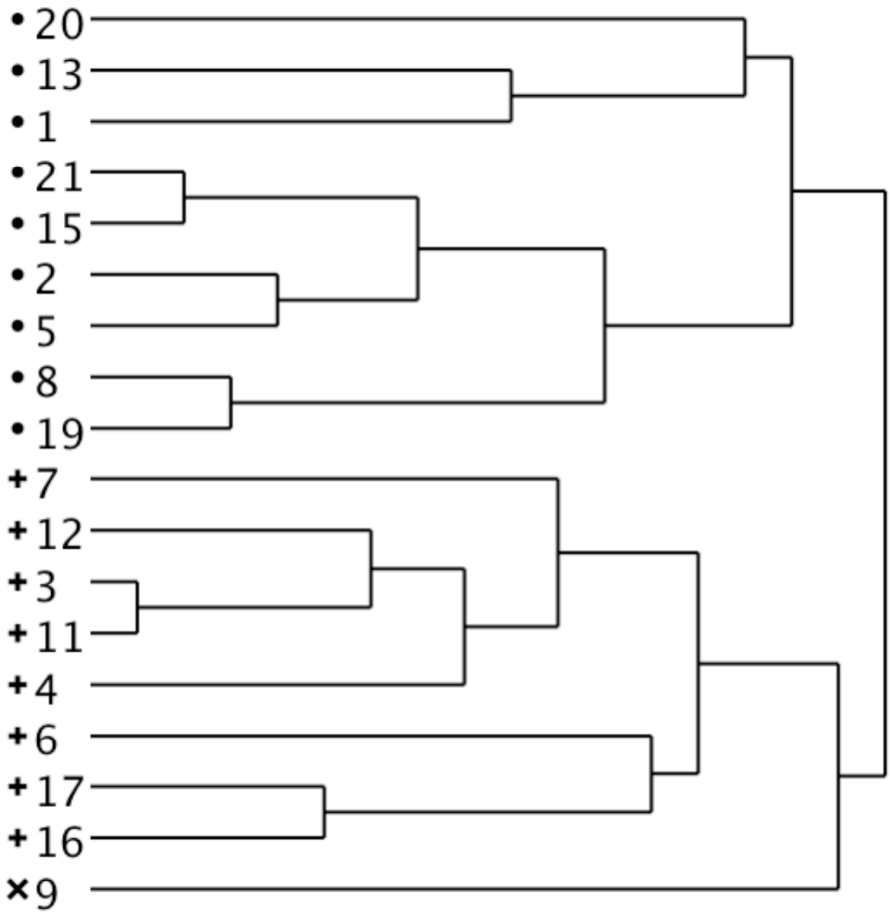

Figure 4.4. Dendrogram of PI clustering determined by Wards hierarchical clustering for the first run of the initial screen to *R. zeae* (ISRZ1). Clusters designated as high resistance (·), medium resistance (+), and low resistance (x)

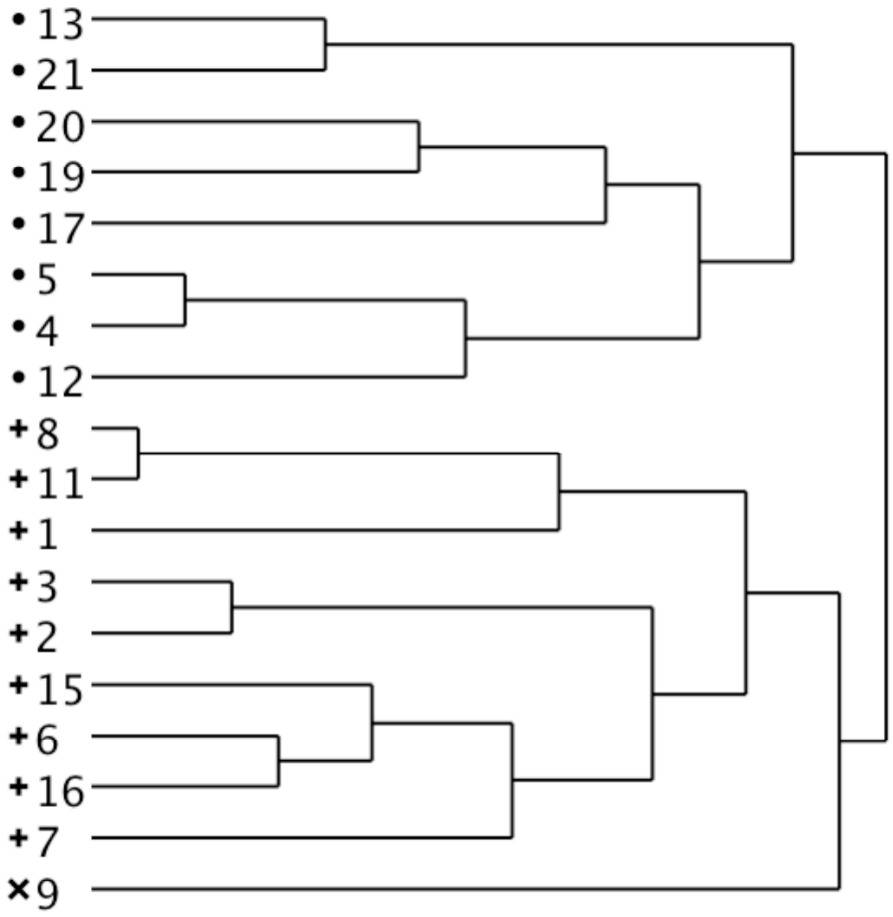

Final Screen

Mean disease severity was similar between screens performed using the same pathogens, but differed by pathogen. Disease values for *R. solani* screens had significantly higher mean disease severity compared to *R. zeae* screens (Figure 4.5). Clones showed high variability in disease susceptibility within a PI or cultivar in all screens (Figure 4.6, Figure 4.7, Figure 4.8, Figure 4.9)

Temperature was inconsistent between experiments. No temperature data are available for the initial screens or FSRZ1 and FSRZ2. Temperature data from within the disease chamber in FSRS1 averaged over the course of the study were 6.5-8.5 °C higher than average daytime temperatures outside the greenhouse. Average daytime temperatures outside for FSRZ1 and FSRZ2 were 26 °C. If temperature differences were consistent with data reported from FSRS1, plants in FSRZ1 and FSRZ2 would have been subject to an average temperature of 32.5-34.5 C. In FSRS1, temperature was, on average, 27-29 °C. Nighttime lows, however, were recorded as dropping to 20 °C for this screen (Figure 4.10). In FSRS2, nighttime temperatures were recorded as dropping to 10 °C in the beginning of the study. Space heaters surrounded by insulation were placed below the chambers. This created temperatures similar to those recorded in FSRS1 for the remainder of the study (Figure 4.10)

There were significant differences in mean disease severity among PIs and cultivars as a whole in FSRS1 ($p < 0.0001$), FSRS2 ($p = 0.0001$), and FSRZ1 ($p <0.0001$). There were no significant differences in mean disease severity among PIs and cultivars as a whole in FSRZ2 ($p = 0.1431$) (Table 4.2). Cluster analysis of the two *R. solani* runs distinguished PIs 1, 2, 4, and 5 as having the highest resistance to *R. solani* (Figure 4.11, Table 4.3). Cluster analysis of the *R. zeae* run distinguished only the established cultivars, MI 18, FA 20, ST 19, and KE 21 as having the highest resistance to *R. zeae* (Figure 4.12, Table 4.3)

There were significant differences in mean disease severity of PI and cultivar clones in FSRS1 ($p < 0.0001$), FSRS2 ($p = 0.0221$), and FSRZ1 ($p < 0.0001$) (Table 4.2). There were no significant differences in mean disease severity among PI and cultivar clones in FSRZ2 ($p = 0.8345$)(Table 4.3). The *R. solani* screen contained twenty-five PI-clones in the cluster exhibiting the highest disease resistance, while the *R. zeae* screen contained nineteen PI-clones in the cluster exhibiting the highest disease resistance (Table 4.4). In the *R. solani* screen, 64% of the top-performing clones were from PIs, while 36% were from established cultivars. In the

Figure 4.5. Scatterplot matrix showing the distribution of disease severity and table showing mean disease severity in final screens to *R. solani* and *R. zeae* (FSRS1, FSRS2, FSRZ1, FSRZ2).

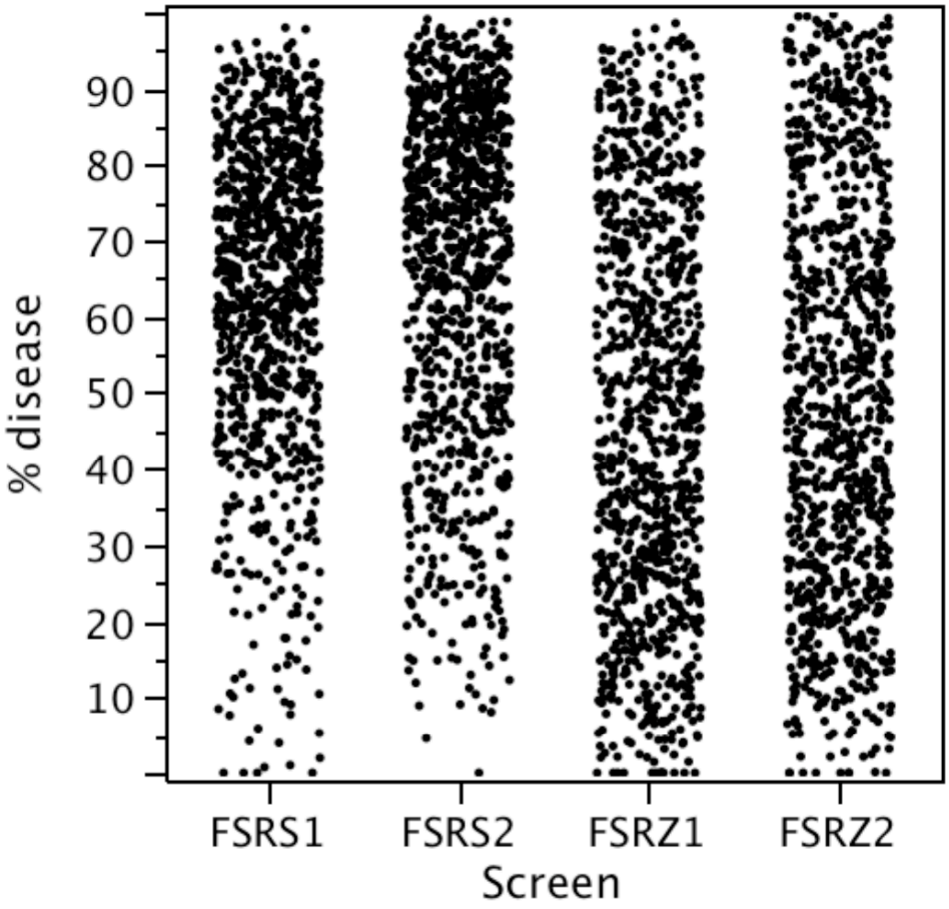

Experiment	Mean % disease	
FSRS1	63.44[y]	B[z]
FSRS2	66.27	A
FSRZ1	47.94	C
FSRZ2	49.94	C

[y] means separated using $ANOVA_{\alpha = 0.05}$

[z] means differentiated using Tukey's $HSD_{\alpha = 0.05}$. Means not connected by the same letter are significantly different

Figure 4.6. ANOVA of mean disease severity by PI or cultivar for the first run of the final *R. solani* screen (FSRS1). The diamond indicates points within the 95% confidence interval and the line across each diamond represents the group mean. The short horizontal lines indicate one standard deviation from the mean. The horizontal line crossing the entire graph indicates the grand mean. Each dot represents the disease severity of the plant within a single conetainer.

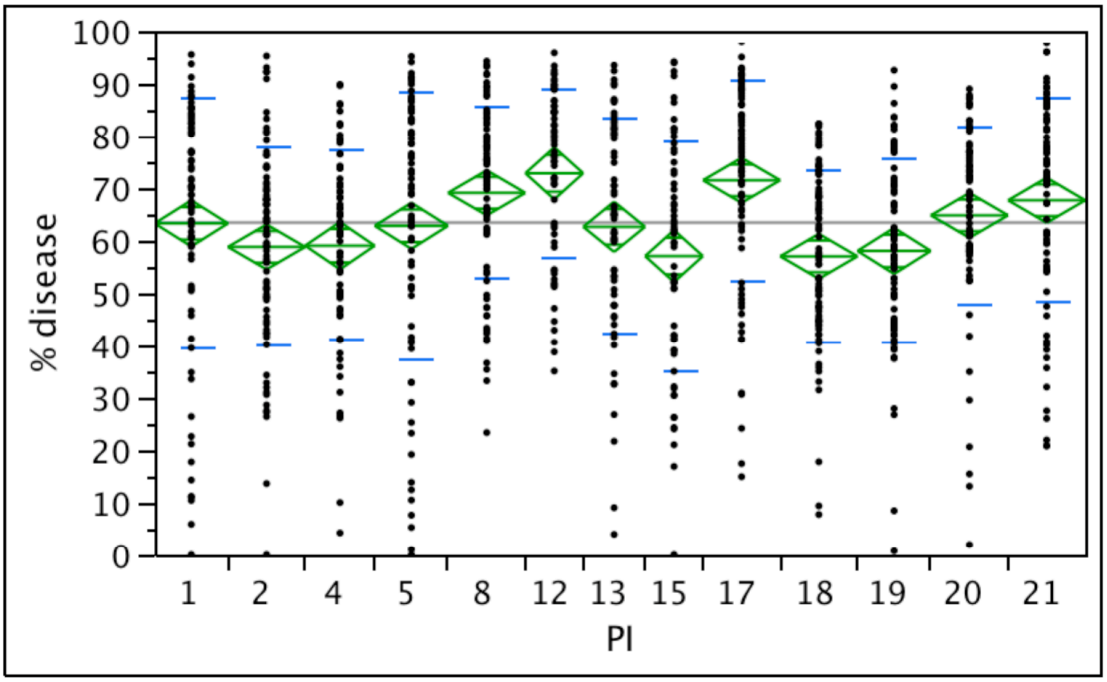

Figure 4.7. ANOVA of mean disease severity by PI or cultivar for the second run of the final *R. solani* screen (FSRS2). The diamond indicates points within the 95% confidence interval and the line across each diamond represents the group mean. The short horizontal lines indicate one standard deviation from the mean. The horizontal line crossing the entire graph indicates the grand mean. Each dot represents the disease severity of the plant within a single conetainer.

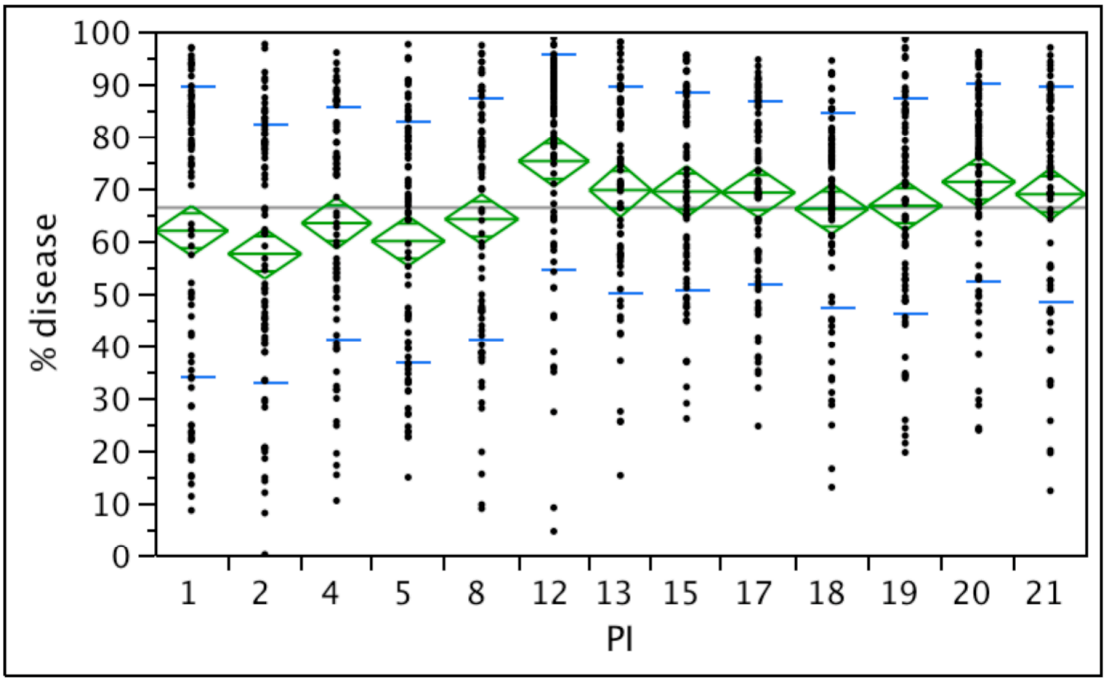

Figure 4.8. ANOVA of mean disease severity by PI or cultivar for the first run of the final *R. zeae* screen (FSRZ1). The diamond indicates points within the 95% confidence interval and the line across each diamond represents the group mean. The short horizontal lines indicate one standard deviation from the mean. The horizontal line crossing the entire graph indicates the grand mean. Each dot represents the disease severity of the plant within a single conetainer.

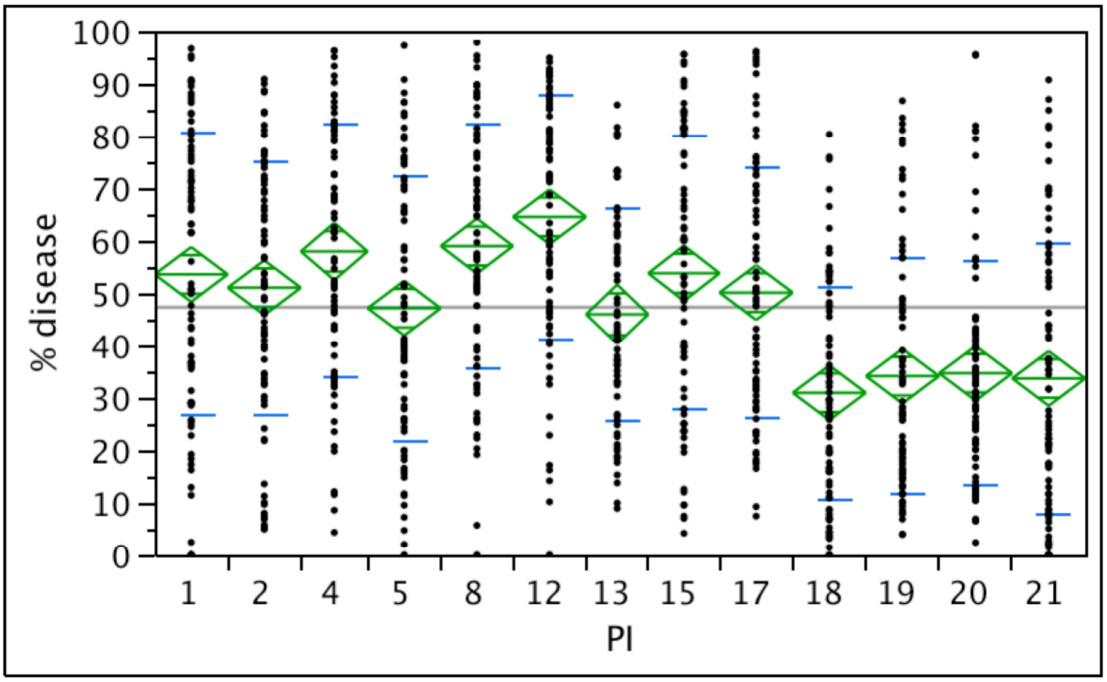

Figure 4.9. ANOVA of mean disease severity by PI or cultivar for the second run of the final *R. zeae* screen (FSRZ1). The diamond indicates points within the 95% confidence interval and the line across each diamond represents the group mean. The short horizontal lines indicate one standard deviation from the mean. The horizontal line crossing the entire graph indicates the grand mean. Each dot represents the disease severity of the plant within a single conetainer.

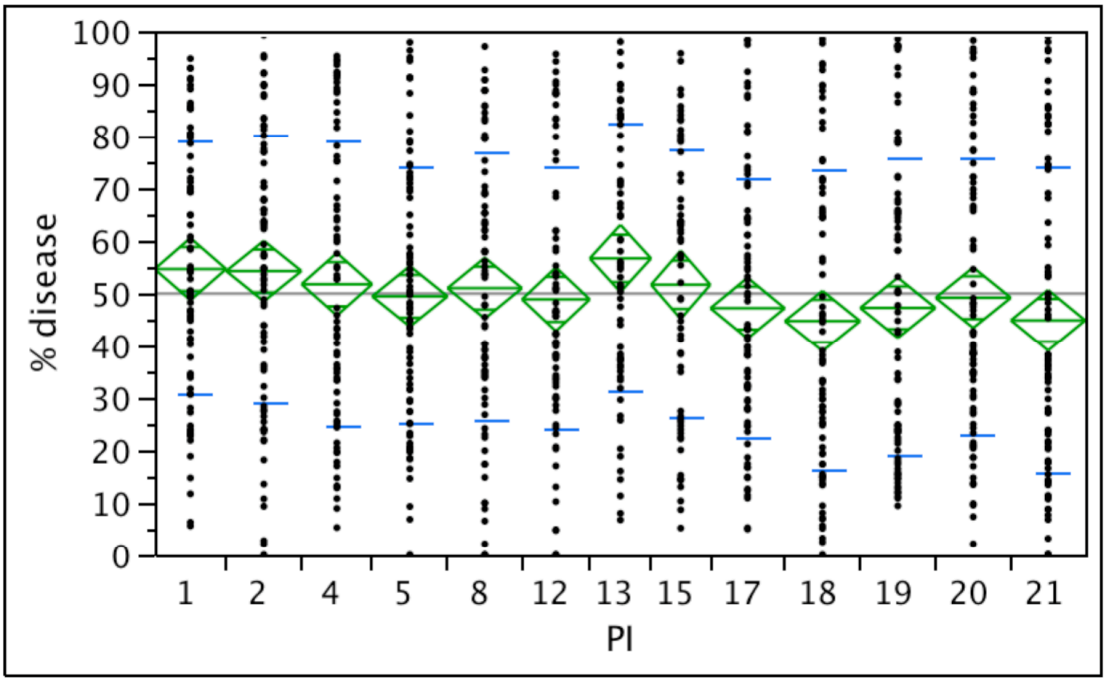

Figure 4.10. Temperature data (C) recorded within the two closed chambers (KC1, KC2) for the two final R. solani screens (FSRS1, FSRS2).

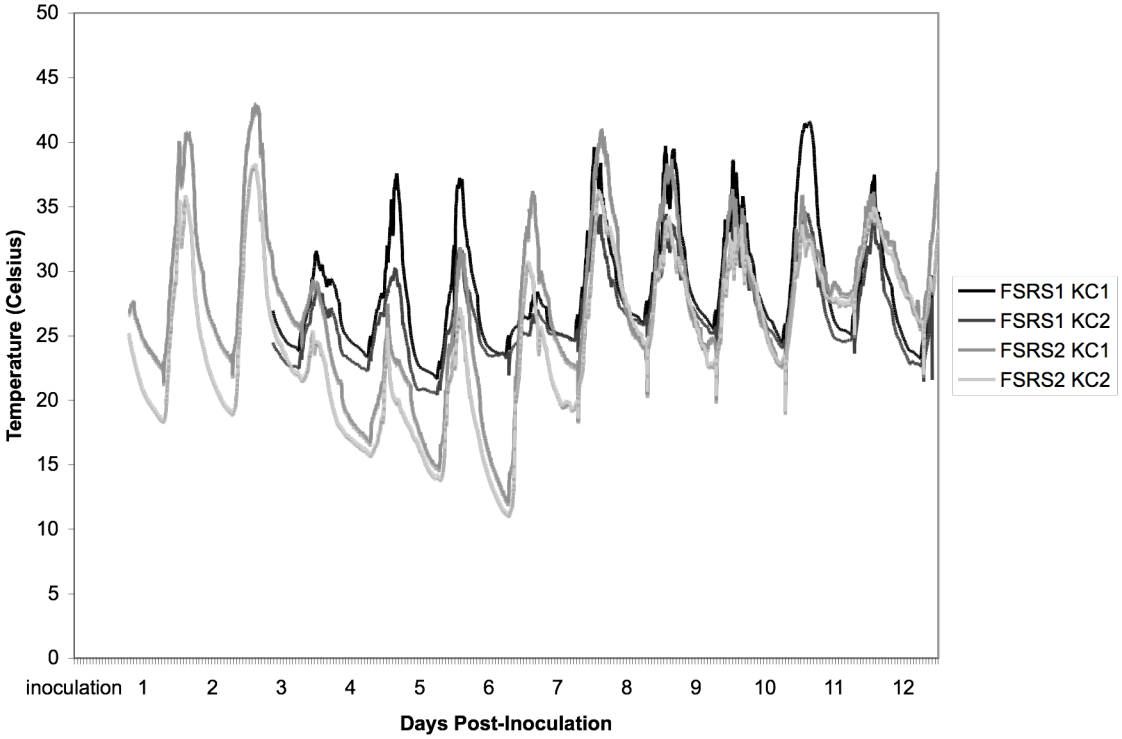

Figure 4.11. Dendrogram of PI and cultivar mean disease severity clustering determined by Wards hierarchical clustering with three clusters (highest resistance (·), medium resistance (x), lowest resistance (+)) for the first and second run of the final screen to *R. solani* (FSRS1, FSRS2). PIs and cultivars are ordered by principal components analysis of the mean disease severity in both runs. The colored columns to the right of the identification number are on a grayscale with black indicating high mean disease severity and white indicating low mean disease severity.

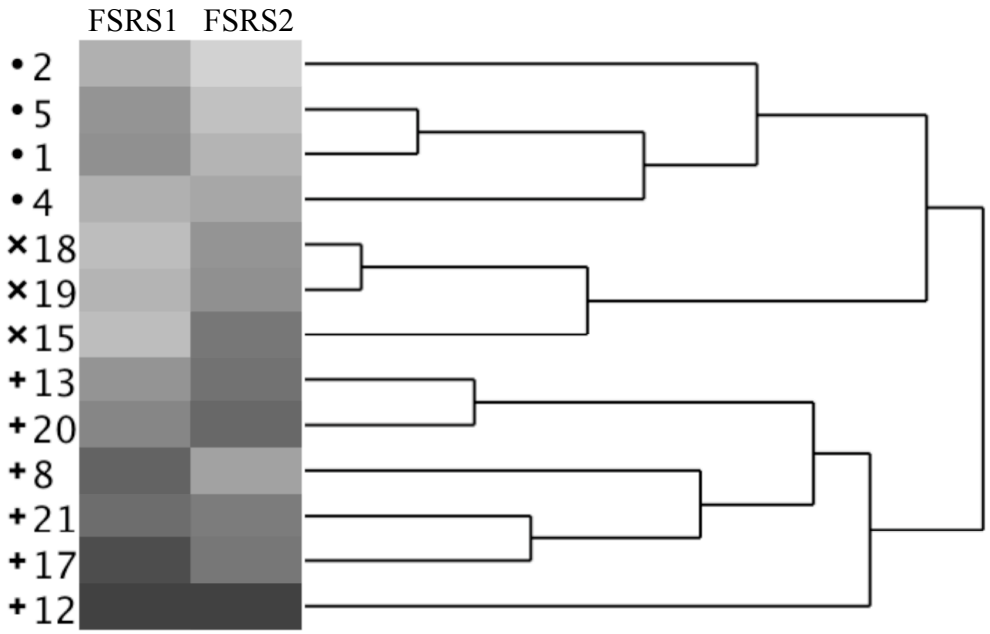

Figure 4.12. Dendrogram of PI and cultivar mean disease severity clustering determined by Wards hierarchical clustering with three clusters (highest resistance (·), medium resistance (x), lowest resistance (+)) for the first run of the final screen to *R. zeae* (FSRZ1).

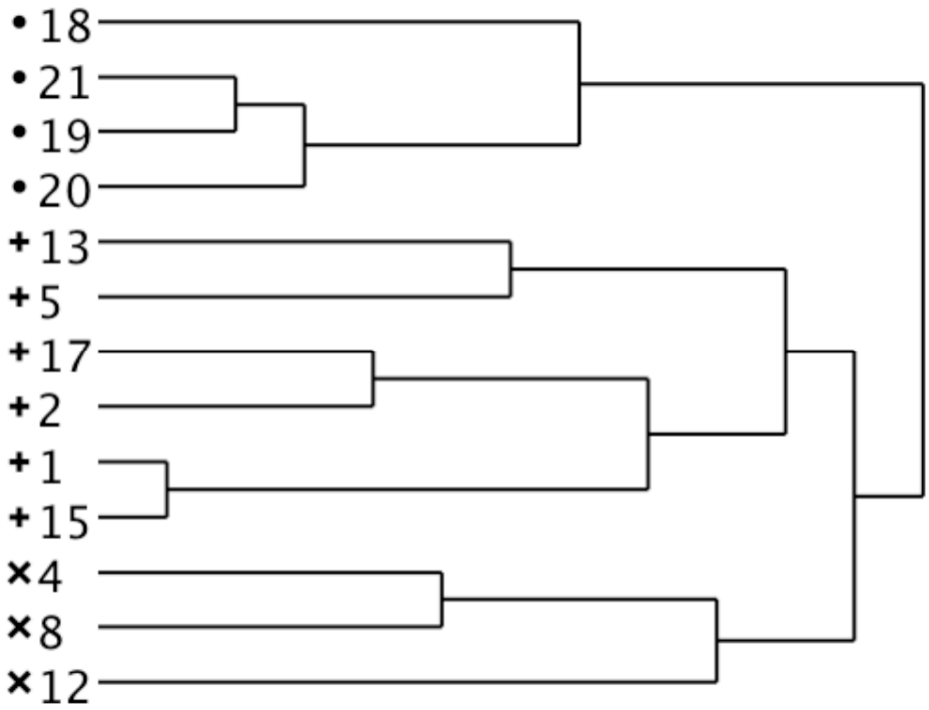

Table 4.2. ANOVA table for the final screens to *R. solani* (FSRS1, FSRS2) and *R. zeae* (FSRZ1, FSRZ2).

	Final Screens			
	FSRS1	FSRS2	FSRZ1	FSRZ2
PI or Cultivar[y]				
R^2	0.15	0.23	0.22	0.06
W – p value	<0.0001*	<0.0001*	<0.0001*	0.1431
Rep – p value	<0.0001*	<0.0001*	<0.0001*	<0.0001*
Clones[z]				
R^2	0.42	0.44	0.44	0.26
C - p value	<0.0001*	<0.0001*	<0.0001*	0.8345
Rep - p value	<0.0001*	<0.0001*	<0.0001*	<0.0001*

[y] means separated using $ANOVA_{\alpha = 0.05}$ with replication (Rep) and plant introductions and cultivars as a whole (W) as effects. An asterisk indicates a significant p-value
[z] means separated using $ANOVA_{\alpha = 0.05}$ with replication (Rep) and clones (C) as effects. An asterisk indicates a significant p-value

Table 4.3. Means and standard deviation (SD) table for plant introductions and cultivars as a whole (W) in the final screens to *R. solani* (FSRS1, FSRS2) and *R. zeae* (FSRZ1, FSRZ2).

	FSRS1			FSRS2			FSRZ1			FSRZ2		
ID	Mean Disease(%)	SD	Cluster[z]	Mean Disease(%)	SD	Cluster	Mean Disease(%)	SD	Cluster	Mean Disease(%)	SD	Cluster
PI 1	63.28	23.82	M	59.23	27.76	H	53.54	26.74	M	54.59	24.20	-
PI 2	58.80	18.85	H	62.34	24.48	H	51.05	24.12	M	54.18	25.54	-
PI 4	59.04	17.96	H	60.41	22.30	H	57.95	24.01	L	51.90	27.27	-
PI 5	62.82	25.74	M	62.76	23.02	H	47.14	25.24	M	49.40	24.52	-
PI 8	69.09	16.48	L	65.41	23.00	M	58.97	23.40	L	50.88	25.57	-
PI 12	72.80	16.26	L	67.62	20.65	M	64.44	23.31	L	48.66	25.11	-
PI 13	62.63	20.46	M	68.19	19.76	M	45.97	20.25	M	55.95	25.42	-
PI 15	60.19	22.05	H	67.61	18.81	M	52.84	26.26	M	51.61	25.60	-
PI 17	71.47	19.23	L	68.76	17.74	M	50.11	23.79	M	47.39	24.67	-
MI 18	57.01	16.47	H	66.29	18.59	M	30.79	20.39	H	44.68	28.73	-
ST 19	58.04	17.55	H	71.31	20.65	L	34.09	22.57	H	47.20	28.34	-
FA 20	64.81	17.00	M	75.56	18.91	L	34.64	21.29	H	49.14	26.25	-
KE 21	67.68	19.39	L	66.88	20.60	M	33.51	25.67	H	44.75	29.28	-
Mean	63.63	19.33		66.32	21.25		47.16	23.62		49.89	26.19	
Mean SD – clones		16.92			20.35			21.62			25.19	
Mean SD - reps		6.99			10.68			7.38			6.28	

[z] Means showing significant differences in ANOVA$_{\alpha = 0.05}$ differentiated into three clusters using Wards hierarchical cluster analysis: highest resistance (H), medium resistance (M), lowest resistance (L).

Table 4.4. Mean disease values for PI clones contained within the high resistant cluster using Wards hierarchical cluster analysis on final screens showing a significant difference in mean disease severity among clones using ANOVA $_{\alpha = 0.05}$ (FSRS1, FSRS2, FSRZ1).

FSRS1 and FSRS2				FSRZ1		
PI Clone[y]		Mean % disease		PI Clone[z]		Mean % disease
		FSRS1	FSRS2			FSRZ1
PI	2-1	29.72	43.77	KE	21-15	7.14
PI	15-7	37.97	53.65	MI	18-17	11.97
FA	19-11	36.38	59.33	KE	21-16	13.23
PI	2-3	44.48	51.73	ST	20-9	16.67
FA	19-9	43.42	53.56	KE	21-8	18.76
PI	2-5	45.26	53.48	PI	5-19	19.35
MI	18-2	44.88	56.32	FA	19-14	20.60
PI	5-8	46.77	57.74	FA	19-6	21.02
PI	15-13	43.16	58.57	PI	13-15	22.33
PI	5-20	46.12	60.32	MI	18-13	22.35
FA	19-12	44.01	44.80	MI	18-18	22.36
PI	5-16	44.90	46.61	MI	18-15	22.42
PI	2-17	45.99	45.74	KE	21-18	22.62
MI	18-11	48.51	45.89	PI	15-6	22.66
PI	4-14	51.27	48.08	ST	20-2	22.74
MI	18-17	50.26	52.24	FA	19-18	23.23
FA	19-7	44.01	44.80	PI	5-7	23.46
MI	18-12	52.82	51.03	MI	18-11	24.15
PI	1-6	54.22	50.34			

[y] ordered by principal components using FSRS1 and FRS2 mean disease severity of clones.
[z] ordered by principal components using FSRZ1 mean disease severity of clones.

R. zeae screen, 21% of the top-performing clones were from PIs and 79% were from established cultivars. None of the PIs, cultivars, PI clones, or cultivar clones contained within the high resistance cluster for *R. solani* were also contained in the high resistance cluster for *R. zeae.*

Discussion

In both screens, mean disease severity differed between pathogens. *Rhizoctonia solani* caused higher disease severity compared to *R. zeae*, even under less than ideal temperature. In both the initial and final screens, cultivar and PI susceptibility differed between *R. solani* and *R. zeae*. Established cultivars tended to show superior performance compared to PIs in the *R. solani* screen, while PIs tended to show equal or superior performance compared to established cultivars in the *R. zeae* screen.

In the final screens, high variability existed within clones. This variability was seen in both PIs and established cultivars, though it was less notable in the established cultivars (Figure 4.6, Figure 4.7). Some of this variability is accounted for by the differences in climate inside and between the two closed chambers. All four final screens showed a significant difference in disease severity among the blocked replications with an average standard deviation among blocks ranging from 6.23 percentage points to 10.68 percentage points in the four screens. Variability within PIs and cultivars as a whole was reduced in the initial screen where all plants were screened in one chamber. Variability may also have been influenced by inherent genetic variability within PIs and cultivars and the age and density of screened plant material.

Variability influenced by genetic differences within PIs and cultivars is consistent with the findings from Curley and Jung (2004) who evaluated genetic relationships in Kentucky bluegrass cultivars and plant introductions using random amplified polymorphic DNA. Three seeds from each plant introduction or cultivar were evaluated. High variability existed in the similarity of genetic markers within seedlings from PIs and cultivars. Variability ranged from 0.05, with nearly all scored bands matching for the three seedlings, to 0.5 with only half of the scored bands matching for the three seedlings. This study corresponded to our own study with the highest genetic variability reported in PIs and only intermediate genetic variability reported in cultivars. Mean standard deviation was lower among clones compared to PIs and cultivars as a whole; however, the standard deviation within clones was still high. Part of this was due to

differences in microclimate within and between chambers, but variability may also have been influenced by differences in the age and density of screened plant material.

The time it took to plant enough replications for each screen caused a distinct difference in the age and density of plant material. Because of the small size of the conetainers in which plants were grown, older plants were more likely to be root bound which may have led to increased plant stress. These older plants also tended to have denser canopies since they had been growing for a longer period of time. Studies have reported increased susceptibility to brown patch in denser turfgrass canopies (Geisler et al., 1996; Nutter Jr. et al., 2006). Variability in canopy density among plants may have contributed to the variability across and within experiments

Plant material age and density were uniform throughout the initial screens and differences in susceptibly to *R. solani* versus *R. zeae* were also seen in these studies. These results, along with the results of the final screens, suggest a difference in PI susceptibly to *R. solani* compared to *R. zeae*. Future studies in which differences in planting material age and density can be reduced may provide more consistent results. An evaluation of the resistance response to both *R. solani* and *R. zeae* for cultivars showing high variability in brown patch resistance response across locations instead of PIs may also be more informative in evaluating differences in tall fescue's resistance response between these two pathogens.

The final screens successfully identified PI clones with equal or superior performance to clones within the evaluated established cultivars. The mean disease values tended to be lowest in the established cultivars when evaluating PIs and cultivars as a whole; however, when evaluating individual PI and cultivar clones, the PI clones dominated the high resistance clusters in the *R. solani* screen. PI clones with equal or superior resistance to *R. zeae* compared to the established cultivars were also identified, though in lesser numbers. These data suggest material within these PIs may possess higher resistance to each individual pathogen compared to established cultivars and further crosses of this material may provide future cultivars with increased resistance to both pathogens. Resistance to *R. solani* and *R. zeae* differed between PIs and PI clones. Screening for resistance to both pathogens may reduce some of the variability observed in the resistance response of brown patch resistant cultivars observed at multiple locations where brown patch-like symptoms may be caused by either *R. solani* or *R. zeae*.

Literature Cited

Curley, J., and G. Jung. 2004. RAPD-based genetic relationships in Kentucky bluegrass: comparisons of cultivars, interspecific hybrids, and plant introductions. Crop Science 44:1299-1306.

Elliot, M.L. 1999. Comparison of *Rhizoctonia zeae* isolates from Florida and Ohio turfgrass. HortScience 34:298-300.

Geisler, L.J., G.Y. Yuen, and G.L. Horst. 1996. Tall fescue canopy density effects on brown patch disease. Plant Disease 80:384-388.

Horst, G.L., M.C. Engelkle, and W. Meyers. 1984. Assessment of visual evaluation techniques. Agronomy Journal 76:619-622.

Horvath, B.J., and J.M. Vargas. 2005. Analysis of dollar spot disease severity using digital image analysis. International Turfgrass Society Research Journal 10:196-201.

Karcher, D.E., and M.D. Richardson. 2003. Quantifying turfgrass color using digital image analysis. Crop Science 43:943-951.

Lindow, S.E., and R.R. Webb. 1983. Quantification of foliar plant disease symptoms by microcomputer-digitized video image analysis. Phytopathology 73:520-524.

Martin, S.B., S.N. Jeffers, and A. Rogers. 2001. Isolation frequency and pathogenicity of Rhizoctonia species from tall fescue crown and leaf tissues from two locations in South Carolina. International Turfgrass Society Research Journal 9:689-694.

McCall, D.S. 2006. Influence of isolate, cultivar, and heat stress on virulence of *Rhizoctonia zeae* on tall fescue, Virginia Polytechnic Institute and State University, Blacksburg.

Niemira, B.A., W.W. Kirk, and J.M. Stein. 1999. Screening for late blight susceptibility in potato tubers by digital analysis of cut tuber surfaces. Plant Disease 83:469-473.

NTEP. 2005. 2002-05 National Tall Fescue Test (NTEP No. 06-12). National Turfgrass Evaluation Program.

Nutter Jr., F.W., P.D. Esker, and R.A.C. Netto. 2006. Disease assessment concepts and the advancements made in improving the accuracy and precision of plant disease data. Phytopathometry 115:95-103.

Nutter Jr., F.W., M.L. Gleason, J.H. Jenco, and N.C. Christians. 1993. Assessing the accuracy, intra-rater repeatability, and inter-rater reliability of disease assessment systems. Phytopathology 83:806-812.

Plumley, K.A. 1988. *Rhizoctonia* spp. associated with golf course turfgrass in southern New Jersey. Phytopathology 78:1510.

Richardson, M.D., D.E. Karcher, and L.C. Purcell. 2001. Quantifying turfgrass cover using digital image analysis. Crop Science 41:1884-1888.

Conclusions

There were no significant differences in the DIA preparation methods for scanning individual leaves. DIA performed on individual leaves (IL) was a good predictor of actual disease values in both experiments (Ex.1: $r^2 = 0.97$, Ex.2: $r^2 = 0.99$). The mean absolute error (MAE) was also low in both experiments (Ex. 1: MAE = 1.85, Ex.2: MAE = 2.51). This method of DIA was very time-consuming and would not be efficient for large-scale disease evaluation. It did provide a good estimate of actual disease values and was used to evaluate the accuracy and precision of less time consuming DIA methods and visual evaluations. The accuracy of DIA evaluations was greater than visual evaluations in two of the four experiments and not significantly different from visual evaluations in two of the four experiments with the hue threshold required to most accurately distinguish lesions varying among experiments. Image variance may have prevented the DIA software from using a set hue threshold value to pick out lesions. The accuracy of the DIA method might be improved by reducing image variance. The precision of the whole pot DIA method using either hue threshold was significantly higher than the precision of visual evaluations. Increased precision in disease evaluations expands researcher's ability to compare results across trials performed by multiple evaluators. Although the accuracy of the whole pot method was not significantly improved compared to visual evaluations, the accuracy of the IL method gave a close estimate to actual disease severity, indicating improvements can be made to alternative DIA methods to increase accuracy in the future. At this time, neither DIA method would be appropriate for in field evaluations of brown patch where DIA is unable to differentiate between biotic and abiotic stress or between symptoms caused by different pathogens.

The whole pot DIA method was able to identify PIs and PI clones with greater *R. solani* and *R. zeae* resistance compared to the established cultivars Millennium, Falcon, Stetson, and Kentucky 31 in greenhouse studies. Overall, plants seemed to be less susceptible to *R. zeae* compared to *R. solani* with lower mean disease severity in both the initial and final screens of *R. zeae* compared to *R. solani* screens. The established cultivars as a whole had the highest resistance to *R. zeae*. The PIs 1, 2, 4, and 5 had equivalent mean disease severity compared to the established cultivars in the initial screen and lower mean disease severity compared to established cultivars in the final screen to *R. solani.* PI clones were dominant among the highest resistance cluster compared to established cultivar clones in the *R. solani* screens. Cultivar

clones were dominant in the *R. zeae* screens, with only four PI clones identified within that cluster. Tall fescue plant introductions appear to be a good source for identifying improved *R. solani* resistance. Although *R. zeae* does not appear to be as aggressive a pathogen on tall fescue compared to *R. solani*, this pathogen can be problematic, causing greater than 90 % disease on some plants within the final screens. Symptoms can be identical to those of *R. solani* and cultivars bred solely for resistance to *R. solani* may perform poorly in trials across multiple locations where *R. zeae* is causing symptoms. Breeding cultivars for resistance to both pathogens may alleviate some of the variability observed in the resistance response of brown patch resistant cultivars evaluated across locations.

Appendix A

(1) Screenshot of a plant image open in APS Assess digital image analysis software. (2) The hue plane was selected. The total plant area was selected by entering a numerical hue threshold range. The area not within that hue threshold range was replaced by selecting "Edit" > "Substitute Background". The intensity color plane was selected. An intensity threshold was used to select the soil, which was then replaced with a blue background (not shown). (3) The hue plane was selected. Numerical hue thresholds were entered to select the total plant area. The total area in pixels within the selection was determined by selecting the "Area" button. (4) Numerical hue thresholds were entered to select the total necrotic area. The total area in pixels within the selection is determined by selecting the "Area" button. (5) Selecting the "% Area" button uses a ratio of necrotic area to total plant area to determine percent disease.

1.

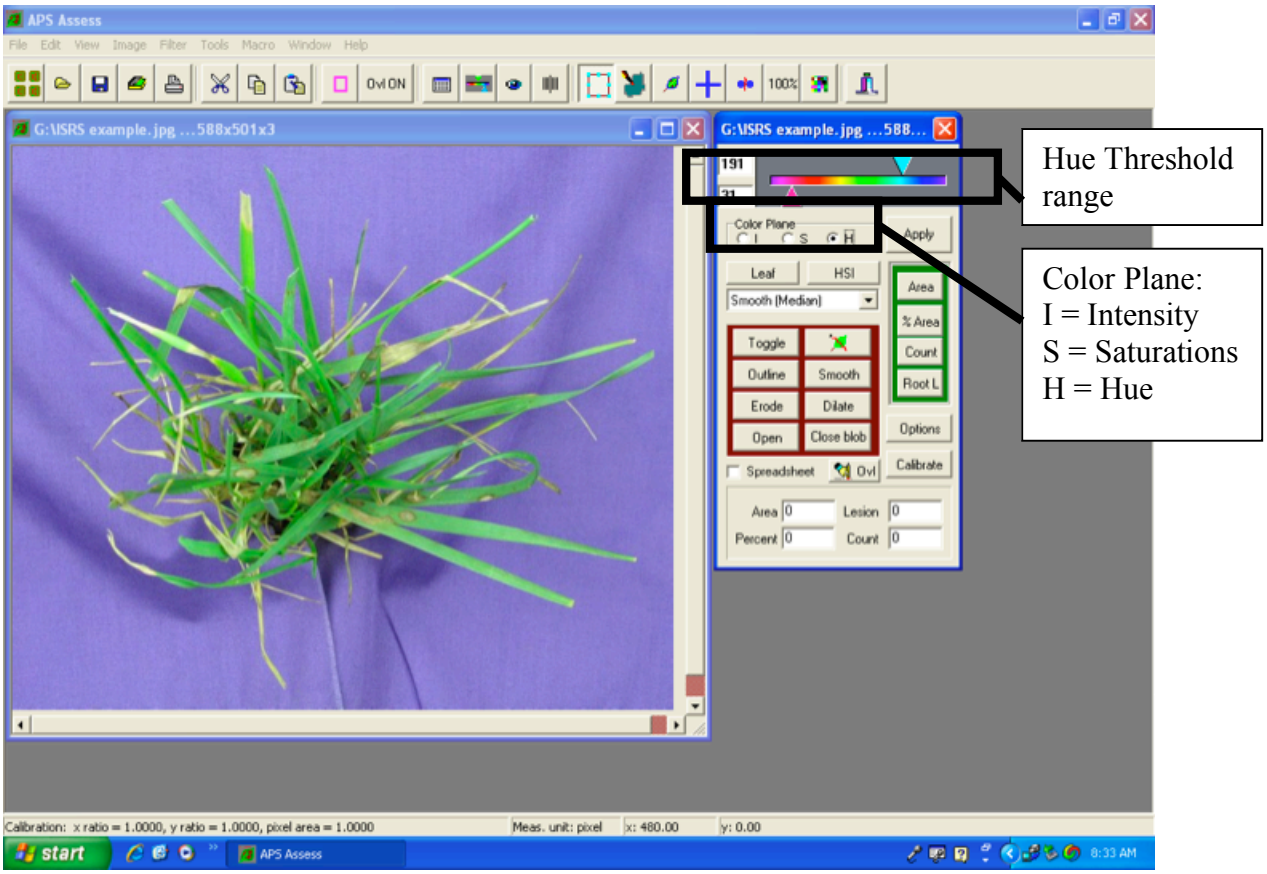

2.

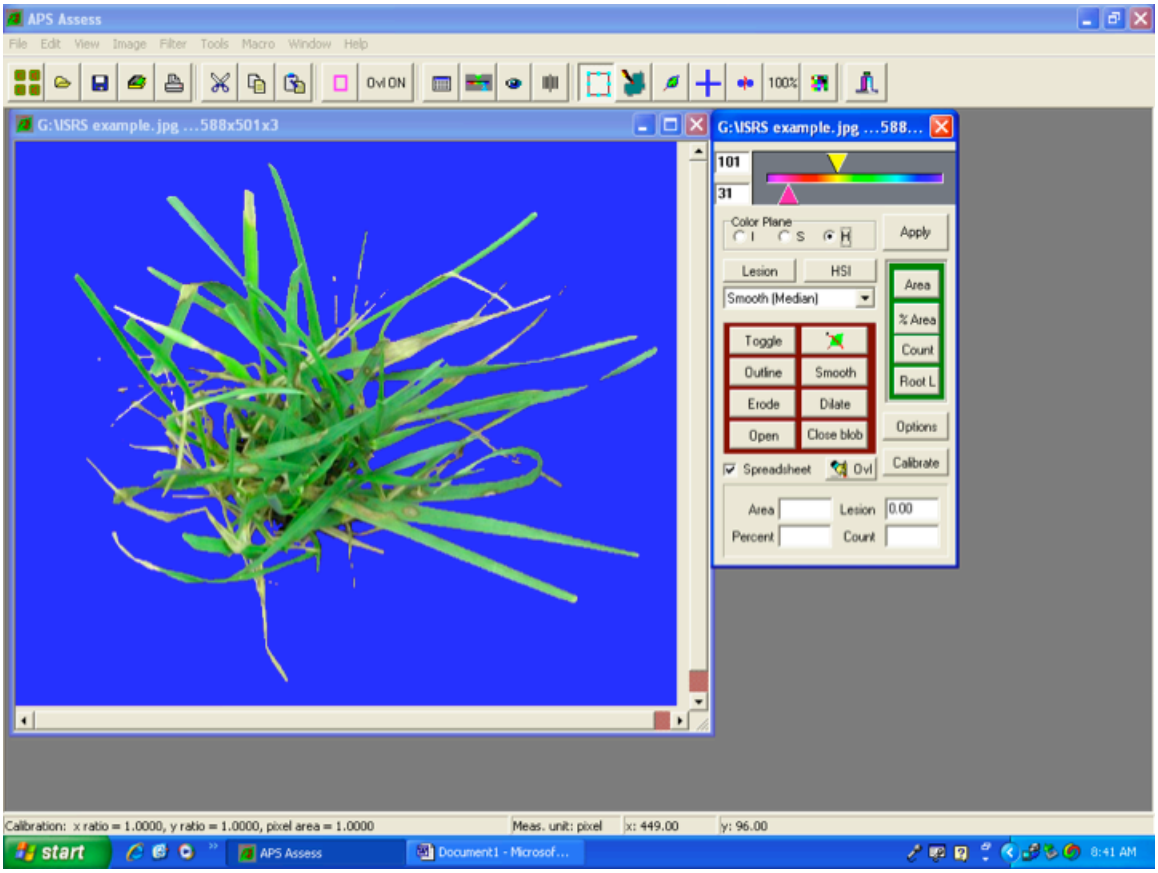
APS Assess
File Edit View Image Filter Tools Macro Window Help
Ovl ON
100%
G:\ISRS example.jpg ...588x501x3
G:\ISRS example.jpg ...588...
101
31
Color Plane
I S H
Apply
Lesion
HSI
Smooth (Median)
Toggle
Outline
Smooth
Erode
Dilate
Open
Close blob
Area
% Area
Count
Root L
Options
Calibrate
Spreadsheet
Ovl
Area
Lesion
0.00
Percent
Count
Calibration: x ratio = 1.0000, y ratio = 1.0000, pixel area = 1.0000
Meas. unit: pixel
x: 449.00
y: 96.00
start
APS Assess
Document1 - Microsof...
8:41 AM

3.

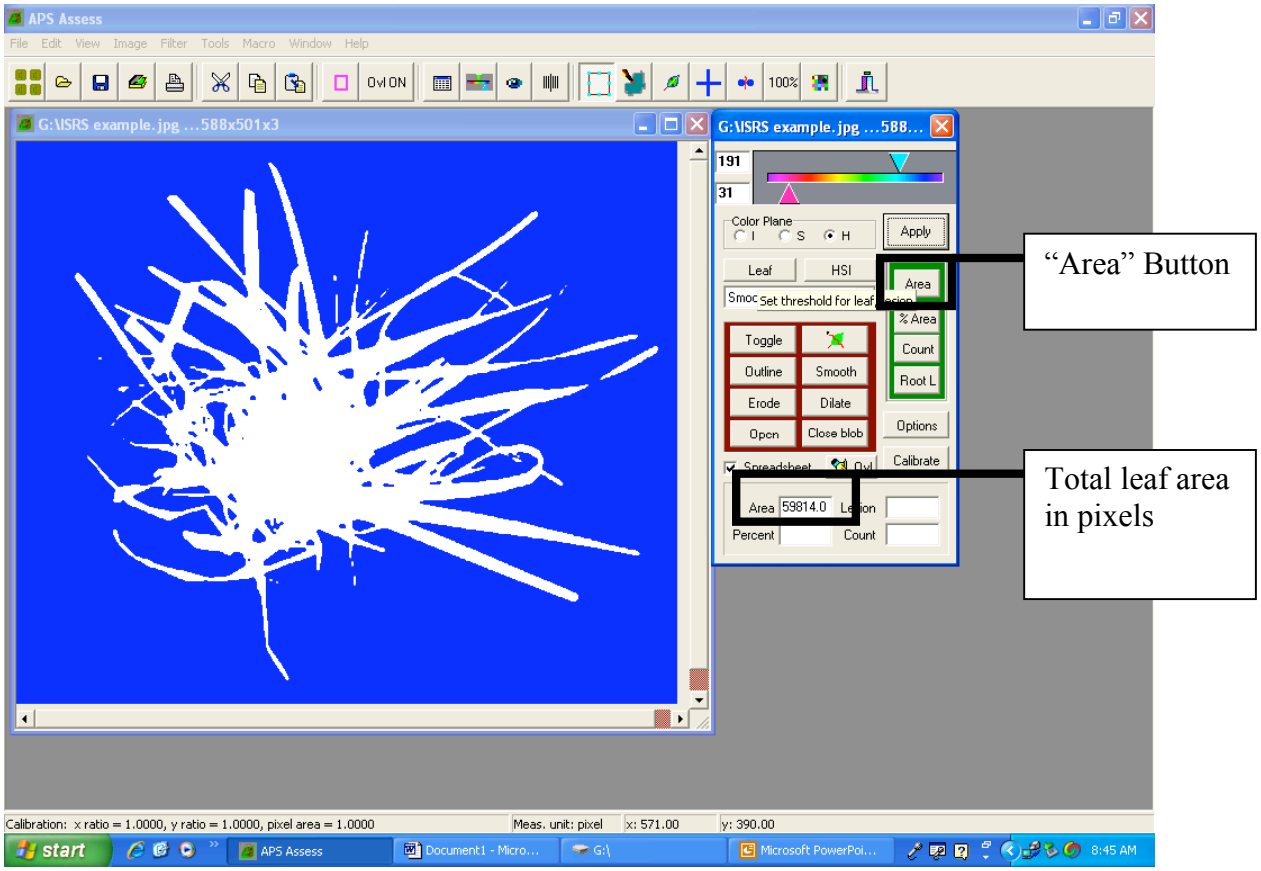
APS Assess
G:\ISRS example.jpg ...588x501x3
G:\ISRS example.jpg ...588...
Color Plane
Apply
Leaf
HSI
Area
Set threshold for leaf
% Area
Count
Root L
Toggle
Outline
Smooth
Erode
Dilate
Open
Close blob
Options
Calibrate
Area 59814.0
Percent
Count
"Area" Button
Total leaf area in pixels
Calibration: x ratio = 1.0000, y ratio = 1.0000, pixel area = 1.0000
Meas. unit: pixel
x: 571.00
y: 390.00
start
8:45 AM

4.

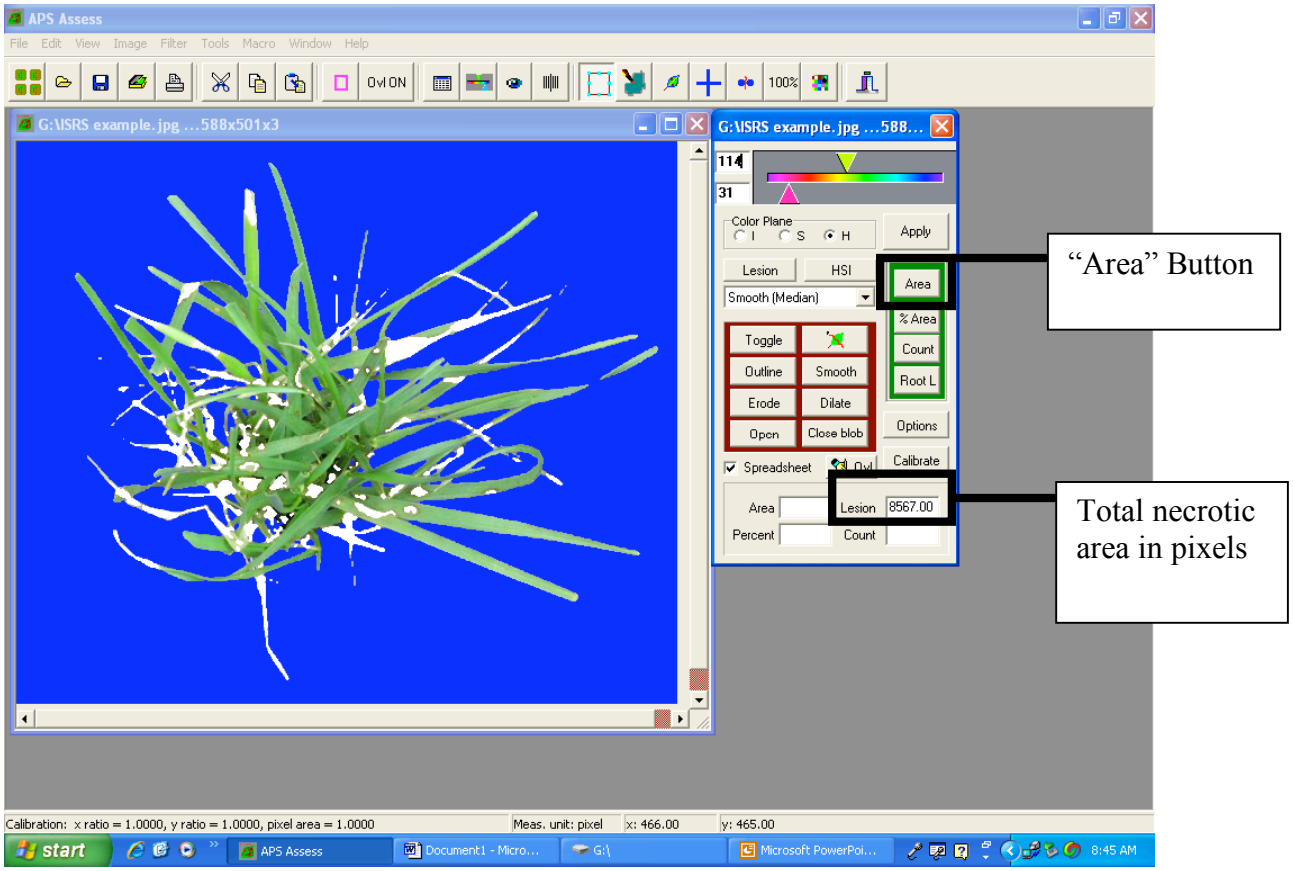
APS Assess
File Edit View Image Filter Tools Macro Window Help
Ovl ON
100%
G:\ISRS example.jpg ...588x501x3
G:\ISRS example.jpg ...588...
114
31
Color Plane
I S H
Apply
Lesion
HSI
Area
Smooth (Median)
% Area
Count
Root L
Toggle
Outline
Smooth
Erode
Dilate
Open
Close blob
Options
Calibrate
Spreadsheet
Ovl
Area
Lesion 8567.00
Percent
Count
"Area" Button
Total necrotic area in pixels
Calibration: x ratio = 1.0000, y ratio = 1.0000, pixel area = 1.0000
Meas. unit: pixel
x: 466.00
y: 465.00
start
APS Assess
Document1 - Micro...
G:\
Microsoft PowerPoi...
8:45 AM

5.

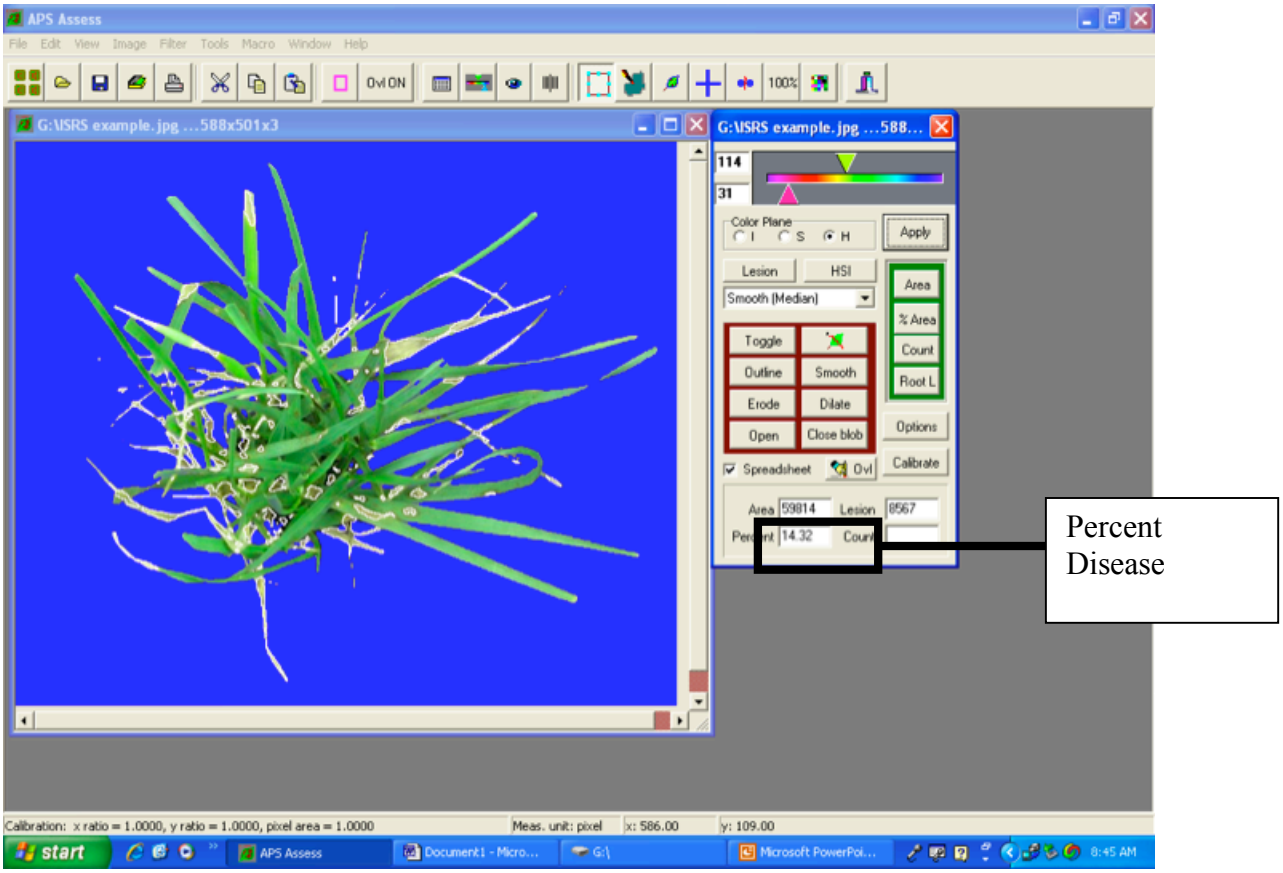
APS Assess
File Edit View Image Filter Tools Macro Window Help
Ovl ON
100%
G:\ISRS example.jpg ...588x501x3
G:\ISRS example.jpg ...588...
114
31
Color Plane
I S H
Apply
Lesion
HSI
Smooth (Median)
Area
% Area
Count
Root L
Toggle
Outline
Smooth
Erode
Dilate
Open
Close blob
Options
Calibrate
Spreadsheet
Ovl
Area 59814 Lesion 6567
Percent 14.32 Count
Percent Disease
Calibration: x ratio = 1.0000, y ratio = 1.0000, pixel area = 1.0000
Meas. unit: pixel
x: 586.00
y: 109.00
start
APS Assess
Document1 - Micro...
G:\
Microsoft PowerPoi...
8:45 AM